164B

Chukchi Sea Transportation Study Ice Component

DICKINS

Joint Industry Study
Chukchi Sea Transportation and
Cost Comparison
1990 Update

Chukchi Sea Transportation Study Ice Component

for

Joint Industry Study

Chukchi Sea Transportation and Cost Comparison

1990 Update

December 1990

prepared by

DF Dickins Associates Ltd.
503, 21 Water Street
Vancouver, B.C.
Canada V6B 1A1

FOREWORD

This report is an update of work submitted as part of a previous joint industry study by Intec Engineering Inc. in April 1986.

Revised sections cover multi-year ice edges, ice retreat and advance, and ice motion. Completely new information is included on summer ice intrusions which are important for scheduling marine operations. The entire text was reviewed for completeness and consistency with the most currently available data; additional information on ridging and ice thickness from more recent icebreaker cruises was inserted into the regional ice summary tables. Nine new references were used in preparing this update, together with more recent ice charts.

The following summary describes the new information together with the characteristics of the Chukchi Sea ice environment.

STUDY TEAM

The authors of the original work were David Dickins, Ingrid Bjerkelund, and Anthony Dickinson. Revisions and new material were developed by Ann Godon, Martin Poulin, and David Dickins.

This work was performed by DF Dickins Associates Ltd. under contract to Intec Engineering Inc.

SUMMARY

This report describes ice conditions along the marine transportation route from the southern Bering Sea to the exploration areas of the northern Chukchi Sea. This route is characterized by gradually increasing thickness and duration of total ice cover from south to north. The greatest variation in ice thickness and concentration occurs within the Bering Sea from the first presence of ice in the vicinity of St. Paul Island to the Bering Strait. Over this section of the route the period of significant ice cover ranges from less than three months in the south to over six months in the north Bering Sea.

Icebreaker Experiences

The Chukchi Sea can be divided into north and south regions with Cape Lisburne as the dividing line. The region between the Bering Strait and Cape Lisburne is often characterized by extensive areas of ice rubble, rafting, and ridging with limited leads and openings during the winter. The combination of ice pressure and deformed ice in this area has led to the greatest number of rams (situations where an icebreaker cannot maintain continuous progress) and the lowest transit speeds during previous winter voyages with the *Polar Sea* and *Polar Star* (Brigham, 1986).

Caution is advised in extrapolating directly from the icebreaker experiences to future commercial vessels; icebreaking tankers with more fuel efficient engines and higher displacement would likely be less affected by severe ice conditions than the Polar Class icebreakers.

North of Cape Lisburne, the frequent presence of leads and thin ice areas along the coast can provide easier conditions for winter operations. The major impediment to marine operations with lower class vessels in the northern Chukchi Sea is the rapidly decreasing open water season north of 71°.

Icebreaker experience in the Chukchi Sea have clearly demonstrated that with the right vessel, safe year-round operations are possible. Interestingly, one of

the conclusions from the joint Maritime Administration/Industry research program was that independent commercial ship operation would be more practical than trying to maintain effective escort operations in the dynamic Chukchi pack ice (Brigham, 1986). Escort vessels may be required as an oil spill countermeasure rather than for operational purposes.

Overview of the Chukchi Sea Environment

The Chukchi Sea ice environment differs significantly from that of the Beaufort Sea. Ice severity in terms of thickness, multi-year encounter, and open water season is related to both latitude and distance from shore. The ice cover is highly dynamic year-round in response to wind and current driving forces; recurring polynyas and lead systems result in preferred transportation corridors which have mild ice conditions even in mid-winter.

Winter ice conditions are dominated by the presence of a broad flaw polynya or lead, comprised of open water and newly forming ice. This recurring feature often extends from Point Hope to Point Barrow with the widest extent occurring between Cape Lisburne and Point Lay.

The flaw polynyas and leads are bounded on one side by a variable zone of fast ice stretching into shoe and on the other side by moving pack ice, with a mixture of ice ages.

There are four characteristic winter ice zones in the Chukchi Sea:

- Variable fast ice (continuous to shore) including a bridge across deep water in Peard Bay and extensions seaward over the shoal area northwest of Icy Cape.

- New ice and open water in recurring polynya areas northeast of Cape Lisburne, south of Point Hope, and along the fast ice edge as far as Point Barrow. Icebreakers have used this zone to advantage in maintaining high transit speeds during winter voyages (Brigham, 1986).

- Predominantly first-year pack ice south of 71° latitude. Thicker floes are interspersed with new and young ice areas. Low concentrations of multi-year ice are often found south as far as Cape Lisburne.

- Polar pack consisting of predominantly multi-year ice north of 72°. The location of the polar pack edge in the Chukchi Sea is highly variable.

Winter ice motion in the Chukchi Sea is dominated by wind and current-driven forces. Along the Chukchi coast from Cape Lisburne to Point Barrow, winter winds from the east and northeast tend to maintain the pack ice away from the coast and cause ice drift in a general southwesterly direction against the northern water flow. Winter ice velocities measured in the Chukchi Sea are over double those commonly used for design purposes in the Beaufort Sea.

The predominantly first-year pack ice zone, which covers the largest portion of the lease areas, is highly variable in terms of ice age and roughness. Unlike the Alaskan Beaufort Sea ice cover, which moves slowly from January to March, the Chukchi Sea ice cover displays a high degree of mobility throughout the mid-winter period. Pressure ridging, rafting, and rubble formation occur during episodes of rapid wind driven ice motion. The resulting mixed ice composition is extremely difficult to categorize in simple statistical terms. For example, in March 1981 the pack ice cover north of Cape Lisburne was described as heavy rubble, 4.5 ft thick level ice floes, and ridges up to 12 ft high, interspersed with young ice, cracks, and refrozen leads (Voelker et al., 1981b).

The patterns of pack ice decay in the summer and ice motion in the winter are strongly influenced by the circulation of relatively warm water flowing north from the Bering Sea. The Alaskan Coastal Current is of particular importance to ice conditions in the lease sale area. There are significant uncertainties regarding the Chukchi Sea water circulation regime. Current reversals along the coast are often associated with northeasterly winds.

During periods of light winds, ice motion is largely controlled by the prevailing currents. In the spring, warm water flowing north into the Chukchi Sea begins to affect both the decay and movement of the ice. Clearing of nearshore areas in the north Chukchi Sea often occurs over a month in advance of the central or more southerly offshore areas.

map (Figure 7) shows less ice retreat by late summer between 161° and 166° Longitude.

The average winter polar pack edge appears to be located up to 30 nmi further south than the corresponding summer old ice edge (based on the longer time period record available in this study); this difference is not considered significant when viewed against the overall variablity of the old ice edge.

Ice intrusions will interfere with summer operations for less than one week on average (median case). One year in ten will encounter interruptions of three weeks or more. Although not significant in the more southern lease areas, interruptions of these durations would seriously affect the operation of conventional marine equipment in the extreme northerly areas.

Additional information on ridging collected during icebreaker voyages, and from aerial photography confirms that a much longer time period record is needed to establish any statistical trends in ice roughness by location.

Knowledge of multi-year ice in the northern Chukchi Sea remains as one of the most serious deficiencies facing offshore installation designers. There has been very limited progress over the past five years towards the collection of better ice baseline data for the Chukchi Sea lease areas.

CONTENTS

APPENDICES

FIGURES

FIGURES

FIGURES

FIGURES

TABLES

1.0 ENVIRONMENTAL ZONES ALONG THE MARINE TRANSPORTATION ROUTE

This study provides an overview of ice conditions along the marine transportation route from the Bering Sea to the Chukchi Sea lease sale area. The route has been divided into 9 Environmental Zones according to the ice conditions characteristic of each zone. The Environmental Zones are mapped in Figure 1. The rationale for the division between each zone is outlined in Table 1.

Ice conditions change dramatically From the south Bering Sea to the north Chukchi Sea. The open water season decreases from about 9 months at St. Paul and St. George Islands (Zone 1) to about 1 month in the Chukchi Sea lease sale area (Zone 8). Maximum first-year ice thicknesses in late winter increase from about 1.5 ft in Zone 1 to at least 5.0 ft in Zone 8. Multi-year ice is rarely encountered in the Bering Sea but can be found at concentrations up to 9+/10 in Zone 8.

Knowledge of the varying ice conditions along the route is critical for evaluating transportation systems (tankers and pipelines). The following material summarizes the important ice characteristics in each zone. Section 2.0 highlights particular features of the Chukchi Sea ice environment.

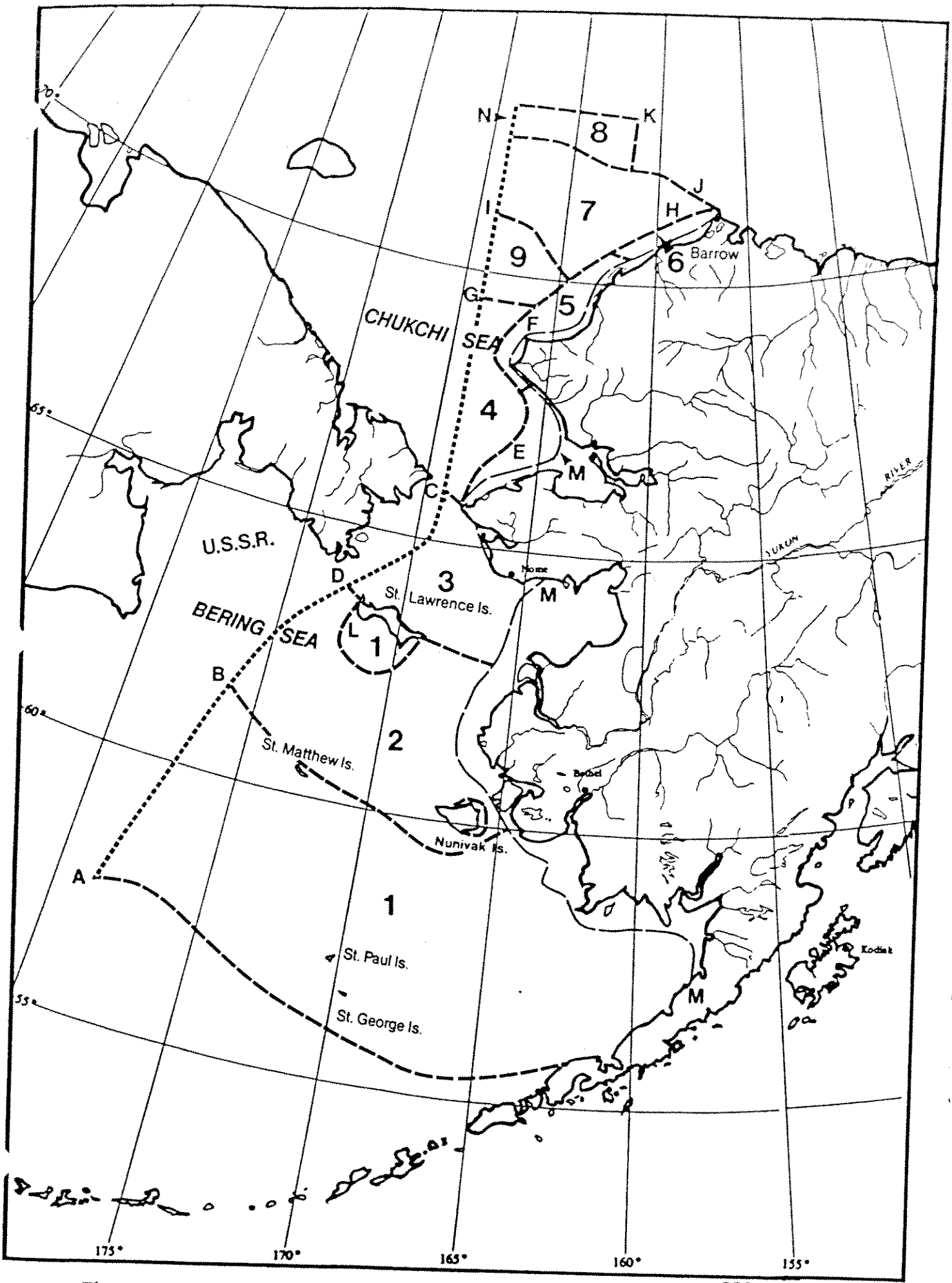

Figure 1 Environmental Zones

DF Dickins Associates Ltd.

Table 1 Key to Environmental Zones

A. South of this line the probability of ≥5/10 total ice concentrations is 0%. Based on the 15 April line - the most southern 0% probability line for ≥5/10 ice concentrations. (Source: LaBelle et al., 1983.)

B. South of this line the probability of ≥5/10 ice concentration is less than 1.0. Based on the 1 March line - the most southern 100% probability line for ≥5/10 ice concentrations. (Source: LaBelle et al., 1983.)

Note: This line is similar to the 100% line for zero ice cover in Webster (1981).

C. Position of the average 9-10/10 ice boundary in January. This is the last month before freeze-up in the Bering Sea. (Edge is based on Potocsky, 1975.)

D. Division of ice zones based on ice concentration data.

E. Extreme location of the fast ice edge in Kotzebue Sound. (Source: LaBelle et al., 1983.)

F. Estimate of polynya and shore lead extent. (Based on satellite image analysis by DF Dickins Associates and LaBelle et al., 1983.)

G. Southern limit of the polar pack (≥5/10 multi-year ice) 1975-1984. (Based on analysis of monthly Canadian Ice Charts by DF Dickins Associates.)

H. Estimate of shore lead extent.

1. Southern limit of 90% of the polar pack edges 1975-1984 (10 out of 11 edges on Canadian Ice Charts were further north).

J. Most northern occurrence of the 50% probability of Ice Free conditions. (Source: Webster, 1981.)

K. Northern boundary of OCS 109 sale area.

L. Zone of recurring flaw polynya off St. Lawrence Island.

M. Limit imposed by the 20 m isobath.

N. US/USSR border.

1.1 Overview of Ice Conditions

Ice summary tables in Appendix A list ice concentrations, ice thicknesses, ridge frequencies and heights, and snow depths, where available, for each zone.

Zone 1 St. Paul and St. George Islands to Nunivak Island

Ice concentrations in the south Bering Sea do not start to increase until January, reflecting the later start of freeze-up and the southward progression of the ice edge from the north Bering Sea. The maximum extent of the ice edge occurs between February and March, and ice cover in this region is usually less than 8/10. East of St. Paul and St. George Islands the maximum southern position may not occur until April.

In heavy ice years, the ice edge extends just south of St. George Island in the east and Cape Navarin in the west, paralleling the continental shelf break (200 m isobath). In light ice years, the ice edge extends just south of St. Matthew and Nunivak Islands and parallels the 50 m isobath (the division between Zones 1 and 2). The northwest flowing current along the continental shelf seems to be the major constraint limiting the southern extent of ice. By May 1 the St. Paul and St. George Islands area is ice-free (Muench and Ahlnas, 1976; Webster, 1981 ; Overland and Pease, 1982).

The ice edge in the south Bering Sea, the marginal ice zone, is defined as a region of broken and rafted floes and is strongly influenced by wind direction. Floe sizes gradually increase while decreasing in thickness with distance from the ice edge (Martin et al., 1982).

Zone 2 Nunivak Island to St. Lawrence Island

The progression of freeze-up in the South Bering Sea (Zones 1 and 2 are both in the south Bering Sea) tends to parallel the alignment of the continental shelf (200 m isobath). By December 1, the ice edge (5/10 total ice concentration) usually stretches between St. Lawrence and Nunivak Islands.

With the predominantly northeasterly winds, polynyas often form along the southern coasts of St. Lawrence, Nunivak, and St. Matthew Islands.

Offshore ice thicknesses and ridge frequencies are less in the south than the north Bering Sea. In February 1981, level ice thicknesses ranged from 0.95 to 1.15 ft and pressure ridge frequencies ranged from 1 to 9 ridges/mi (Voelker et al., 1981b).

The area between Nunivak and St. Lawrence Islands is ice-free by early June, except for a few areas. Ice persists south to southwest of St. Lawrence Island through June due to minimal water circulation in this area.

Zone 3 St. Lawrence Island to Bering Strait

Bering Sea ice is formed in-situ. The first ice forms north of St. Lawrence Island, in the shallow waters of Norton Sound and along the Alaskan coast from October to December. The ice advances south in mid-winter due to the predominantly northerly and northeasterly winds (Muench and Ahlnas, 1976; Pease, 1980; Overland and Pease, 1982) and reaches 9/10 concentration by January 1.

Flow through the Bering Strait is usually northward year round, although local winds can cause surface currents to reverse. Temporary current reversals can last up to 1 week. During these events some ice from the Chukchi Sea can move south into the Bering Sea (Muench and Ahlnas, 1976; Pease, 1980). Multi-year ice rarely encountered in the Bering Sea; one such instance occurred during the *Polar Star* voyage of 1984 (Voelker et al., 1984).

Ridge frequencies are generally greater in the north than the south Bering Sea. The most intense ridging occurs in the vicinity of St. Lawrence Island. St. Lawrence Island forms a barrier to southward ice drift from the north Bering Sea. Ice convergence north of St. Lawrence Island causes an "ice dam" to form between the island and the Siberian mainland. This can result in severe ice deformation and ridging, with 18 to 23 ridges/mi being reported under the worst conditions (Voelker et al., 1981b).

Extensive grounding of ridges also occurs between the island and the Alaskan mainland, in water depths up to 10 fathoms (18 m) due to the presence of numerous shoals. Level ice thicknesses measured in February 1981 in this area were between 1.9 and 2.2 ft (Voelker et al., 1981b).

The limited number of winter ship observations in the area show a great variability in the occurrence of rough ice throughout the Bering Sea These observations are not representative of north/south trends in ice severity which can only be confirmed by long-term observations for ten years or more; such data does not exist for the study area.

Polar Class voyages have encountered ridge frequencies ranging from almost non-existent in 1984 to over 8 ridges per mile in 1981. Caution is advised in interpreting the ship observations too literally; data collected while a vessel is in transit represents only a "snapshot" of local conditions and cannot be considered representative of regional conditions. Shipboard observations are included in Appendix A as examples only.

Ice break-up in the area of the Bering Strait and in Norton Sound starts in early June. By mid-June the Bering Strait is usually ice-free. The most rapid rates of ice edge advance and retreat occur in the north Bering Sea during freeze-up and break-up (Potocsky, 1975 ; Webster, 1981).

Zone 4 Bering Strait to Point Lay

Predominantly first-year ice is found in the southern Chukchi Sea, although trace concentrations of multi-year ice have been encountered in the vicinity of Cape Lisburne. The northern boundary of Zone 4 is formed by the extreme southern limit of the polar pack edge (5/10 multi-year ice concentration).

By November 1, the median ice edge (5/10 total ice concentrations) has advanced as far south as the Bering Strait. The Chukchi Sea ice cover is highly mobile throughout the mid-winter period. Pressure ridges, rafting, and rubble formation occur during periods of wind driven motion. Ice edge retreat usually occurs by July 1.

Zone 5 Cape Lisburne to Icy Cape

The nearshore area of the Chukchi Sea is characterized by a recurring shore lead that extends from Cape Lisburne to Point Barrow and by polynyas or thin ice areas northeast of Cape Lisburne and south of Point Hope. The shore lead is the widest between Cape Lisburne and Point Lay, in Zone 5. Predominantly east to northeast winter winds maintain the ice away from the coast and cause ice drift in a generally southwesterly direction.

The patterns of ice retreat in the summer and ice motion in the winter are most strongly influenced by the circulation of relatively warm water from the Bering Sea northward. The Alaskan Coastal Current branches off the main flow at Point Hope and follows the 20 fathom (37 m) isobath north of Cape Lisburne. This flow then branches into two streams; one flows north and the other channels into Barrow Canyon. The influence of the Alaskan Coastal Current causes the ice to clear from the nearshore areas over a month in advance of the central or more southern areas of the Chukchi Sea. The shore lead between Cape Lisburne and Point Lay and the polynyas offshore of Cape Lisburne and Point Hope can open as early as May. The number of weeks of open water during the summer ranges from 16 to 18 weeks between Cape Lisburne and Point Lay and 20 weeks or more offshore of Point Hope (open water is defined as <3/10 total ice concentrations).

By early November the contiguous ice, or fast ice, starts to extend seaward from shore. The contiguous ice reaches its maximum extent (approximately the 20 m isobath) in late winter, between January and March. The edge of the contiguous ice often marks the inshore boundary of the flaw lead or young ice area. Northeast of Cape Lisburne, a large ridge system tends to anchor the contiguous ice arching across Ledyard Bay. However, due to the large distance from shore, the ice appears susceptible to break away. Contiguous ice is also unreliable in the areas of recurring polynyas offshore of Cape Lisburne and Point Hope.

Zone 6 Icy Cape to Point Barrow

North of Point Lay, the shore lead along the coast shrinks as the Alaskan Coastal Current is channeled into the narrow Barrow Canyon. Freeze-up along the shore at Point Barrow begins in early October, but the offshore ice takes longer to consolidate. A winter flaw lead normally exists along the fast ice edge to Point Barrow. In some years this fast ice (or contiguous ice) may not extend further seaward than the barrier islands between Point Lay and Wainwright. Retreat of the median ice edge (defined as 5/10 total ice concentration) occurs by July 15.

Zone 7 Point Lay to Point Barrow - Offshore

The annual southern limit of the summer polar pack edge (5/10 multi-year ice concentration) occurs at about 71°N in 11 out of 15 years (1975 to 1989, Canadian Ice Charts). Some multi-year ice may be encountered year round in Zone 7. Predominantly first-year ice is found south of 71°N, the southern boundary of Zone 7.

Ice concentrations can reach 8/10 as far south as 70°N by early November. Retreat of the ice edge (defined as 5/10 total ice concentration) occurs by late August with a 50% frequency of occurrence. During the summer, the number of weeks of open water ranges between 9 and 5 weeks, from south to north, (open water is defined as <3/10 total ice concentration for operational purposes).

Zone 8 Northern Limit of OCS Lease Sale Area 109

The maximum ice retreat in the Chukchi Sea occurs in late September when the ice edge (5/10 total ice concentration) recedes to 72°30'N (at a 50% probability level). This ice edge corresponds approximately to the boundary between Zones 7 and 8. Less than 4 weeks of open water occur north of 72°N, and the ice edge typically starts to advance south in early October.

The occurrence of multi-year ice is common in Zone 8. However, in extreme summers, the polar pack edge can retreat beyond the continental shelf break at

75°N. With the limited clearing of ice in the summer and high probability of encountering old ice, Zone 8 represents the most severe environmental zone in terms of ice severity.

Zone 9 Cape Beaufort to Point Lay - Offshore

Zone 9 is located outside the influence of the recurring shore lead system (Zones 5 and 6) and is not favoured as a shipping route. While the southern limit of the polar pack edge is usually at 71°N (between Zones 7 and 9), in extreme years the polar pack edge can remain close to shore and as far south as 69°N. First-year ice predominates in Zone 9.

Advance of the median ice edge (5/10 total ice concentration) occurs between mid-October and early November. Ice edge retreat occurs between July and August. The number of weeks of open water during the summer ranges between 15 and 10 weeks, from south to north, respectively.

2.0 INTRODUCTION TO THE CHUKCHI SEA ICE ENVIRONMENT

The Chukchi Sea ice environment differs significantly from that of the Beaufort Sea. Ice severity in terms of thickness, multi-year encounter, and open water season is related to both latitude and distance from shore. The ice cover is highly dynamic year-round in response to wind and current driving forces; recurring polynyas and lead systems result in preferred transportation corridors which have mild ice conditions even in mid-winter. Although the Chukchi Sea ice cover is characterized by extreme spatial and temporal variability, there are distinct features and trends in ice characteristics. These characteristics are described in the following introduction.

Winter ice conditions are dominated by the presence of a broad flaw polynya or lead, comprised of open water and newly forming ice. This recurring feature often extends from Point Hope to Point Barrow with the widest extent occurring between Cape Lisburne and Point Lay.

The flaw polynyas and leads are bounded towards shore by a variable zone of fast ice and seaward by moving pack ice, with a mixture of ice ages. Figure 2 is a NOAA satellite image showing four zones characteristic of the Chukchi Sea winter ice cover:

- Fast ice bridging across deep water in Peard Bay and extending seaward over the shoal area northwest of Icy Cape. Fast ice in the Chukchi Sea often forms large, unstable extensions subject to unpredictable break-up (see Section 5.0).

- New ice and open water in recurring polynya areas northeast of Cape Lisburne and south of Point Hope and along the fast ice edge as far as Point Barrow. This zone persists throughout the winter (see Section 6.0).

- Predominantly first-year pack ice south of 71° latitude. Thicker floes (white in tone) are interspersed with new and young ice areas (darker tones). Trace to moderate concentrations of multi-year ice are often found south as far as Cape Lisburne.

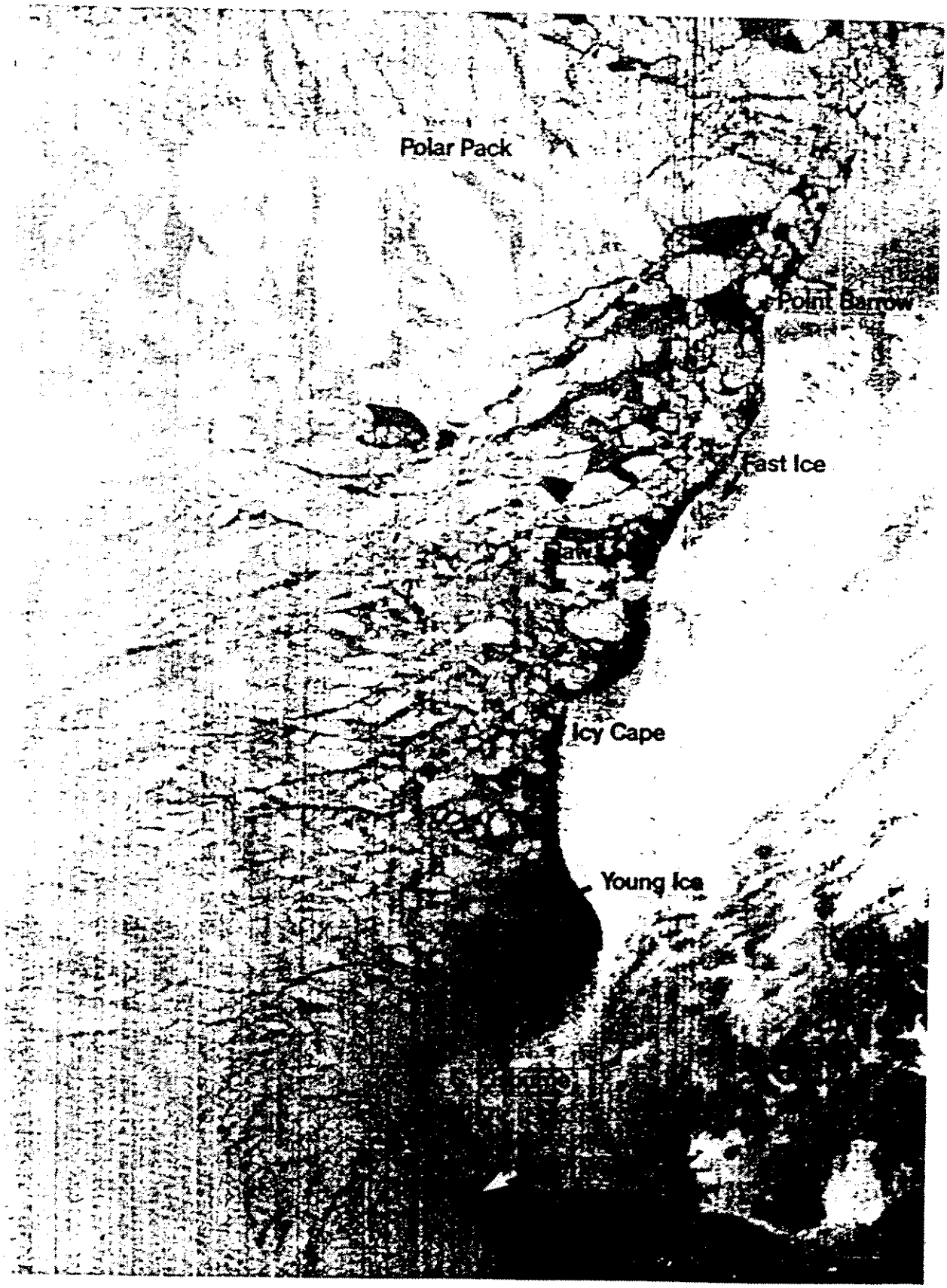

Figure 2 Chukchi Sea Winter Ice Zones: NOAA Satellite Image, 23 December 1974

- Polar pack consisting of predominantly multi-year ice. The region shown here is an approximate location inferred from November 25 imagery. The location of the polar pack edge in the Chukchi Sea is highly variable.

Winter ice motion in the Chukchi Sea is dominated by wind and current-driven forces. Along the Chukchi coast from Cape Lisburne to Point Barrow, winter winds blow from the east and northeast over half of the time (Brower et al., 1977) . These winds maintain the pack ice away from the coast and cause ice drift in a general southwesterly direction against the northern water flow. Winter ice speeds measured from satellite buoy records and satellite imagery, for the period 1974 to 1983, averaged between 0.2 and 0.4 knots. Peak velocities exceeded 3 knots (Thorndike and Cheung, 1977; Murphy et al., 1982). The maximum winter ice velocities measured in the Chukchi Sea are over double those commonly used for design purposes in the Beaufort Sea (average 0.1 knots, maximum 1.2 knots - In Marcellus and Morrison (1982) derived from Gulf Canada Resources Ltd. buoy data).

The predominantly first-year pack ice zone, which covers the largest portion of the lease area, is highly variable in terms of ice age and roughness. Unlike the Alaskan Beaufort Sea ice cover, which moves slowly from January to March, the Chukchi Sea ice cover displays a high degree of mobility throughout the mid-winter period. Pressure ridges, rafting, and rubble formation occur during episodes of rapid wind driven ice motion. The resulting surface roughness is extremely difficult to categorize simply in terms of ridging statistics. For example, in March 1981 the pack ice cover north of Cape Lisburne was described as heavy rubble, 4.5 ft thick level ice floes, and ridges up to 12 ft high, interspersed with young ice, cracks, and refrozen leads (Voelker et al., 1981b). Figure 3 is an illustration of typical Chukchi Sea pack ice appearance looking aft from the *Polar Sea* conning station in early February 1981.

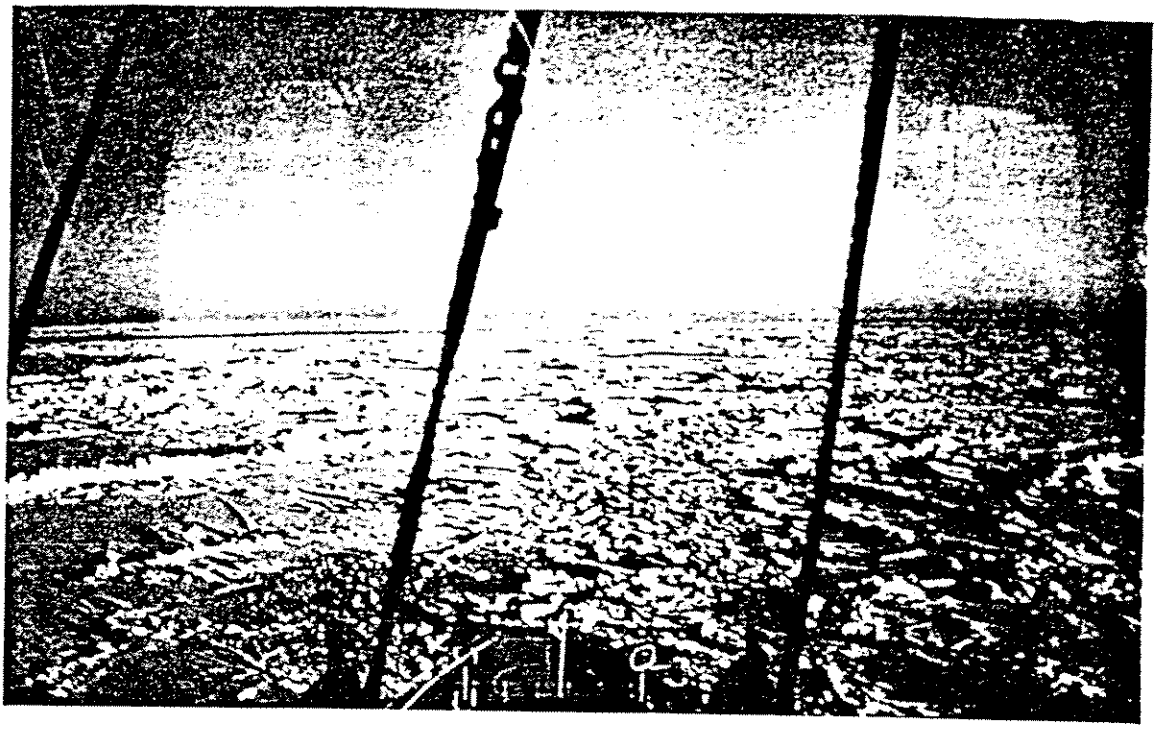

Figure 3 **North Chukchi Sea Pack Ice Viewed from the *Polar Star*, February 1981 (Voelker et al., 1981b)**

Accurate estimates of level first-year ice thickness offshore are extremely difficult to predict. Variables of ice motion, climate, and the different proportions of first-year ice ages combine to create a wide range in possible level ice thickness. In practice, thick level first-year ice is a rare commodity in the Chukchi Sea, as evidenced by the Maritime Administration's needs to send the *Polar Sea* to Antarctica to find enough level ice to conduct performance trials (Siebold, 1985).

Deformed ice predominates over level ice. Most level ice areas which do exist consist of young to medium (less than 4 ft thick) ice which has developed under relatively calm conditions. Before this ice reaches the thick first-year category a storm event will often cause an episode of ice deformation which transforms large areas of level ice into rubble, rafting, or ridges. Maximum and average offshore first-year ice thickness values for the Chukchi Sea are presented in Appendix A.

The patterns of pack ice decay in the summer and ice motion in the winter are strongly influenced by the circulation of relatively warm water flowing north from the Bering Sea. Figure 4 shows the general bathymetry of the Chukchi Sea area (Paquette and Bourke, 1981). The arrows suggest channeling of the northward flow through the various troughs and canyons (Paquette and Bourke, 1981). The Alaskan Coastal Current is of particular importance to ice conditions in the lease sale area. This current originates from a branching of the main flow off Point Hope. The coastal current follows along the 20 fathom (37 m) isobath north of Cape Lisburne and then branches into two main streams; one flows north and the other increases in velocity as the water is channeled into the narrow Barrow Canyon (Paquette and Bourke, 1981).

There are significant uncertainties regarding the Chukchi Sea water circulation regime. Russian scientists have reported average current speeds of 1.5 ft/second during summer and 0.3 ft/second during winter (Wilson et al., 1982). Current reversals along the coast are often associated with northeasterly winds. Observations in the fall of 1970 indicated that the expected northeasterly current set only occurred when winds were weak and variable.

Outside of the Alaskan Coastal Current, a significant southwesterly current has been observed off Point Franklin (Wilson et al., 1982). This observation agrees with the depiction of a counter clockwise current eddy shown encircling a broad mound in the sea floor north of Wainwright.

Another eddy is identified over the broad flat shelf in Ledyard Bay, with weak, wind driven southwesterly currents inshore circling to join the stronger Alaskan Coastal Current at about the 22 fathom (40 m) depth (Potocsky, 1975). General circulation maps also indicate southerly, water mass generated surface flow in the vicinity of 72°N, 166°W (Wilson et al., 1982).

A stagnant area of minimal circulation exists in the vicinity of 71°N, 164-166°W; this area corresponds roughly to where a broad band of southeasterly flowing Arctic Ocean water meets the northerly Bering Sea flow (Coachman et al., 1975).

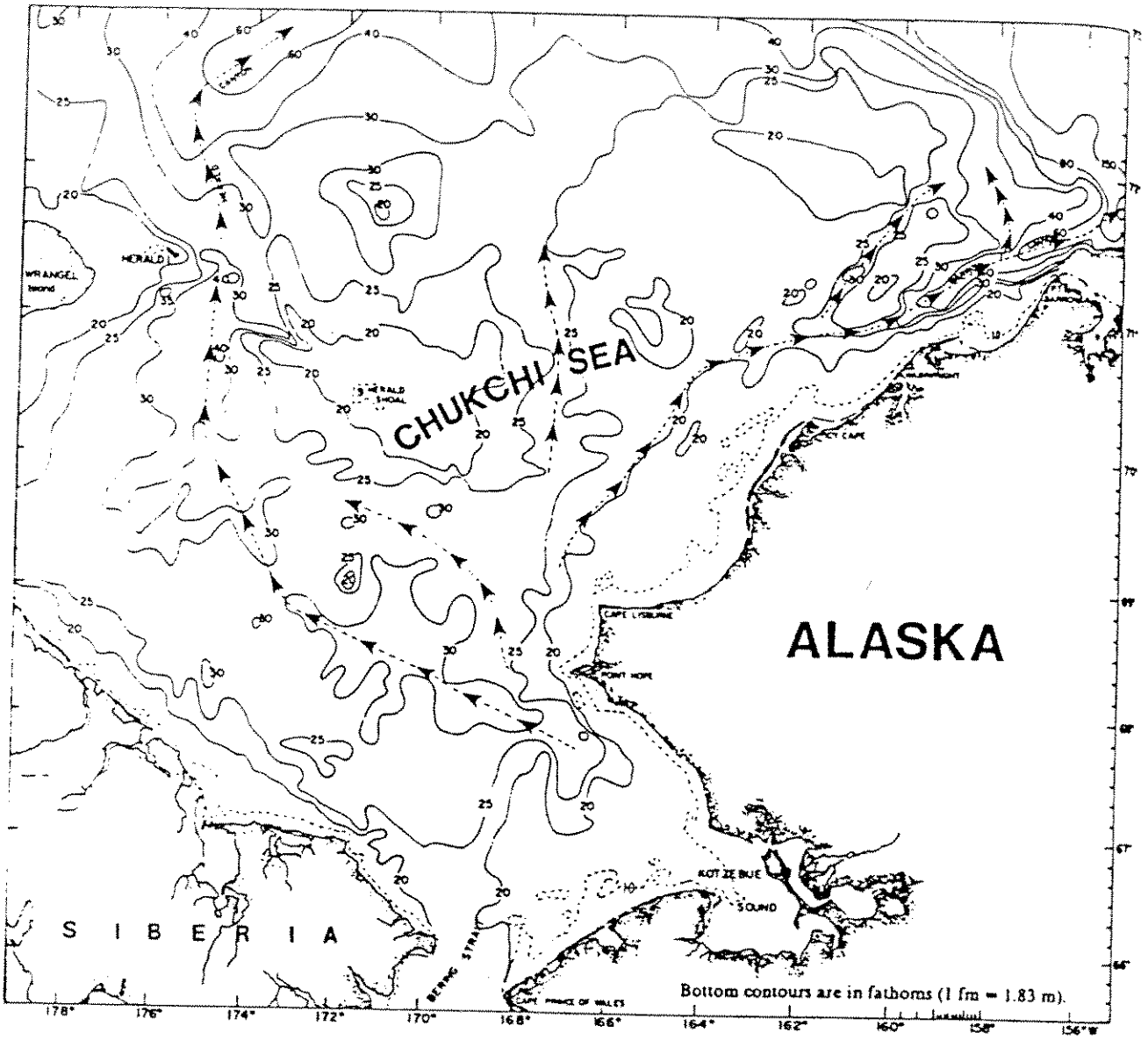

Figure 4 Chukchi Sea Bathymetry (Bourke, 1983)

During periods of light winds, ice motion is largely controlled by the prevailing currents. In the spring, warm water flowing north into the Chukchi Sea begins to affect both the decay and movement of the ice. Assisted by offshore winds, the warm surface water influx from the Bering Sea, supplemented by the Yukon River discharge, rapidly erodes the first-year pack ice within the area of influence of the Alaskan Coastal Current.

Figures 5 and 6 are satellite images showing how wind and warm water influx can combine to accelerate the clearing of ice in the Point Hope to Point Barrow area as early as mid-May. Clearing of nearshore areas in the north Chukchi Sea often occurs over a month in advance of the central or more southerly offshore areas.

As the ice edge progressively retreats to the north, a series of recurring bays in the ice margin develop in association with the bathymetric steering of the warm Bering Sea waters (Paquette and Bourke, 1981). This phenomenon is mapped and discussed in more detail in Section 3.2.

The maximum ice retreat in the Chukchi Sea occurs in late September, when the median edge of close pack ice (5/10) recedes to near 73° north latitude. In extreme summers, this ice edge can remain close to shore and as far south as 69°, or retreat beyond the continental shelf margin at 75° north latitude (Webster, 1982). See Section 3.1 for maps of average ice edge retreat.

The past two years, 1990 and 1989, are representative of very moderate open water seasons. For instance, at 71° latitude the open water season was 16 weeks in 1989. In a severe summer, the open water season may be as short as 3 weeks.

Freeze-up begins along shore at Point Barrow in early October and progresses south to Cape Lisburne by late October. The offshore ice cover takes longer to consolidate. Average ice concentrations in the lease sale area reach 8/10 as far south as 70° latitude by early November, and as far as the southern lease sale boundary by late November (Potocsky, 1975) .

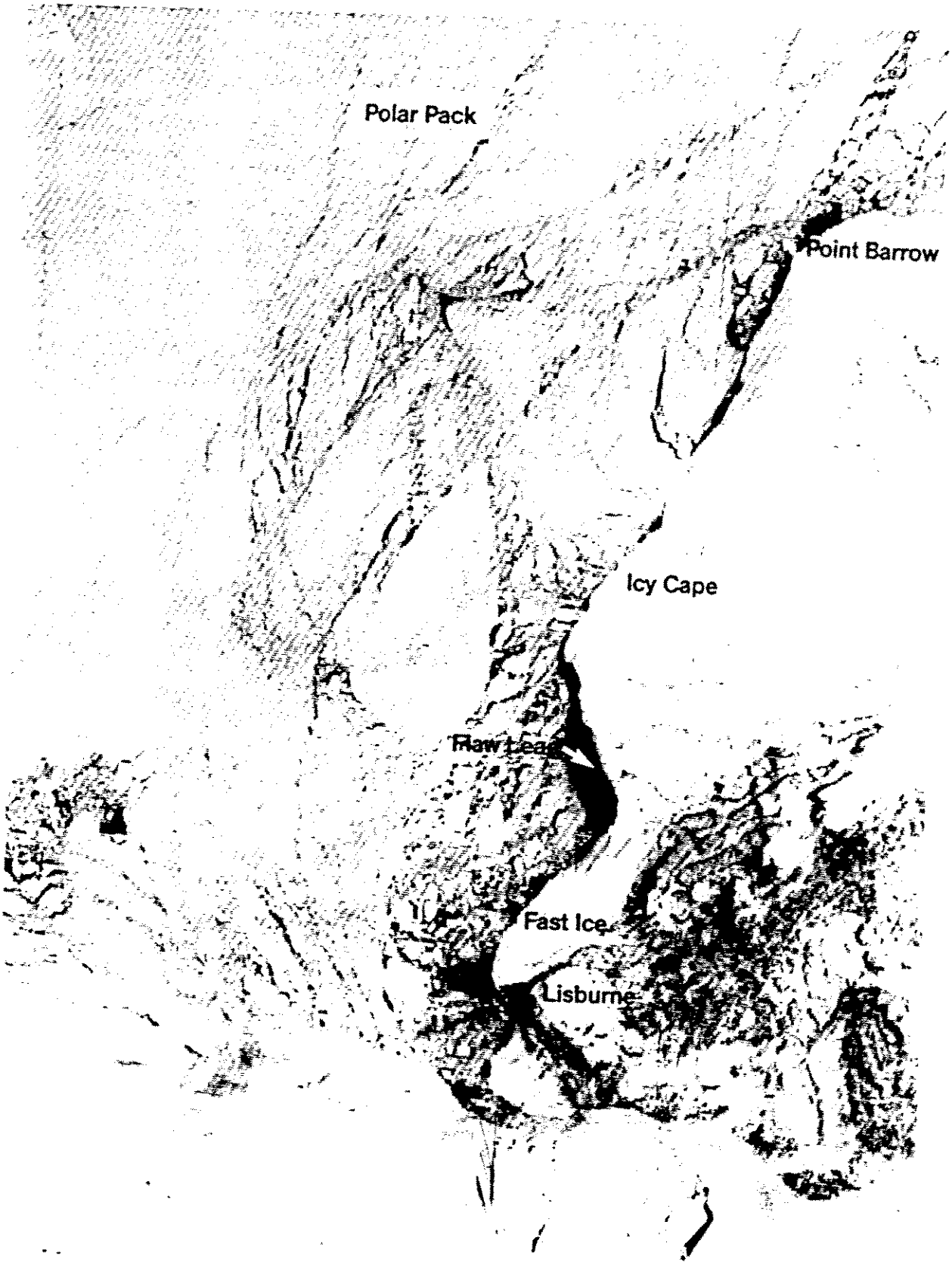

Figure 5 NOAA Satellite Image of the Chukchi Sea, 2 May 1978

Figure 6 DMSP Satellite Image Showing Early Ice Clearing, 17 May 1978 (compare with Figure 5)

There is a considerable north/south variation in the number of weeks of open water within the lease sale area. Values range from 20 weeks in the vicinity of Cape Lisburne to less than 4 weeks north of 72° latitude. Contours of open water weeks are mapped in Section 3.3.

In summary, the Chukchi Sea ice environment is highly mobile year round and is characterized by sudden, short term changes in ice deformation and concentration. Winds and currents play a major role in maintaining recurring polynyas and leads throughout the winter and in controlling the retreat and advance of ice in the spring and fall. Ice conditions in the Chukchi Sea can be considered as a transition in severity between the marginal ice zone of the Bering Sea and the arctic ocean environment of the Beaufort Sea. The following sections discuss the important ice characteristics in more detail.

3.0 PATTERNS OF ICE RETREAT AND ADVANCE

3.1 5/10 Total Ice Concentration Boundaries

Figures 7 and 8 show the locations of the median 5/10 ice concentration boundaries in the Chukchi Sea from June 15 to November 15. The boundaries are derived from 15 years of ice charts produced by the Canadian Atmospheric Environment Service (AES). The AES ice charts are based on satellite imagery and are produced every week for the summer months. The ice edges for June 15 and November 15 are derived from 13 years of ice charts as two years of ice charts are missing for these dates. For the year 1980, information on the ice edges west of 163°W is missing; 14 years of data are used to determine the median ice edges in these areas.

The weekly AES ice chart dates do not correspond exactly with the first and the fifteenth of each month; consequently, the closest available date is substituted. The error involved is plus or minus three days from the first or the fifteenth of each month.

The median boundary for the week of July 1 was difficult to plot because the ice boundaries were very random northwest of Cape Lisburne. This area corresponds with the initial retreat of the ice north into the lease sale area.

The same generic term "ice edge" is often used to denote the boundaries of 1/10 ice (essentially separating open water from any ice), 5/10 ice (marking the beginnings of closer pack ice), or polar pack ice (an area of predominantly multi-year ice). In terms of marine operations, these three ice conditions represent very different degrees of difficulty. The critical location of predominantly multi-year ice is discussed in Section 4.1. This section is concerned solely with the location of the 5/10 <u>total</u> ice (first-year and multi-year ice) concentration boundary which marks the effective northerly limit for unassisted, non-ice strengthened vessel operation.

There is little practical difference between the 1/10 and 5/10 ice boundary locations during freeze-up when ice concentrations are increasing rapidly, During the summer period, however, the Chukchi Sea ice edge can be diffused

by wind and currents, leaving broad bands of loose floes in the marginal ice zone. The distance between the median 1/10 and 5/10 ice concentration boundaries can then be as great as a degree of latitude (60 nmi).

3.1.1 Ice Retreat

Figure 7 indicates that the 5/10 ice edge in the Chukchi Sea begins to retreat north in the lease sale area beginning in early July. The maximum northerly retreat occurs in late September. Coastal areas north of Cape Lisburne can be clear of ice by mid-May in favorable years, over a month in advance of Kotzebue Sound or the central Chukchi Sea (see Figure 6).

The 15 August 5/10 ice boundary shows a wave-like configuration with shallow embayments in the ice edge (Figure 7). These embayments are considered directly related to bathymetric steering of warm Bering Sea waters (see Section 3.2 for a more detailed discussion).

3.1.2 Ice Advance

Figure 8 shows the southerly advance of new ice, beginning with freeze-up in early October in the most northerly lease sale areas. Freeze-up tends to proceed along an advancing northwest/southeast oriented front. Coastal areas are first to have complete ice cover. The extreme western areas of the lease sale are often not completely ice covered until mid-November. The influence of warm, northward flowing Bering Sea surface waters is probably an important factor in modifying freeze-up patterns and rates.

New ice is susceptible to rapid break-up and dispersal by wind action. Strong winds predominate from a northwesterly or easterly direction during October and November, and tend to disperse the newly forming ice to the southwest, away from the area of maximum ice production.

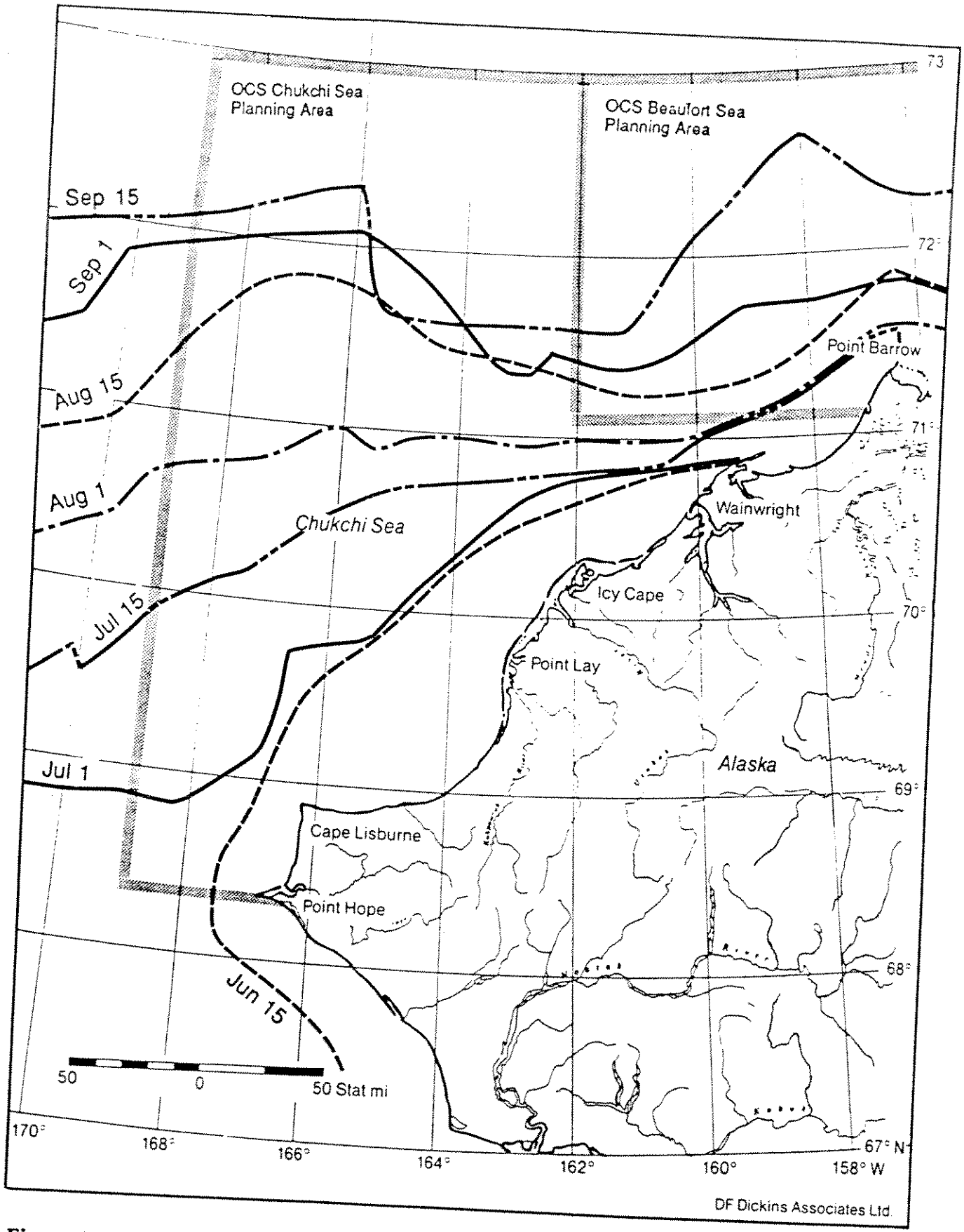

Figure 7 **Retreat of the Median 5/10 Ice Concentration Boundary**

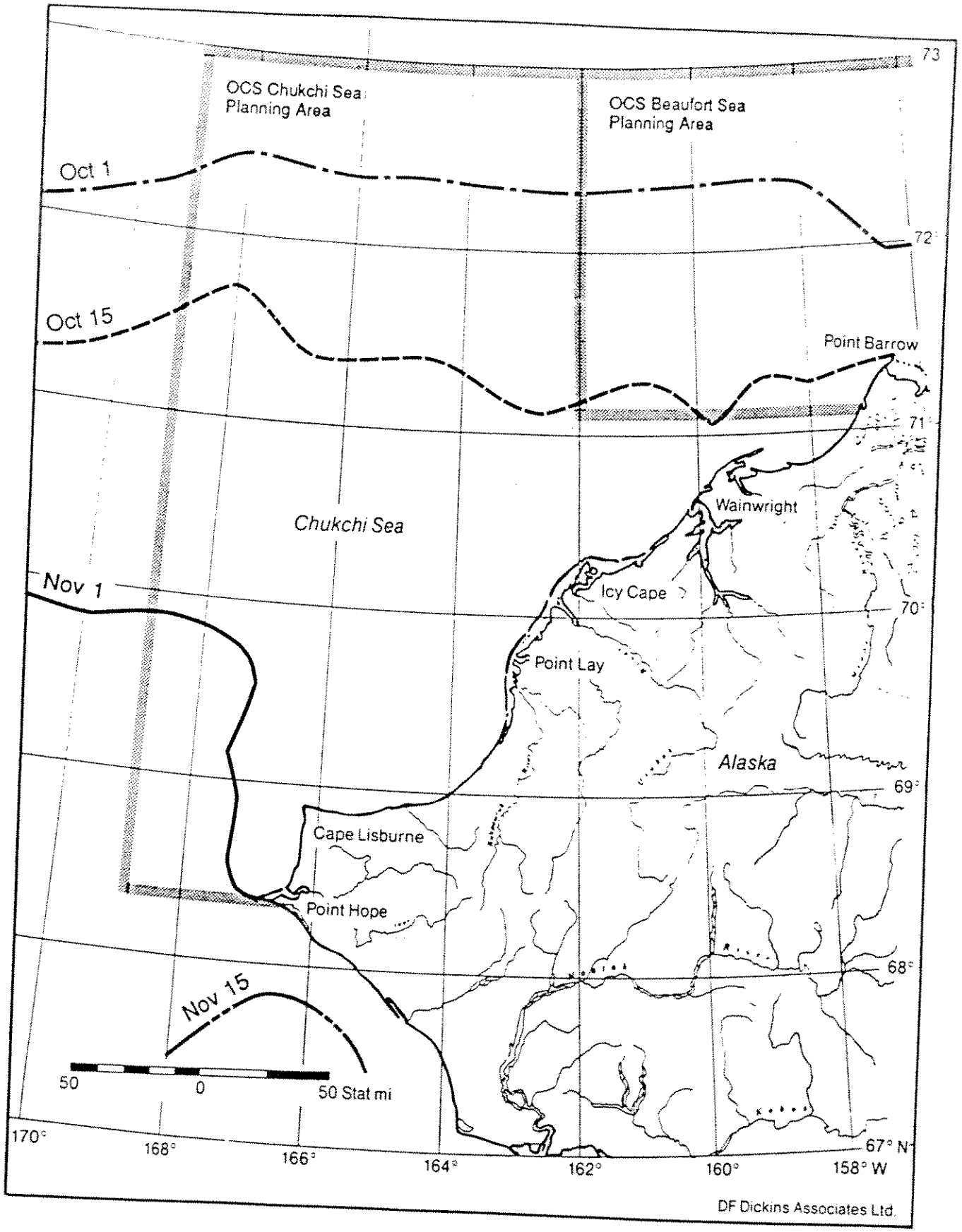

Figure 8 **Advance of the Median 5/10 Ice Concentration Boundary**

3.2 Ice Embayments During Summer Retreat

Ice melt-back in the Chukchi Sea is characterized by a series of recurring bays in the ice margin. These bays are associated with bathymetric troughs which steer the warm, northward flowing currents from the Bering Sea to create preferential melting of the ice edge (Paquette and Bourke, 1981 ; Bourke, 1983). Four major melt-back features were identified in previous studies, a large bay at 170° to 175°W, another bay at 167° to 168°W, the shore lead along the coast from Cape Lisburne to Point Barrow, and a small bay northwest of Point Barrow (Paquette and Bourke, 1981). Most of the lease sale area lies between the bay at 170°W and the bay northwest of Point Barrow.

Figure 9 maps the typical configuration of the melt-back bays within the lease sale area. The ice edge positions were mapped from cruises in the Chukchi Sea in late July-August 1977 and 1978 (Bourke, 1983). A satellite image from June 29, 1979 (Figure 10) shows that the characteristic melt-back features were already well developed early in the season for that year. The melt-back features have even been observed in such extreme ice years as 1975 when the ice pressure from the north might be expected to overwhelm the oceanographic influences.

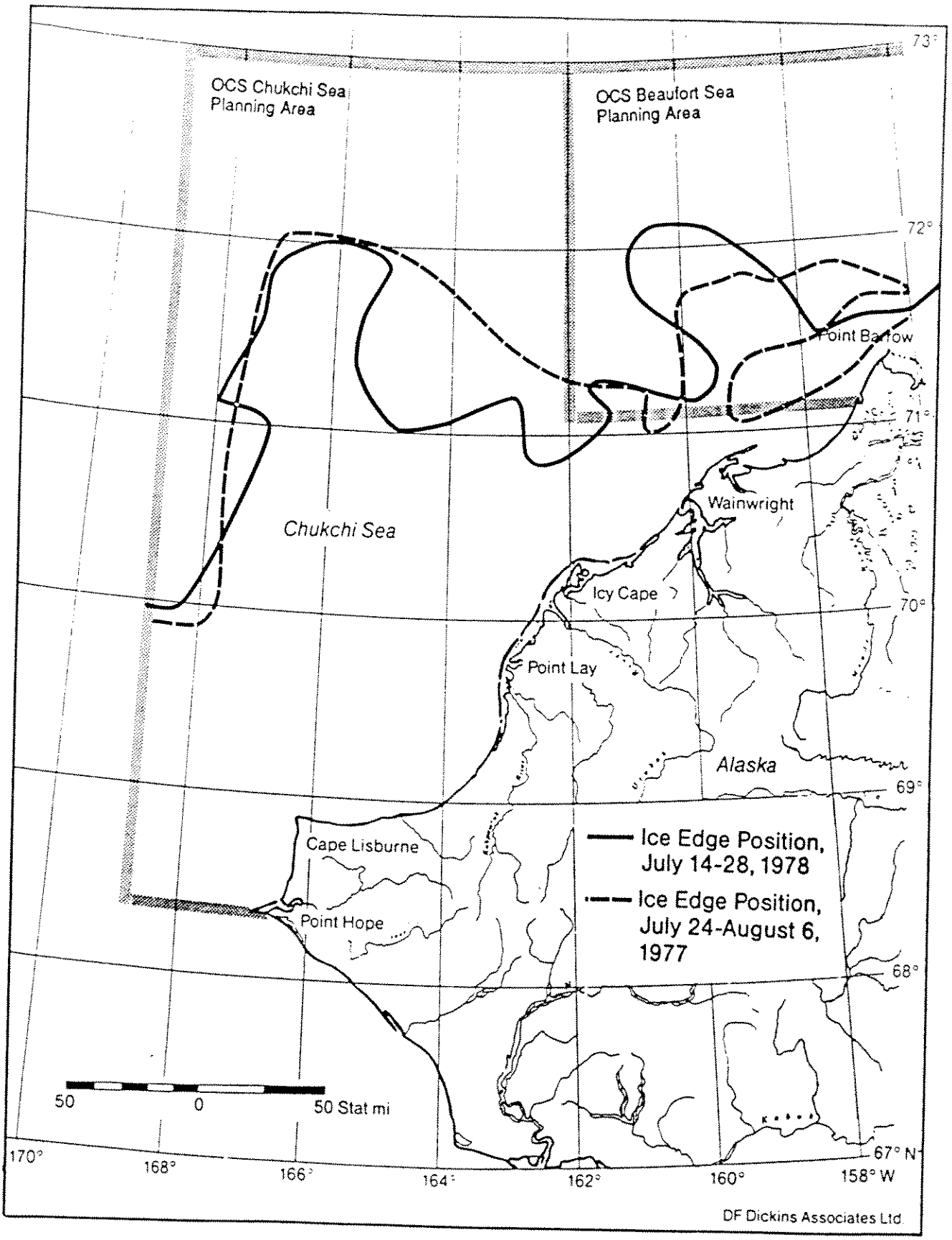

Figure 9 Configuration of Recurring Embayments in the Retreating Ice Edge (Bourke, 1983)

Figure 10 DMSP Satellite Image Showing an Early Example of Ice Edge Embayments, 29 June 1979

3.3 Open Water Season

The annual number of weeks of open water within the lease sale area were determined for the following criteria:

1. Average total ice concentrations less than 3/10 (Figure 11).

2. Average total ice concentrations less than 6/10 (Figure 12).

3. Average total ice concentrations less than 8/10 (Figure 13).

4. 20% probability of total ice concentrations less than 6/10 (Figure 14).

5. 80% probability of total ice concentrations less than 6/10 (Figure 15).

The number of weeks of open water does not merely represent the time span from break-up to freeze-up, but represents the net open water season. Summer intrusions of ice in concentrations greater than the specified criteria were subtracted from the total open water season for each case. Ice intrusions are discussed separately in Section 3.4. The open water season contours are based on six years of Canadian ice chart information, 1978 to 1979 and 1981 to 1984. The ice charts missed break-up and freeze-up prior to 1978, and in 1980 they did not cover the Chukchi Sea.

Figures 11 to 13 show the average, annual open water season decreasing from 22 to 20 weeks offshore of Point Hope to less than 3 or 2 weeks at 73°N. Note that changing the criteria for defining open water conditions from <3/10 to <6/10 and to <8/10 only extends the length of the average, annual open water season by 1 to 2 weeks at any location.

The length of the open water season is highly variable in the Chukchi Sea. For example, at 71°N there was a 3 week season in 1983 and a 16 week season in 1984. The dramatic differences in the open water season are apparent in Figures 14 and 15 which show the number of weeks of open water at 20% and 80% probability levels for ice concentrations <6/10, respectively. The open water season decreases from 23 weeks (20% probability - Figure 14) to 18 weeks

(80% probability - Figure 15) offshore of Point Hope. North of 71°N, the open water season decreases from 14 weeks (20% probability) to 6 or 7 weeks (80% probability).

The length of the open water season is the most variable and uncertain between Wainwright and Point Barrow. Note the steep gradient in Figure 15 of the weeks with an 80% probability of ≤ 6/10 ice: 11 weeks at Wainwright reduces to 2 weeks at Point Barrow.

Figure 14 is representative of the open water season of the past two years: 16 weeks of open water in 1989 at 71°N and 17 weeks in 1990. 1989 and 1990 represent one end of the spectrum of variability in the open water season.

The shape of the contours in Figures 11 to 15 reflects the melt-back bays in the ice margin that occur during August (Section 3.2). The shore lead that opens in May between Cape Lisburne and Point Lay is also apparent in the contours; however the narrow flaw lead north of Point Lay and the flaw polynya east of Point Hope (outside the lease sale area) are not as well defined. More detailed ice data is required to map local ice features.

The close spacing of the contours north of 70°30' (Wainwright) reflects the influence of the polar pack position in limiting the open water season within the northern portion of the lease sale area (see Section 4.1). This is especially pronounced in Figure 15 (80% probability of ice concentrations <6/10).

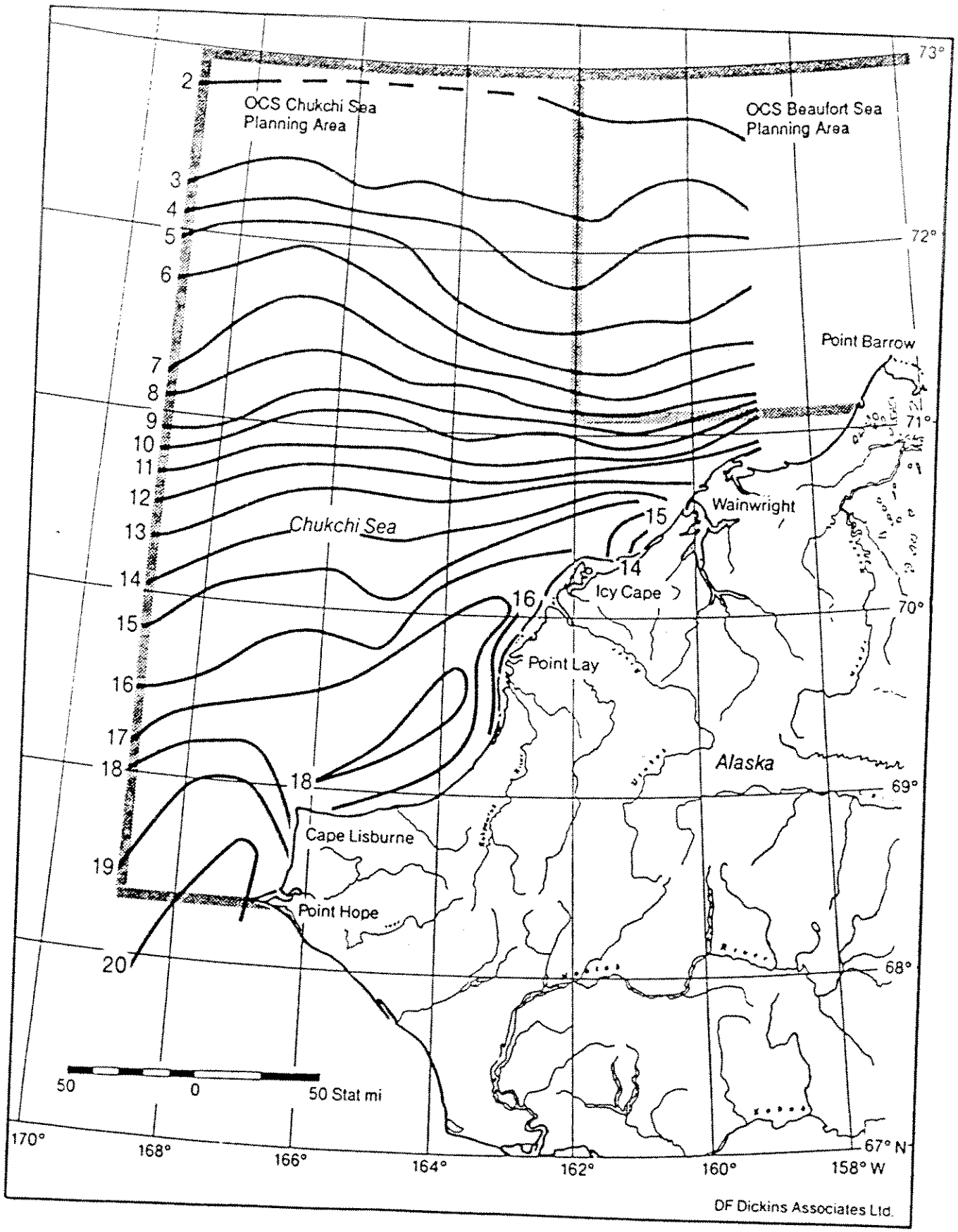

Figure 11 **Average Number of Weeks with Ice Concentrations Less Than 3/10**

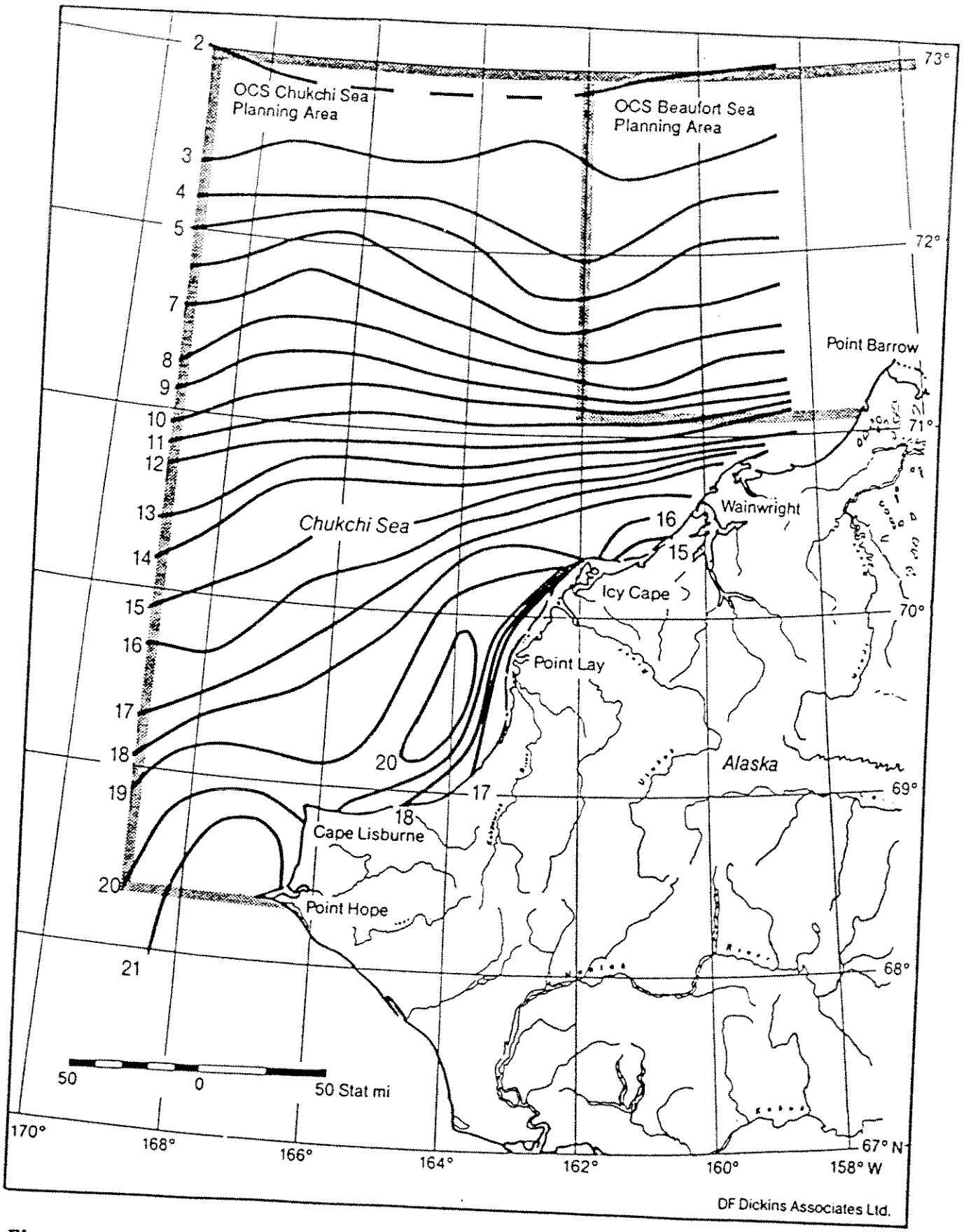

Figure 12 **Average Number of Weeks with Ice Concentrations Less Than 6/10**

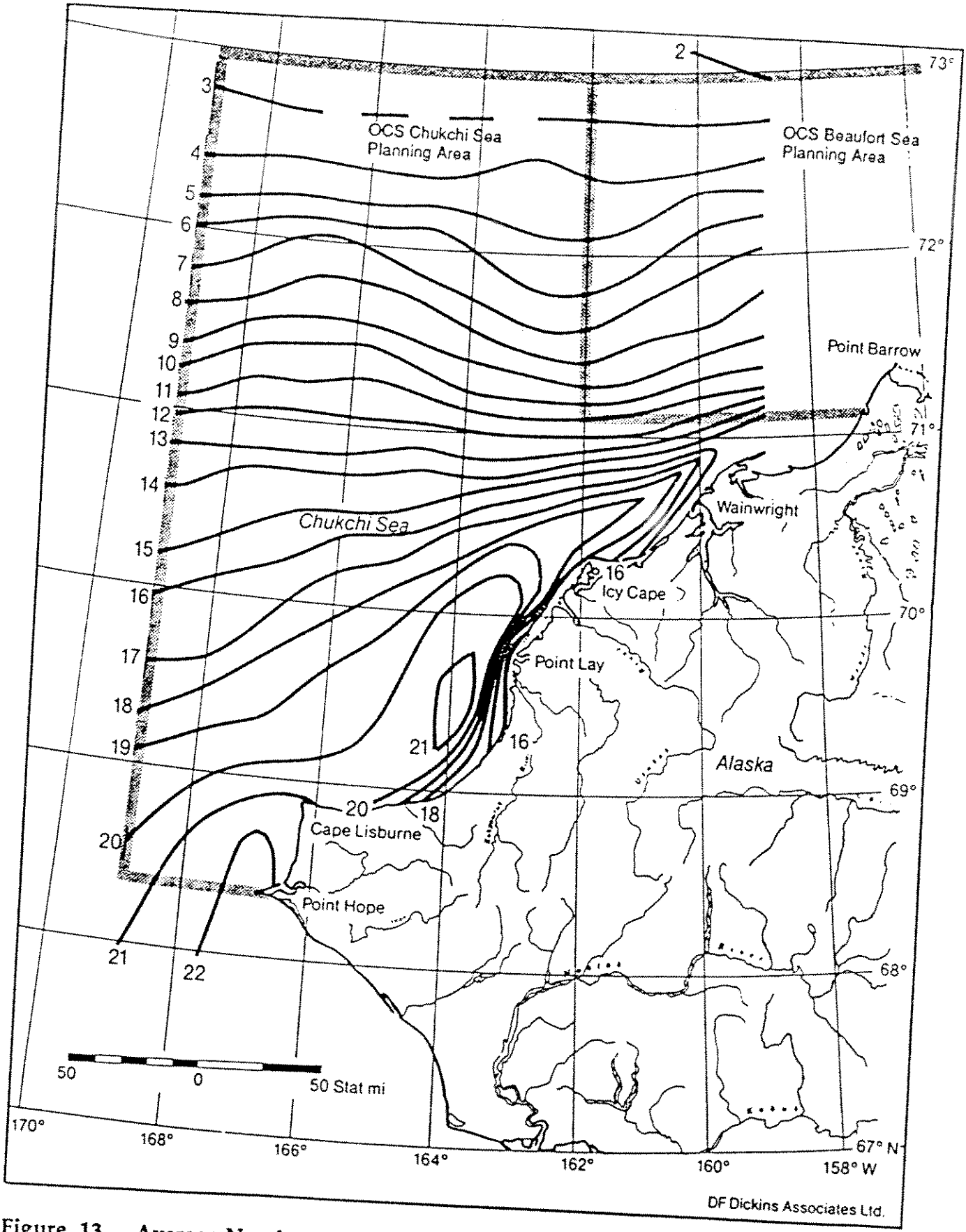

Figure 13 **Average Number of Weeks with Ice Concentrations Less Than 8/10**

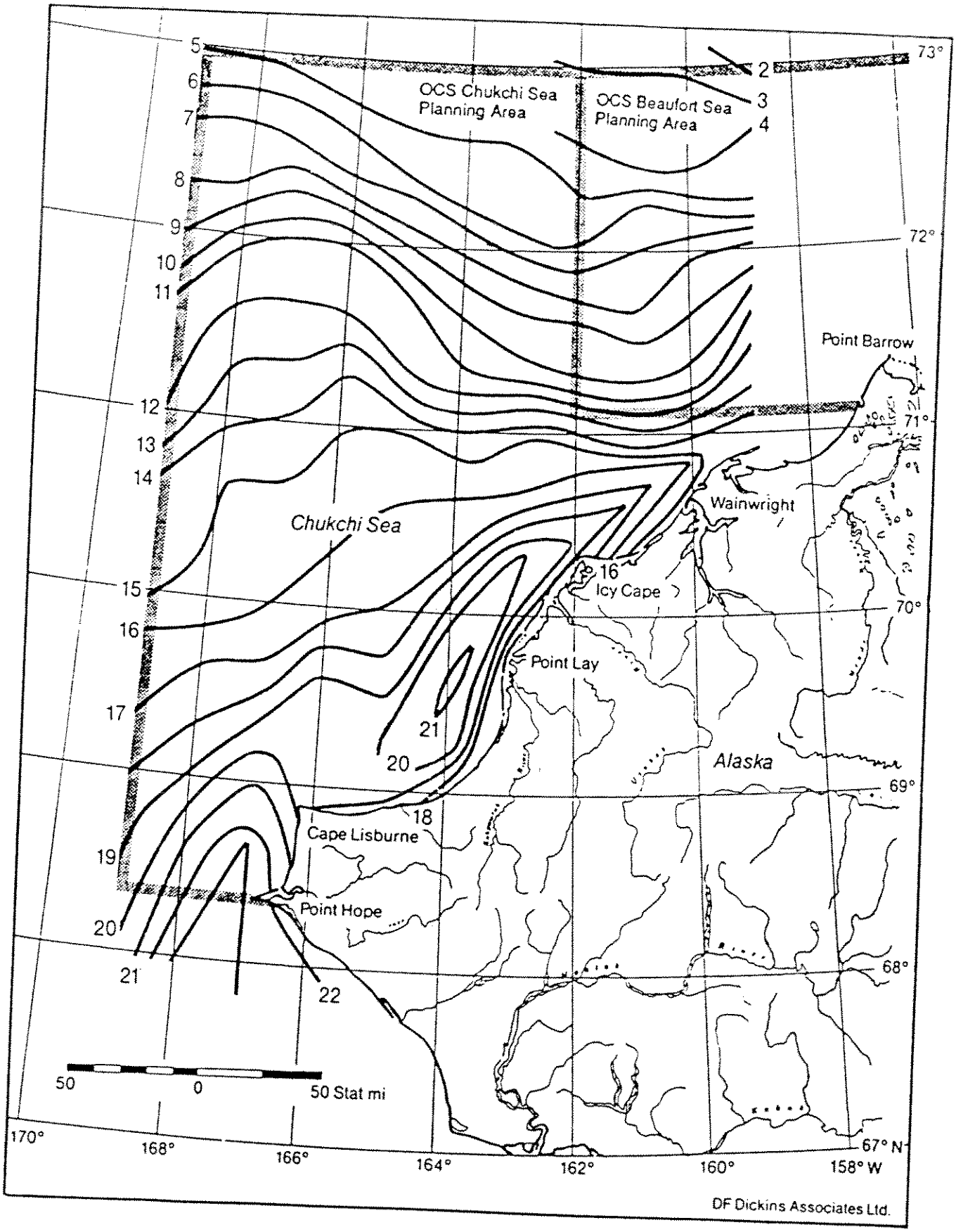

Figure 14 Number of Weeks with a 20% Probability of Ice Concentrations Less Than 6/10 (representative of a moderate open water season)

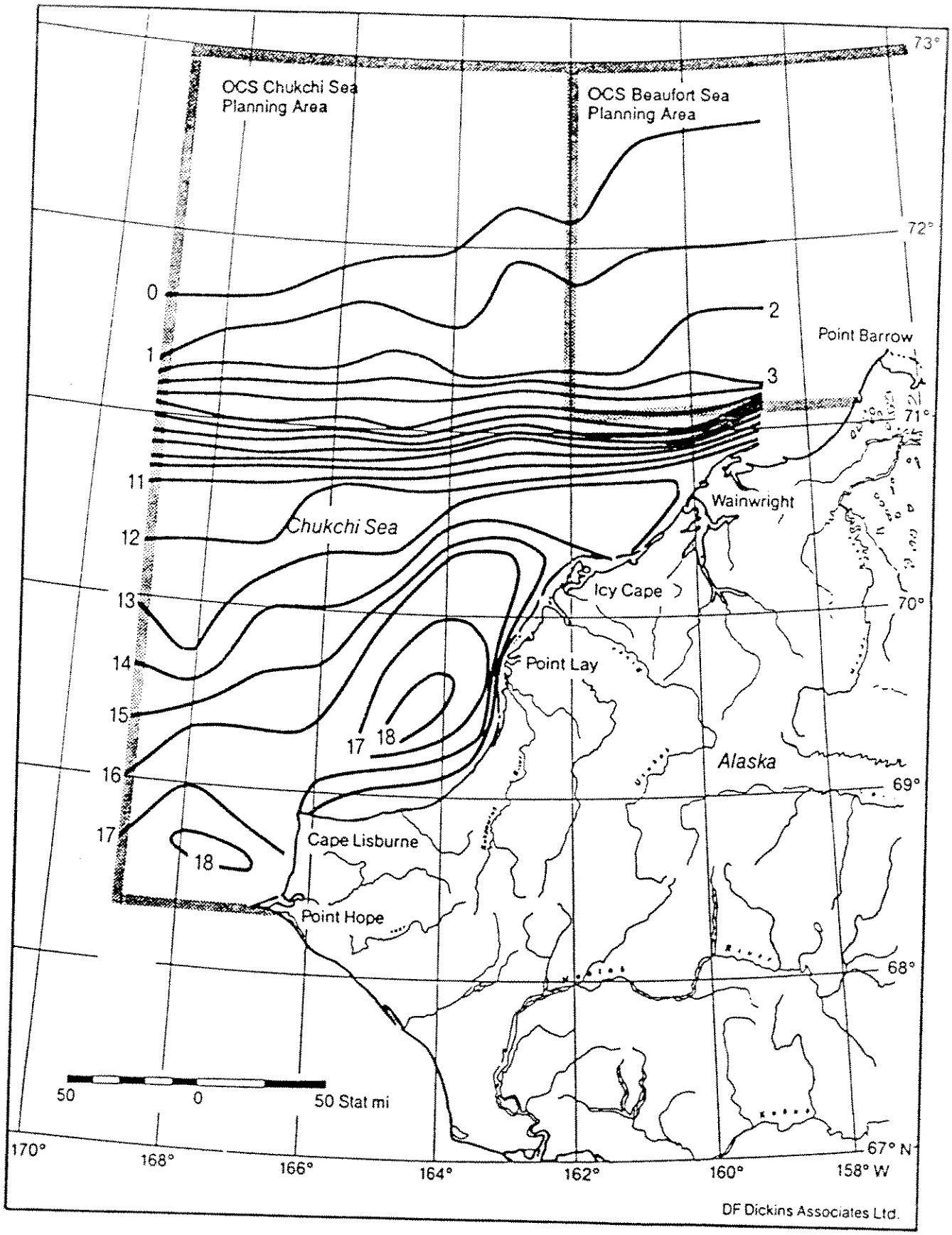

Figure 15 **Number of Weeks with an 80% Probability of Ice Concentrations Less Than 6/10 (representative of a severe open water season)**

3.4 Summer Ice Intrusions

This section presents the probability of ice intrusions in the Chukchi Sea, and the probability of encountering multi-year ice during the intrusions. Ice intrusions occur when the polar pack or remaining seasonal pack ice moves into an ice-free area and then recedes again.

In this section, intrusions are defined as periods of ice concentration greater than or equal to 3/10 that occur between break-up and freeze-up. Break-up is considered complete when the ice concentration drops to 3/10 or less; freeze-up is classed as when the ice concentration reaches and remains at 7/10 or more.

Ice intrusions have been analyzed by latitude. As shown in Figures 7 and 8, the retreat and advance of the ice edge is roughly parallel to lines of latitude. To compile the ice intrusion data a grid point was selected on each line of latitude. The longitude of the point was chosen to correspond to longitudes typical of exploration drilling sites. The exact location of the grid points is given below.

Latitude	Longitude
68°	168°
69°	168°
70°	164°30'
71°	164°
72°	166°

The data presented in Figures 16 and 17 was compiled from 14 years of data (1975-1979, 1981-1989) derived from weekly Canadian ice charts (AES).

Figure 16 shows the cumulative probability of ice intrusions as a function of latitude. It appears from Figure 16 that north of 69° the probable number of weeks of ice intrusions is independent of the latitude. However, as Table 2 shows, the time available for intrusions between break-up and freeze-up decreases with latitude. Even though the probability of 2 weeks or less of intrusions is 70% at 72°N and 80% at 68°N, the median open water season at

72°N is 8.5 weeks compared to 19 weeks at 68°N. At higher latitudes, a much greater portion of the open water season is affected or lost due to ice intrusions.

Table 2 Weeks Available for Ice Intrusions to Occur

Latitude	Minimum	Median	Maximum
68°N	17	19.0	≥24
69°N	13	18.0	≥25
70°N	12	17.5	≥23
71°N	3	14.5	18
72°N	0	8.5	14

Source: 14 years of Canadian ice charts

Figure 16 represents the probability of total weeks of ice intrusions. This means any combination of weeks adding up to the total. For instance an 80% probability of 3 weeks of intrusions could take the form of any number of intrusions which add up to 3 weeks (i.e., one 3 week intrusion or three 1 week intrusions). Intrusions were counted in units of integer weeks.

The strict definition of ice intrusions given above presents a conservative picture of the conditions in the southern Chukchi Sea. At 68°N, 10 of the 15 intrusions were caused by premature freeze-ups which left the area before the final freeze-up. The ice in these intrusions would consist mostly of young ice types (≤ 12 in.) and would present a much lower hazard than intrusions of thick first-year and multi-year ice.

The presence of multi-year ice in intrusions increases to the north. Concentrations of multi-year ice found in intrusions are presented by latitude in Figure 17. Multi-year ice was absent from intrusions at 68°N, while in the northern Chukchi Sea, multi-year ice was found in every intrusion at 72°N.

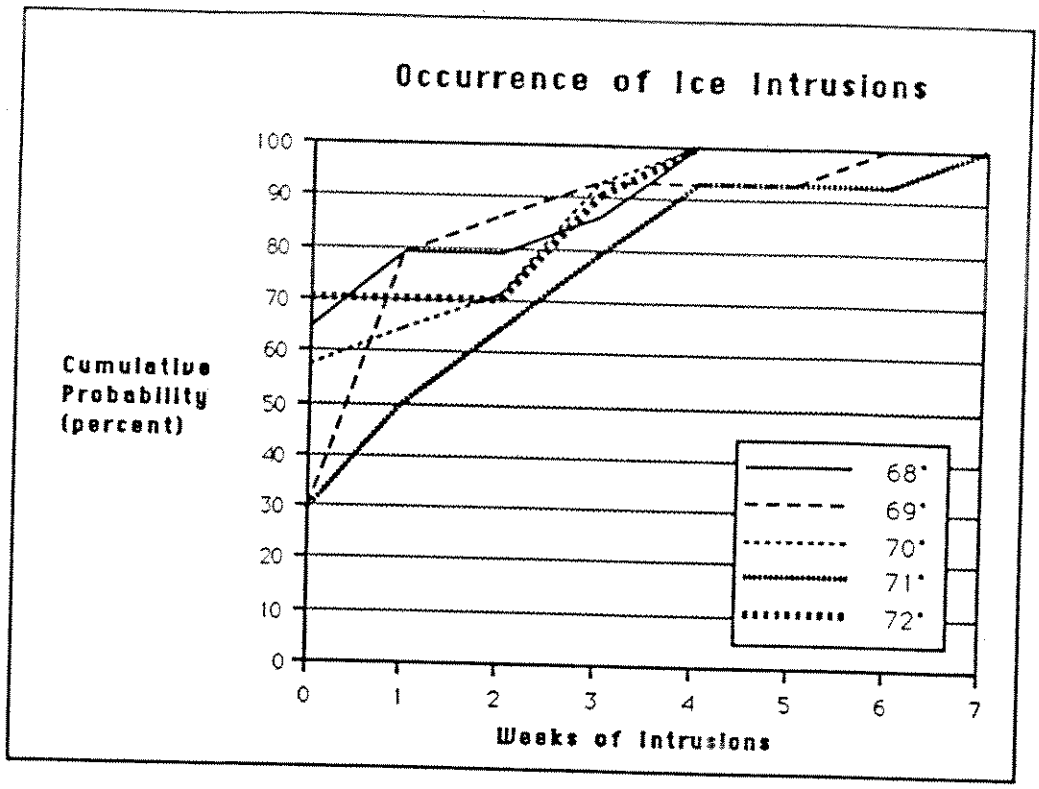

Figure 16 Occurrence of Ice Intrusions ≥ 3/10 in the Chukchi Sea

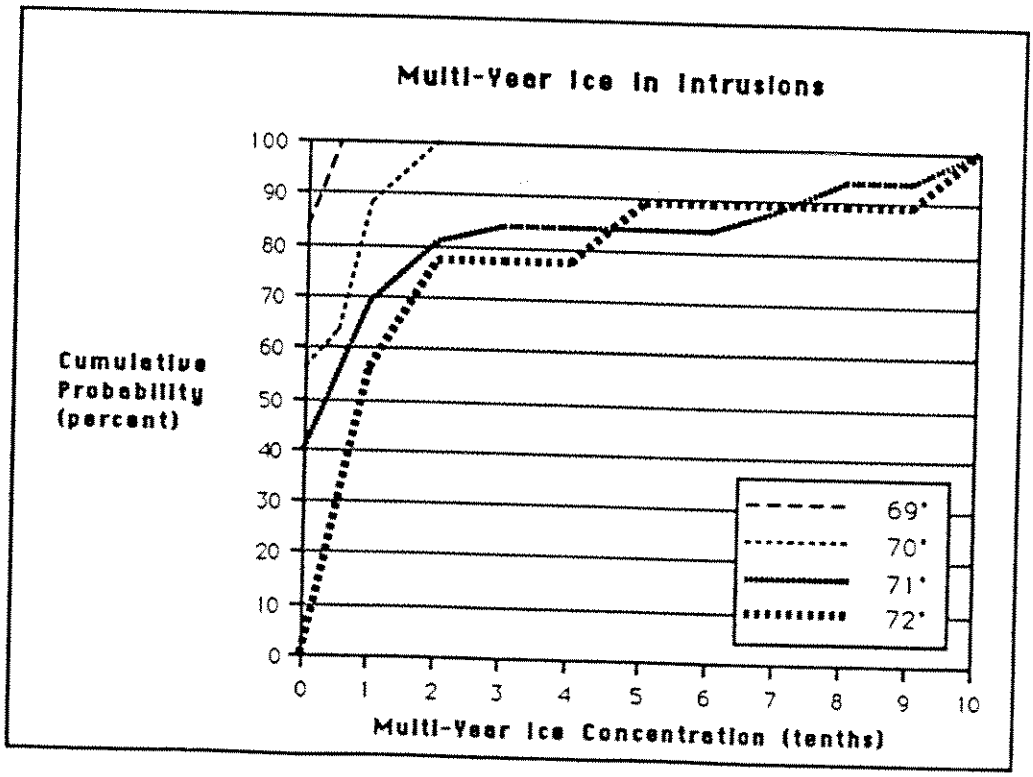

Figure 17 Presence of Multi-Year Ice in Intrusions

4.0 MULTI-YEAR ICE

4.1 Polar Pack Boundaries

The polar pack edge is defined as the boundary north of which multi-year ice concentrations are greater than or equal to 5/10.

The polar pack edges were mapped from the Canadian ice charts between 1975 and 1989. The ice charts were initially separated according to summer and winter edges. Summer was considered to extend from June to September, inclusive, and winter was considered to extend from October to May, inclusive (The winter data set is limited by the availablity of charts; prior to 1980, the Canadian ice observations extended from mid-June until the end of October.)

The most southerly extent of the polar pack was plotted for each season over the fifteen year period. To simplify the presentation, the extreme limits of the polar pack boundary are presented along with the median boundary. Refer to Appendix B for the presentation of all the plotted boundaries.

Figures 18 and 19 show that multi-year ice is a common feature in the Chukchi Sea north of 71°N. This is the annual southern limit of the summer polar pack edge in about 11 out of 15 years (Figure 18) . In extreme years, such as 1975 and 1976, the polar pack edge advanced as far south as 69°30' and inshore of the 17 fathom (31 m) water depth. In 1976 the pack edge remained south of 71°N throughout the entire summer.

There is no statistical evidence to support the widely accepted view that the polar pack advances south towards the coast in October, and continues to move south throughout the winter (e.g., Wilson et al., 1982). The plots of the polar pack edges shown in Appendix B indicate the considerable annual variability in the most southern locations of the polar pack edge. The polar pack edge tends to be located about 30 miles further south in the winter than in the summer according to the median ice edges shown in Figures 18 and 19. However, over fifteen years, the overall north/south range in the polar pack edges is about the same (73°N to 69°30'N), summer and winter.

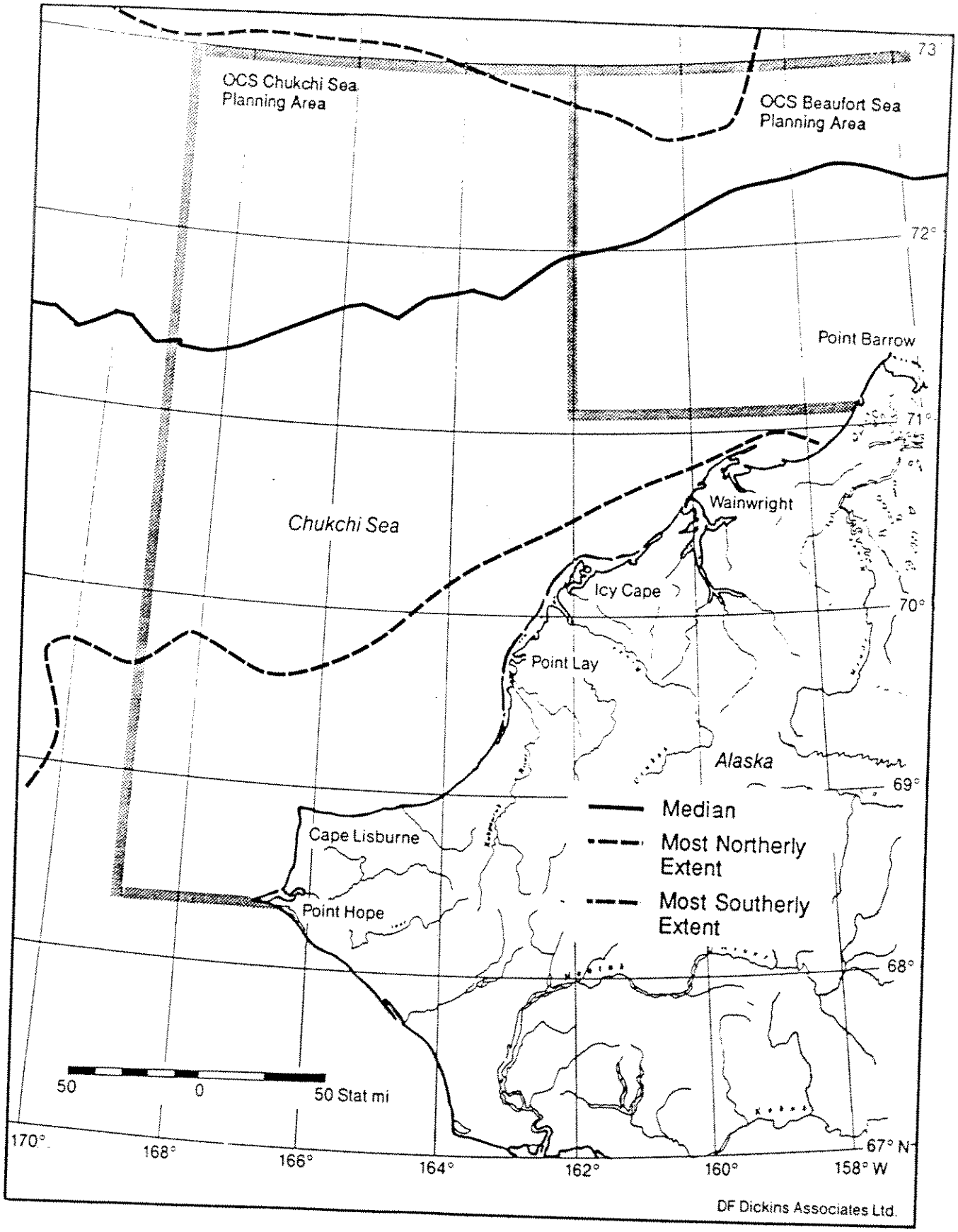

Figure 18 **Locations of the Most Southerly Annual Summer Polar Pack Edges (June to September, 1975-89)**

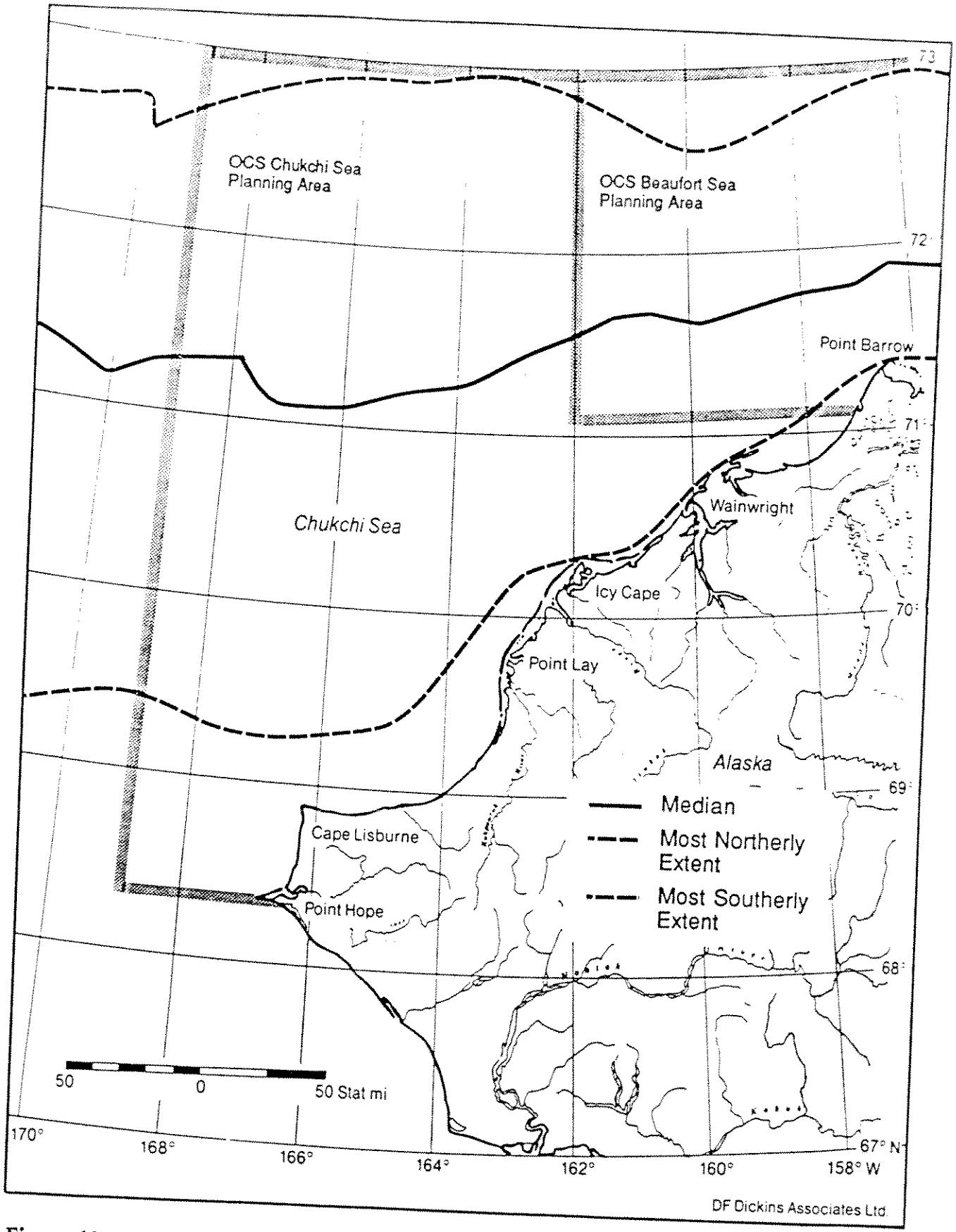

Figure 19 **Locations of the Most Southerly Annual Winter Polar Pack Edges (October to May, 1975-89)**

A survey of weekly polar pack edges between 1975 and 1989 confirms that there is no clear seasonal cycle of pack ice advance and retreat.

The extreme variability in polar pack locations, both from year to year, and within a given ice season, makes the definition of an average multi-year ice edge somewhat academic. Multi-year ice can occur within the lease sale area throughout the year, although concentrations of greater than 5/10 multi-year ice are not encountered south of 71°N more than 5 years in 14.

The occurrence of high multi-year ice concentrations is critical to tanker loading operations. The ice edge locations shown on the ice charts are based on large scale satellite imagery (NOAA imagery, original scale 1:7,000,000) . Identification of multi-year ice concentrations from satellite imagery is highly subjective (Intera, pers. comm.). The only time of year that the polar pack edge can be mapped with any certainty from satellite imagery is during the late summer or early fall.

Experience has shown that regional ice conditions interpreted from satellite imagery are often more severe than the actual ice condition at a specific location. Operating experience from the Canadian Beaufort Sea and from icebreaker voyages has confirmed this trend. Unfortunately, there is limited, publicly available field data to calibrate multi-year ice concentrations interpreted from satellite imagery (satellite imagery is used to prepare the ice charts). Lack of field data on multi-year ice concentrations is a continuing deficiency which affects long-term planning for Chukchi Sea development.

4.2 Multi-Year Floe Sizes

Public data on multi-year floe sizes is unavailable for most of the study area. One study by Weeks et al. (1977) used SLAR imagery to record multi-year floe sizes along a line northwest of Point Barrow (data replotted as Figure 20). The floe sizes in Figure 20 were assumed to have a circular shape. Mean diameters were grouped into 650 ft (200 m) bins.

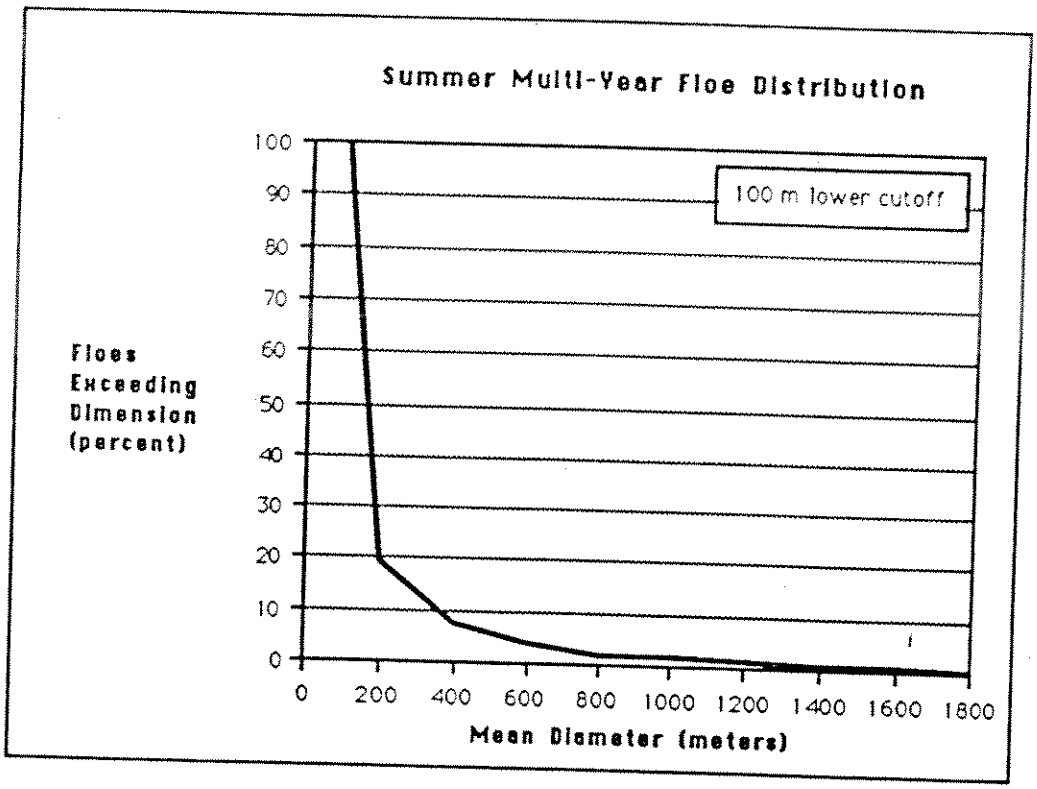

Figure 20 **Summer Multi-Year Floe Distribution for the North Chukchi Sea (Weeks et al., 1977)**

A second study measured the major and minor axes of 922 multi-year floes near the polar pack edge using aerial photo-stereo analysis (Gulf Canada, 1980), which has a higher degree of accuracy than other types of imagery such as Synthetic Aperture Radar (SAR). The photo-stereo information allowed the floes to be grouped into high, medium, and low freeboard categories. The percent exceedance versus the major axis dimension (floe length) is shown in Figure 21.

Despite the fact that the data was collected in the Canadian Beaufort Sea, it is considered reasonable to extrapolate this data to the Chukchi Sea. Multi-year ice in the northern region of the Chukchi Sea originates at the southern limits of the polar pack. Data from multi-year ice studies near the polar pack edge in the Beaufort Sea will be representative of the multi-year floe sizes likely to be encountered in the northern Chukchi Sea during the winter and early summer (mid to late summer floes will likely be reduced in size due to

dynamic interactions). Comparison of Figure 20 with the medium to high freeboard floes documented by Gulf (Figure 21) shows good agreement.

A third study analyzed multi-year floe dimensions for the Chukchi Sea based on SAR data acquired in February 1981 (Intera, 1982). Floes were counted in bins of 160 m with a lower cutoff of 91 m in the 0-160 m bin. Although less certain than aerial photography in identifying old ice, SAR offers the advantage of a wide swath which includes much larger floes than can be viewed in a single air photo strip. Figure 22 shows the floe distributions from the Intera data.

The data in the first two bins (91-320 m) was not included in Figure 22 because the number of floes reported below 320 m (17%) is unusually low. Researchers usually describe the distribution of floe sizes as either a power law or exponential function, both of which predict higher frequencies as floe sizes decrease. The apparent discrepancy in the Intera data (1982) may be caused by the resolution of the SAR imagery. SAR can have difficulty adequately differentiating small pieces of multi-year ice when the pieces are either surrounded by first-year rubble or so heavily deformed in their own right that they appear like first-year ice in the radar return.

To avoid presenting data which may be misleading, only data for floe sizes greater than 320 m were included in Figure 22.

Figures 21 and 22 present two snapshots of floe size distributions in the winter. The general trend of each data set is the same. In comparison to Figure 20, the winter ice regime has a higher percentage of floes >500 m. As multi-year ice moves away from the confines of the polar pack it will be subject to increased summer ablation and more dynamic interactions with surrounding features. Floe size distributions would then tend towards smaller mean diameters with higher freeboards (assuming that the last floes to fragment tend to be rougher and thicker). This hypothesis seems to be in agreement with the many small multi-year floes profiled on the *Polar Sea* cruises.

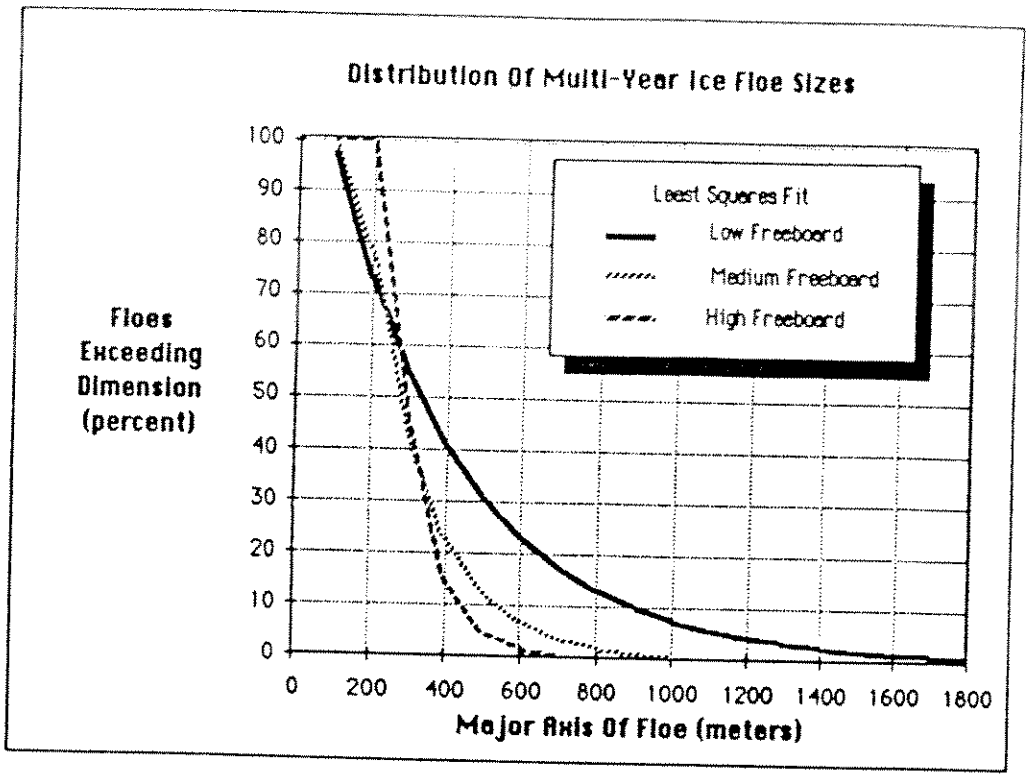

Figure 21 Winter Multi-Year Floe Distributions Measured Near the Polar Pack Edge in the Canadian Beaufort Sea (Gulf, 1980)

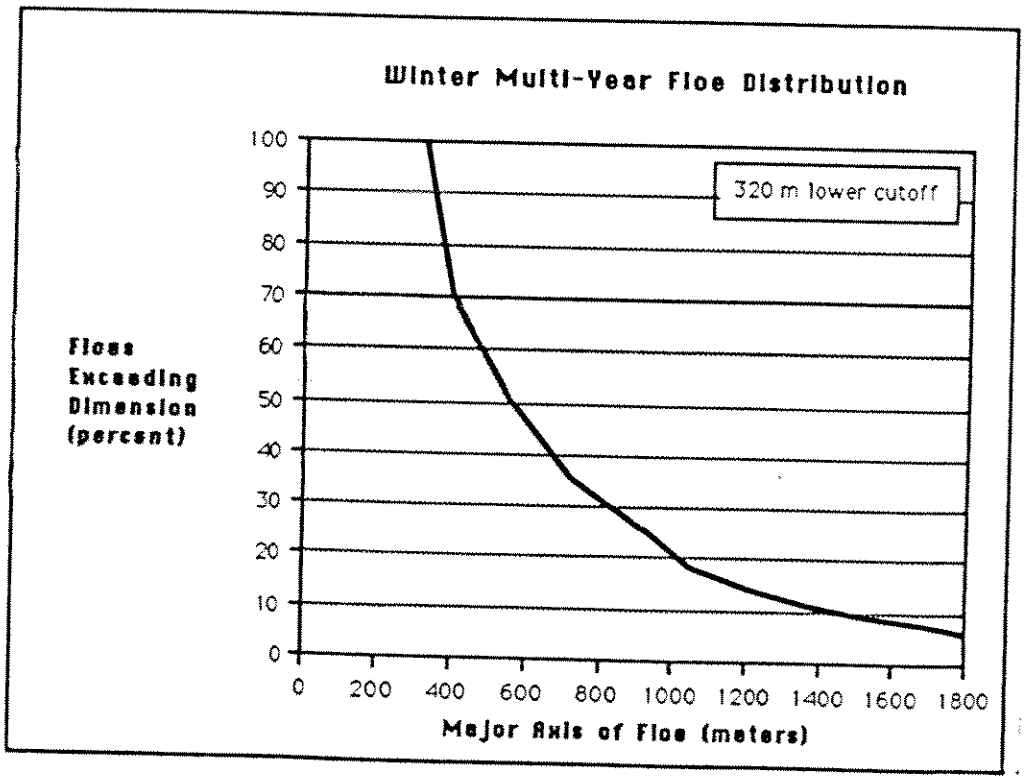

Figure 22 Winter Multi-Year Floe Distributions Measured in the Chukchi Sea, February 1981 (Intera, 1982)

4.3 Multi-Year Ice Floe Thickness

Multi-year ice thicknesses reported by published sources are tabulated in Table 3 below. These values indicate that multi-year ice floe thicknesses (ridges excluded) will likely range between 10 and 14 ft in the northern Chukchi Sea. Much higher thicknesses, in excess of 90 ft, will be associated with multi-year pressure ridges. The *Polar Sea* observed a multi-year ridge sail of 49 ft during the 1981 winter voyage in the north Chukchi Sea, indicating a total potential thickness in excess of 150 ft. (Voelker et al., 1981b).

Sixteen multi-year profiles were obtained in small floes (< 500 ft) during the April 1983 *Polar Sea* voyage in the Chukchi Sea (Voelker et al., 1983); results of deliberate drilling through the ridges showed a mean sail height of 6.8 ft and a mean keel depth of 16 ft (in reasonable comparison with the general thickness of rough floes (ridges excluded) measured in the Canadian Beaufort (Dickins, 1989).

Floes encountered at lower concentrations in the south Chukchi Sea will tend to be smaller and thicker (more likely to be multi-year fragments). The data collected by Dickins (1989) for rough multi-year floes in the Beaufort Sea represents a conservative upper bound for old ice thickness which could be encountered in the south Chukchi Sea.

Table 3 Multi-Year Ice Thicknesses

Reference	Mean (ft)	Standard Deviation (± ft)	Upper Decile Thickness (ft)	Comments
Tucker (1977)	11.8	5.0	-	31 drill holes on one floe
Wetzel (1971-75)	9.5	-	14.8	Sverdrup Basin 6300 data pts
Maykut (1977)	10.5	-	22.3	Based on theoretical thermodynamic mass balance
Wadhams and Horne (1978)	12.8	6.9	-	2600 nmi of submarine sonar profiles
C-CORE (1980)	12.1	4.9	-	50 nm of airborne radar data
Dickins (1989)	13.8	4.6	17.8	116 holes in 6 smooth floes
	17.8	5.6	25.9	56 holes plus sonar in 7 rough floes

5.0 CONTIGUOUS ICE EXTENT

Contiguous ice is defined as ice continuous to shore. This zone includes ice that may temporarily extend from shore into areas beyond the zone of most grounded ridges (7 to 12 fathoms (13 to 22 m)). The term contiguous ice has been used by Stringer to conveniently map those ice areas which, although they appear continuous to shore on satellite images, may not satisfy the stability requirements inferred by the term fast ice. According to Stringer et al. (1980), the contiguous ice edge is largely controlled by season, extending seaward as the winter progresses.

The Chukchi Sea nearshore ice environment is much more dynamic and variable than that of the Beaufort Sea (see Section 9.0). In the Beaufort Sea, the fast ice zone is relatively static throughout the winter and typically extends out beyond the 10 fathom (18 m) water depth to merge with the slowly moving pack ice offshore. Along the Chukchi coast the edge of the contiguous ice often marks the inshore boundary of an active flaw lead or young ice area (see Section 6.0) .

The stability of contiguous ice is strongly related to the nearshore bathymetry and bottom slope. In the Chukchi Sea, the distances between the 10 and 17 fathom (18 and 31 m) water depths range from about 15 to 35 nmi. By comparison, distances in the Beaufort Sea range from 5 to 20 nmi. The resulting differences in bottom slope mean that, to reach a given water depth, the contiguous ice has to extend much further from shore in the Chukchi Sea. At the same time, the lack of a distinct shelf break in the Chukchi Sea means that the grounded pressure ridges that serve as anchor points for fast ice in the Beaufort Sea are not as frequent or effective. The net result is that the contiguous ice cover in the Chukchi Sea is unreliable and subject to sudden break-away.

The average seasonal nearshore ice regimes of the Beaufort Sea and Chukchi Sea are compared in Table 4.

Table 4 Nearshore Ice Cycles in the Beaufort and Chukchi Seas[1]

Ice Phase	Central Beaufort Sea Coast	Central Chukchi Sea Coast
New Ice Forms	3 October	10 October
First Continuous Fast Ice	Mid-October	Early November
Extension/Modification of Fast Ice	Nov-Jan/Feb	Nov/Dec-Jan/Feb
Stable Ice Sheet Inside 15 m Isobath	Jan/Feb-Apr/May	Feb-Apr/May[2]
River Flooding Fast Ice	25 May	1 May
First Melt Pools	10 June	10 May
First Openings and Movement	30 June	10 June
Nearshore Area Largely Free of Fast Ice	1 August	5 July

1 These dates are based on available Landsat imagery for 1973-77. An identifiable event may occur anywhere between the dates of available clear frames which bracket the latest date of recognized non-occurrence and the earliest date of its identified occurrence; the average of these dates is used here.

2 Locally, the ice may not achieve any prolonged stability.

Source: LaBelle et al. (1983).

Figures 23, 24, and 25 map the range in contiguous ice extent in the Chukchi Sea for three periods: early winter (November and December), mid-winter (January to March), and early spring (April and May), respectively. Contiguous ice edges were mapped from 54 DMSP (Defence Meteorological Satellite Program) images for the years 1975 to 1984 and 26 NOAA (National Oceanic and Atmospheric Administration) images for the years 1975 to 1982. In mapping the ice edges from the imagery it was often difficult to determine the extent of true fast ice. Small leads inshore of the contiguous ice edge could not always be detected.

Figure 24 shows the contiguous ice edge at its maximum extent in late winter, between January and March. In some years, especially in the early winter period and in January, contiguous ice may not extend further seaward than the barrier islands between Point Lay and Wainwright (Figures 23 and 24).

Where the edge of the contiguous ice is poorly anchored, the ice tends to move seaward and leave large areas of open water behind. The recurring polynya between Point Hope and Cape Lisburne is an example of this. Another polynya formed by southward motion of the ice occurs southeast of Point Hope. In both areas the contiguous ice extent is unreliable.

Northeast of Cape Lisburne a large ridge system develops that serves to anchor the contiguous ice arch between Point Lay and Cape Lisburne (Stringer et al., 1980). However, due to the large distance involved, the contiguous ice sheet in Ledyard Bay is not stable and appears susceptible to break-away during the winter (Figures 23, 24, and 25).

In spring, the seaward limit of the contiguous ice recedes from its winter maximum, as the flaw lead expands to expose the ice edge (Figure 25). The minimum ice edge extent during April and May is greater than during the mid-winter period. This reflects the increased ice thickness and, hence, stability of the ice close to shore.

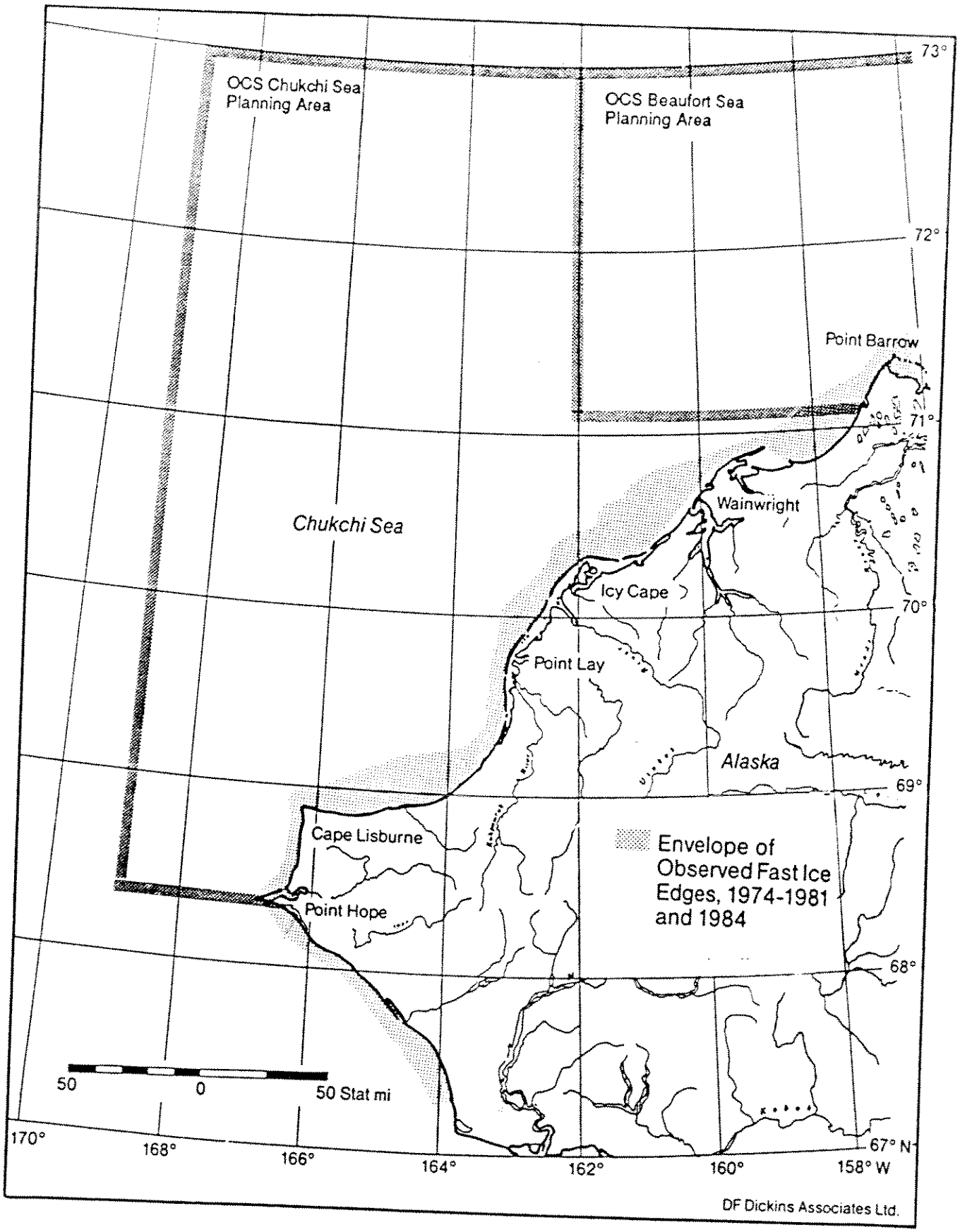

Figure 23 **Early Winter Contiguous Ice Extent (November-December)**

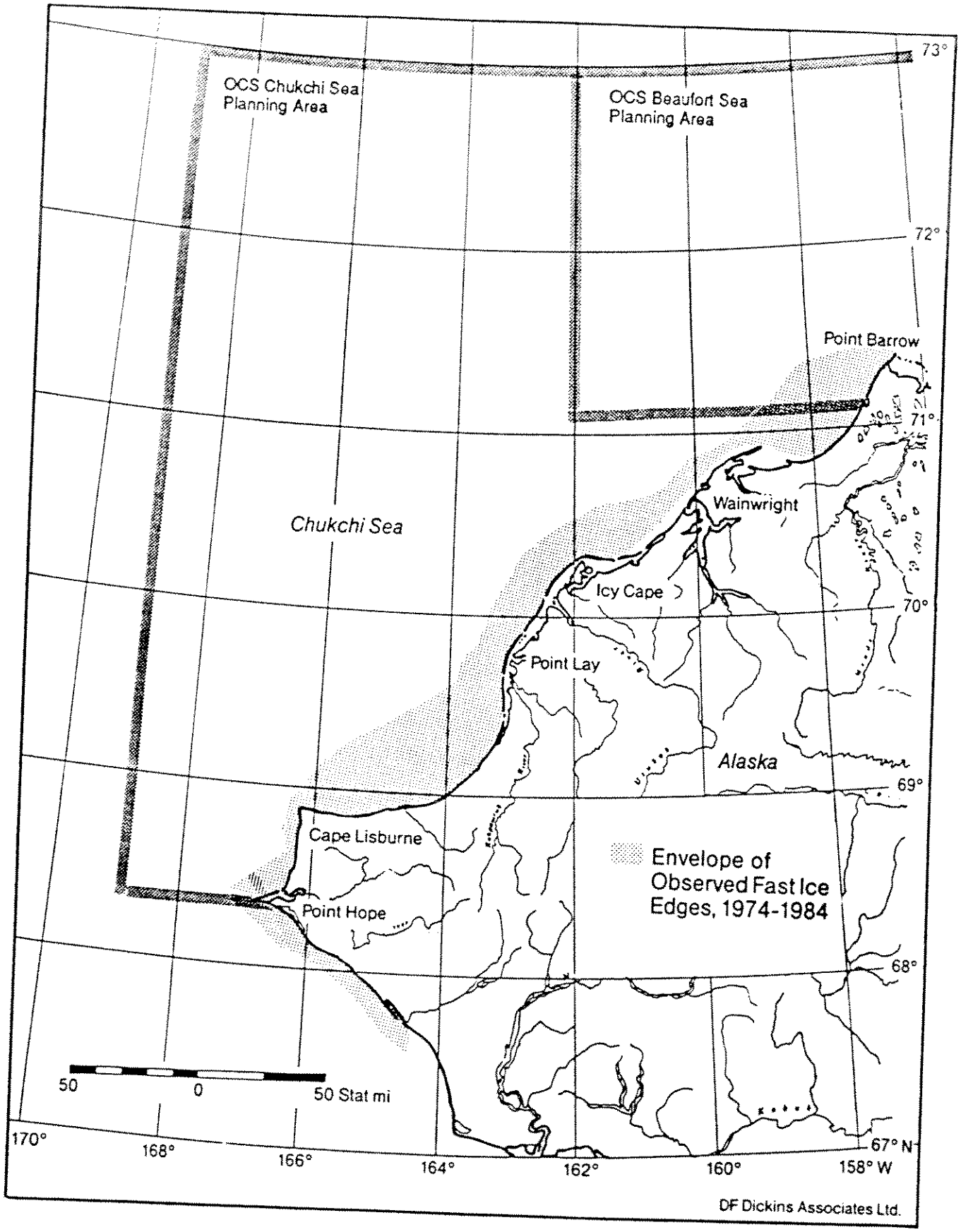

Figure 24 **Mid-Winter Contiguous Ice Extent (January-March)**

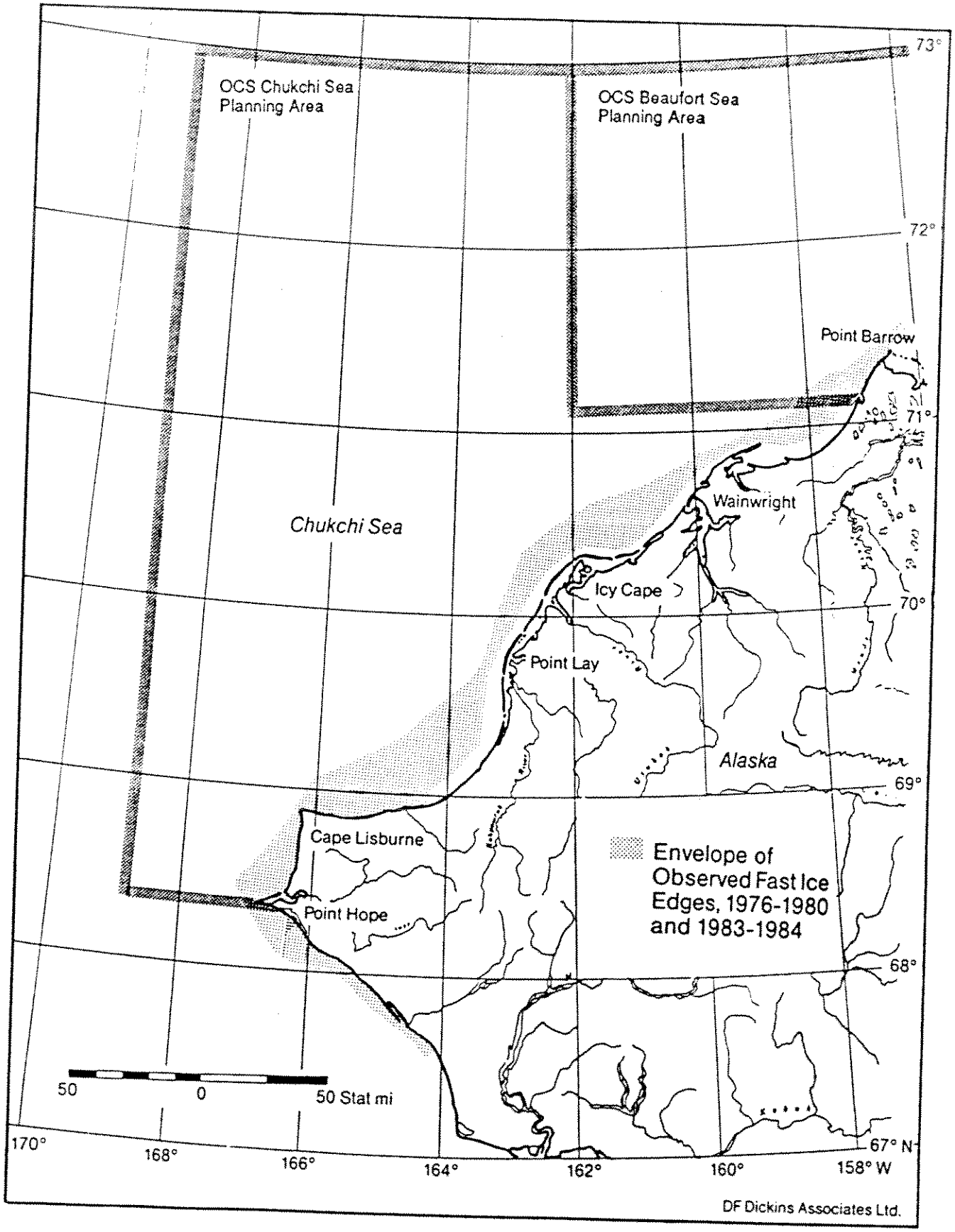

Figure 25 **Early Spring Contiguous Ice Extent (April-May)**

6.0 RECURRING FLAW POLYNYAS AND LEAD SYSTEMS

As described in Section 2.0, the nearshore ice environment in the Chukchi Sea is dominated by the presence of broad flaw polynyas, leads, and thin ice areas. These features are most persistent in the Point Hope/Cape Lisburne area but often extend as far north as Point Barrow.

Satellite images, acquired for the months November to June from 1974 to 1985, show that the flaw polynyas and leads along the Chukchi Sea coast are not limited to the spring period, but have a high probability of occurring in any month.

Figures 26 and 27 are satellite images obtained in January and February. These images show two common features of the Chukchi Sea winter ice cover, young ice stretching for 10 to 80 nmi from the coast, and major east/west oriented leads offshore covering the lease sale area. The area between Cape Lisburne and Point Lay is most often associated with a large expanse of young ice. North of Point Lay the flaw lead can narrow to less than a mile or become non-existent.

There is a problem with defining polynyas and leads in mid-winter; the formation of new ice is so rapid that true open water becomes a transient phenomenon. Leads and polynyas quickly develop a cover of new and young ice which can be as good as open water to an ice class vessel. (By definition new ice is less than 4 in. thick and young ice is from 4 to 12 in. thick.)

The persistence of the Chukchi polynya was evaluated in detail by Stringer et al. (1982) for the period February to October. During February and March, considered as winter months in this study, Stringer found that 20 to 30% of satellite observations showed a flaw lead adjacent to the fast ice edge. Stringer reported the average lead width as less than 0.3 nmi (including zero width situations). Qualitative observations of images for the November to January period show that when a flaw lead exists, it is likely to be at least several miles in extent, if only open water or new ice areas are measured. If young ice areas are included, the frequency and width of the lead increases well beyond those values indicated in previous studies.

Figure 26 NOAA Satellite Image Showing Increasing Ice Thickness Away from the Coast and Characteristic East/West Leads, 15 February 1975

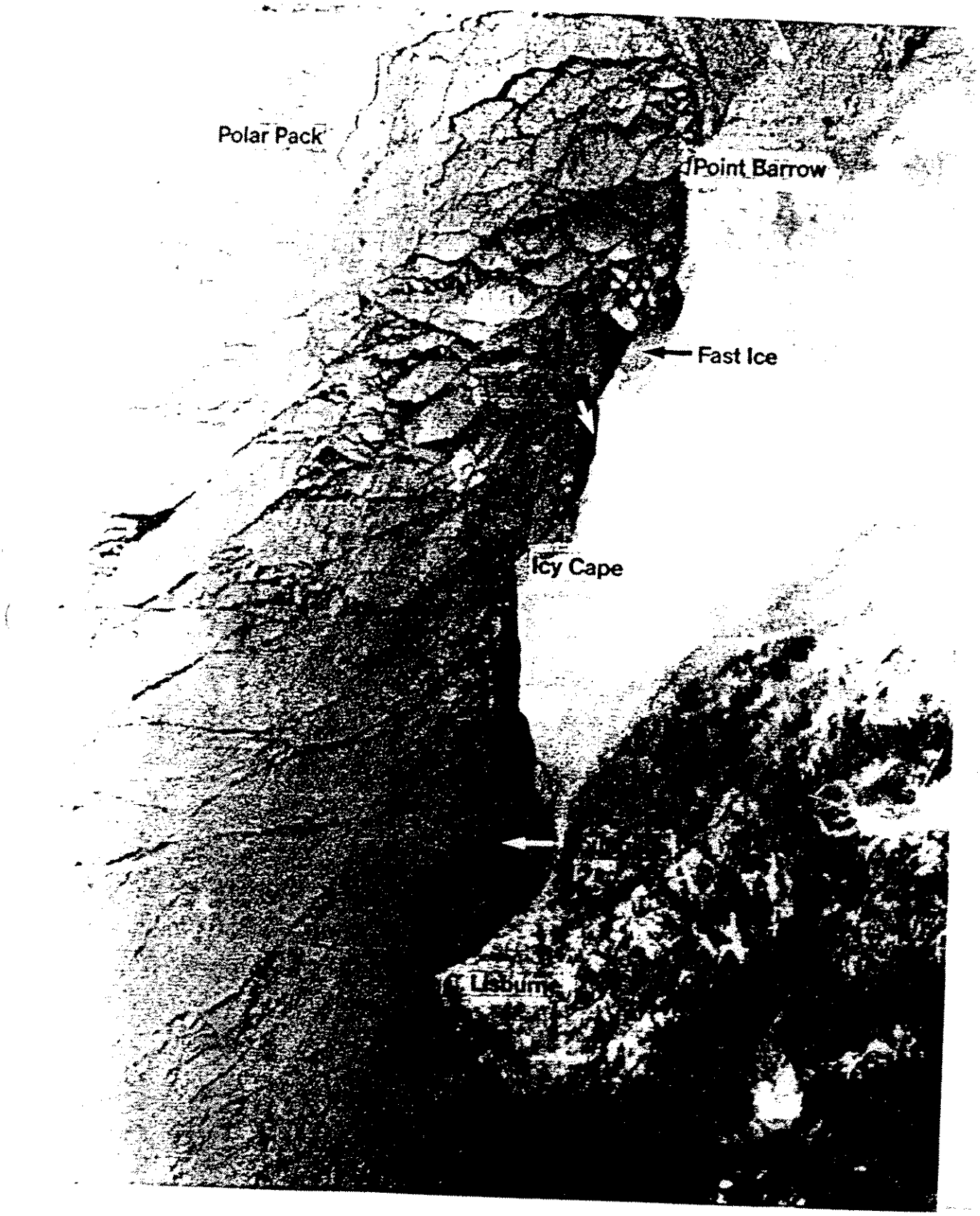

Figure 27 NOAA Satellite Image Showing North/South Gradation in Ice Thickness and New Ice Along the Fast Ice Edge, 14 January 1982

6.1 Ice Pressure

The environmental driving forces which inhibit or promote the development of leads and polynyas are currents, winds, and the Beaufort Gyre (influencing the northern sections of the lease area).

Winter current data is almost non-existent in the Chukchi Sea. Speeds under the ice are expected to be significantly lower than surface currents during periods of open water.

Winds are likely to be the most dominant driving force controlling the extent of transient open water and young ice along the Chukchi shore. Stringer et al. (1982) noted a qualitative correlation between the average ice motion away from the coast and the mean vector wind.

Four ice motion situations are related to the wind strength and direction as follows:

1. **Winds - Calm or Light (<7 kt)**
   Ice movement is current driven at speeds typically less than 0.2 kt. Leads will tend to be randomly oriented except off Point Barrow where current shear may cause an arching effect as the ice adopts the eddy motion of the near surface water. Pack ice may move up the coast slowly with a northerly set until all openings are closed and pressure builds up to resist further northerly ice movement.

2. **Winds - West to North (>6 kt)**
   Pack ice will be pushed towards shore without well defined lead systems. An exception may be direct northerly winds which could produce east/west leads along the polar pack/first-year pack ice boundary.

3. **Winds - Southwest (>6 kt)**
   Pack ice will be driven north, assisted by the nearshore currents. Pressure will build to the north as the first-year pack is driven into the polar pack. The Point Hope polynya will close. Open areas and break-away of the fast ice can occur in Ledyard Bay, northeast of Cape Lisburne. Northerly ice drift will be short lived, lasting only until openings and thin ice areas are closed or deformed.

4. **Winds - Southeast to the Northeast (>6 kt)**
Flaw leads and polynyas will develop as the pack ice is moved away from the fast ice edge. Winds from the prevailing northeast winter direction will develop the characteristic situation of wide thin ice zones parallel to shore, starting off Point Barrow and expanding towards Cape Lisburne. As the pack ice is driven southwest, a series of tightly spaced east/west lead systems will tend to arch away from the coast. There will be an increasing gradation in ice thickness from southeast to northwest away from the thick fast ice edge.

Of these four postulated wind-driven situations, number 4 is considered most likely. This conclusion is confirmed by satellite imagery and wind statistics. Table 5 summarizes the average percent occurrence of the different wind speed/direction groupings associated with situations 1 to 4 described above. The table combines data from Point Barrow, Wainwright, Point Lay, and Cape Lisburne (Brower et al., 1977).

Table 5 **Average Wind Statistics for North Chukchi Coastal Sites - Cape Lisburne to Point Barrow**

Wind Class	Percent Occurrence						
	Nov	Dec	Jan	Feb	Mar	Apr	May
1. Calm or Light <7 kt	26	37	33	38	36	35	35
2. West to North >6 kt	14	14	13	12	12	11	10
3. South to Southwest >6 kt	14	12	13	12	12	12	10
4. Southeast to Northeast >6 kt	49	43	45	46	47	48	48

Source: derived from Brower et al. (1977)

Note: Trace occurrences of winds were included in percentages. Totals may exceed 100% by up to 7%.

This table indicates that the wind class most favouring ice movement away from shore occurs between 40 and 50% of the time during the winter period. The next most common condition is calm or light winds which will lead to limited ice pressure or motion.

Wind class 3, favouring closure of the Point Hope polynya, occurs about 12% of the time. This agrees with Shapiro and Burns (1975). They associated polynya closure with short periods of southerly winds producing a northerly ice drift.

The percentage values in Table 5 should be interpreted as a relative guide to the likely proportions of different onshore/offshore ice movement patterns. The absolute values will not necessarily correspond with the actual percent occurrence of polynya formation. The rate and magnitude of ice movement associated with a particular wind will depend heavily on the duration and strength of the wind, as well as the previous history of ice development for that winter. Situations where a loose pack exists offshore may lead to an initially rapid retreat of ice away from shore with the onset of a period of relatively light north to northeasterly winds. As the pack closes and ice pressure develops, the wind strength necessary to maintain ice motion will steadily increase. If the offshore pack is already well consolidated with limited room for contraction, there may be almost little or no motion of the ice away from shore, even with a strong northeasterly wind.

The Chukchi wind climate implies a low probability of severe ice pressure situations along the shipping route. The presence of leads and thin ice areas, as the most often observed ice condition, indicates that ice pressure in the area is likely to be infrequent and short lived. Unfortunately, the state of knowledge concerning the causes and effects of ice pressure precludes any rigorous statistical treatment of the frequency of pressure situations or the actual shipping delays likely to be experienced.

Wind is the dominant driving force causing ice pressure, but there is no agreement as to what wind duration, sustained speed, or direction is necessary to generate a severe ice pressure situation. Bradford (1972) recounts the following general relationships observed between wind and ice pressure from personal observations onboard the *Manhattan*, *John A. MacDonald*, and *Louis St. Laurent*:

- up to a 25 knot wind speed the percentage occurrence of pressure increased by roughly an order of magnitude for every 9 knot increase in speed

- pressure was noted on 76% of all occasions of onshore winds (considered as winds between 30° and 150° angles to shore) and 51% of offshore winds

- on average, pressure situations observed during onshore winds outlasted those during offshore winds by a factor of 10.

The frequency of ice pressure situations has been interpreted from several studies of Landsat imagery. Hall (1977) measured a state of ice convergence (implying pressure) on 23% of 161 images over a three year period at a point near 77°N, 135°W. Dickins (1979) inferred a maximum winter frequency of ice pressure situations in the Chukchi Sea of 25% (January to July).

In summary, the limited database on actual ice pressure situations, combined with known wind statistics (shown in Table 5), indicates that ice pressure will not cause significant interruptions to the operation of high ice class vessels in the Chukchi Sea.

6.2 Leads Available for Tanker Transit

Recurring leads and young ice areas are an important part of the ice environment affecting icebreaking vessel operations and offshore structures in the lease sale area. Figures 28 to 30 are maps drawn from a typical cross section of DMSP and NOAA satellite images used in this study. In almost every month of every year polynyas and leads were visible on the images.

Table 6 lists the dates of all available DMSP images and the percentage of the tanker route that appears to be easily transited for a given date. The route was assumed to follow outside the 14 fathom (26 m) isobath, around Cape Lisburne, north to Icy Cape (Zone 5) and then head west to the central production site (Zone 7). Leads, open water, and thin or young first-year ice visible on the images define what was considered easily transited. The percentages are conservative visual estimates made from the DMSP images by an experienced icebreaker designer from the Valmet Corporation (A. Keinonen).

Table 6 indicates that between November and May, open water, leads, and thin ice areas occur frequently along the tanker route.

In an attempt to calibrate the ice conditions visible on the large scale DMSP and NOAA images, nine Landsat images of the lease sale area were found for dates that correspond closely to the dates of the DMSP and NOAA images. The availability of suitable Landsat images is limited by time of year (no images are available for the November to February period), by location (Landsat covers the nearshore Chukchi Sea area but not the offshore area in the vicinity of Zones 7 and 8), and by cloud cover (no images with over 50% cloud cover were ordered).

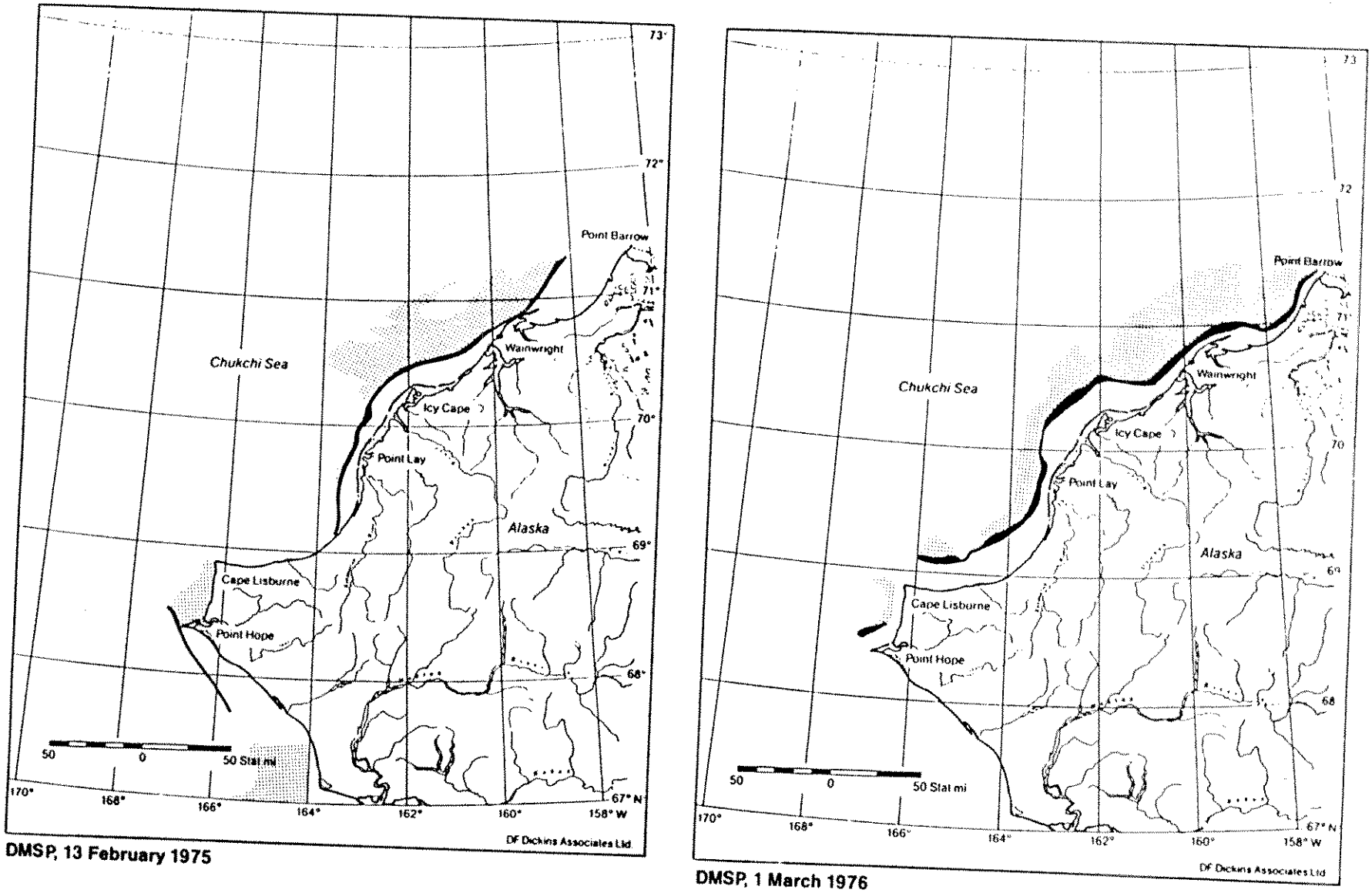

Figure 28 **Examples of the Winter Flaw Lead and Young Ice Areas, 1975 and 1976**

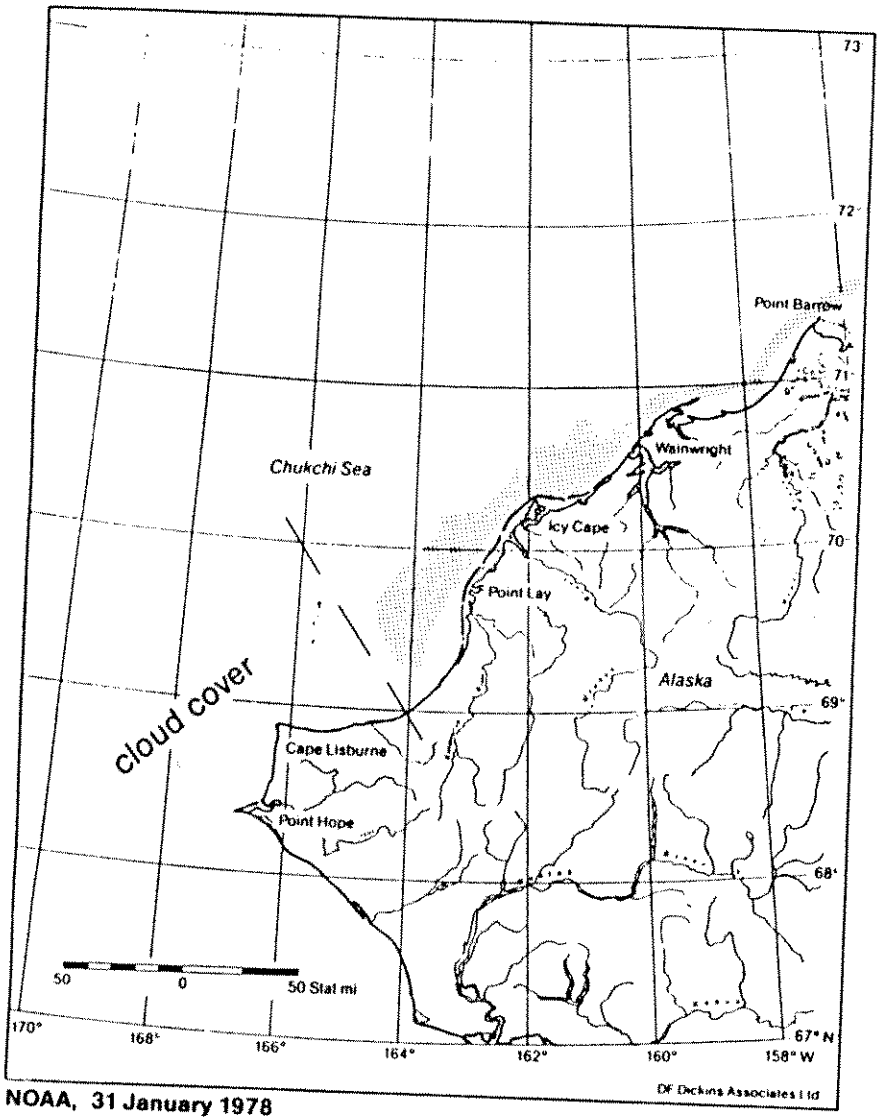

NOAA, 31 January 1978

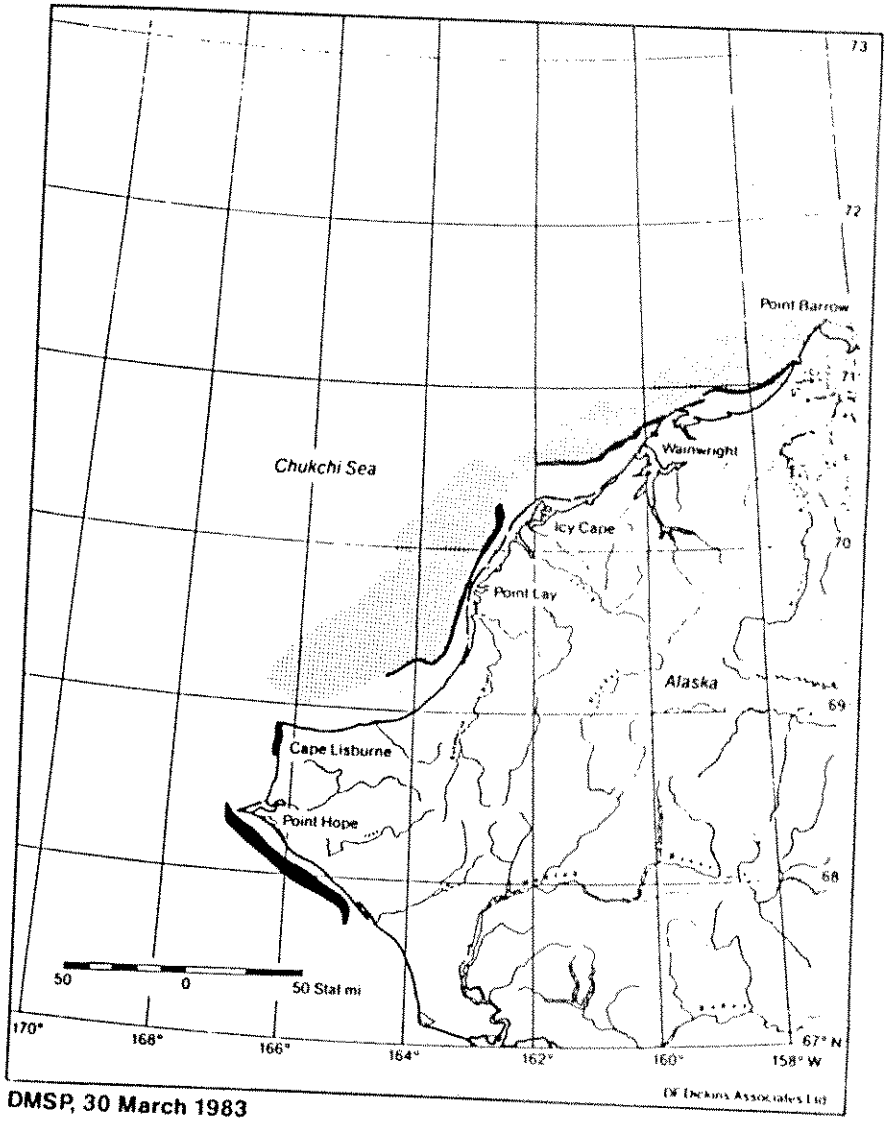

DMSP, 30 March 1983

Figure 29 **Examples of the Winter Flaw Lead and Young Ice Areas, 1978 and 1983**

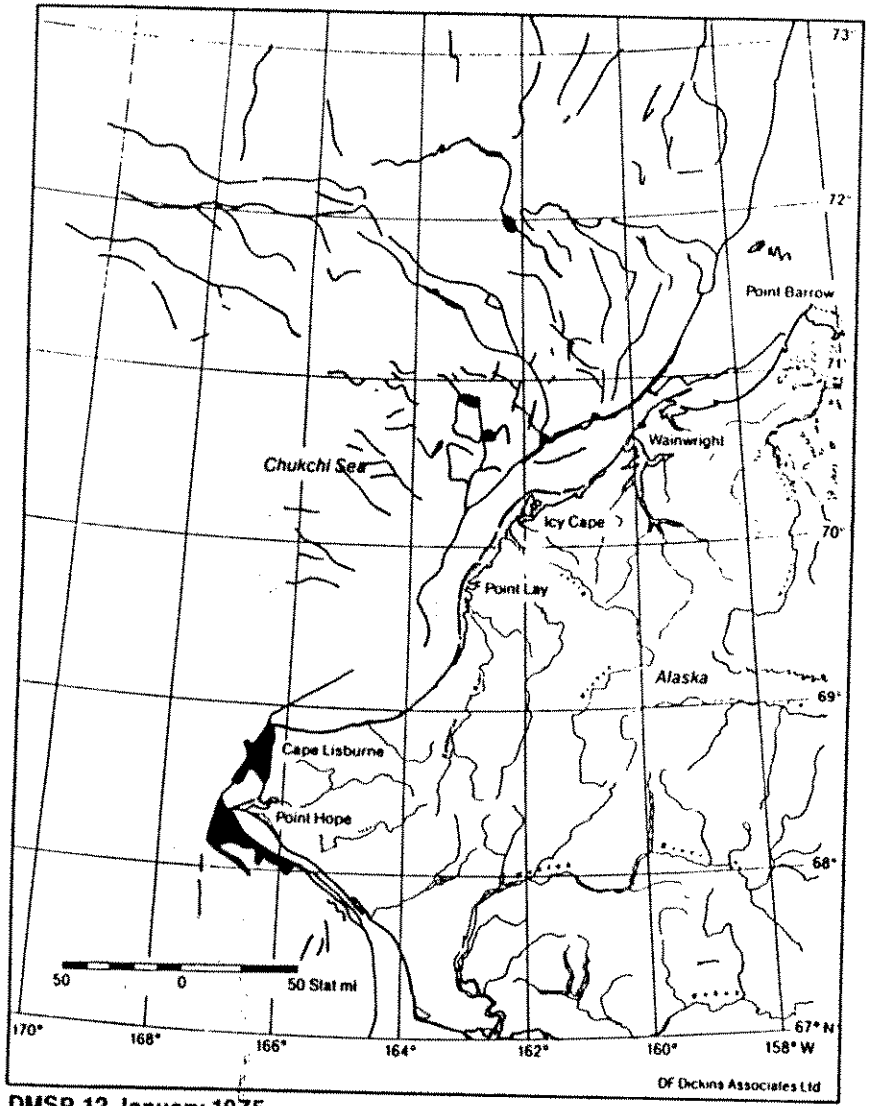

DMSP, 12 January 1975

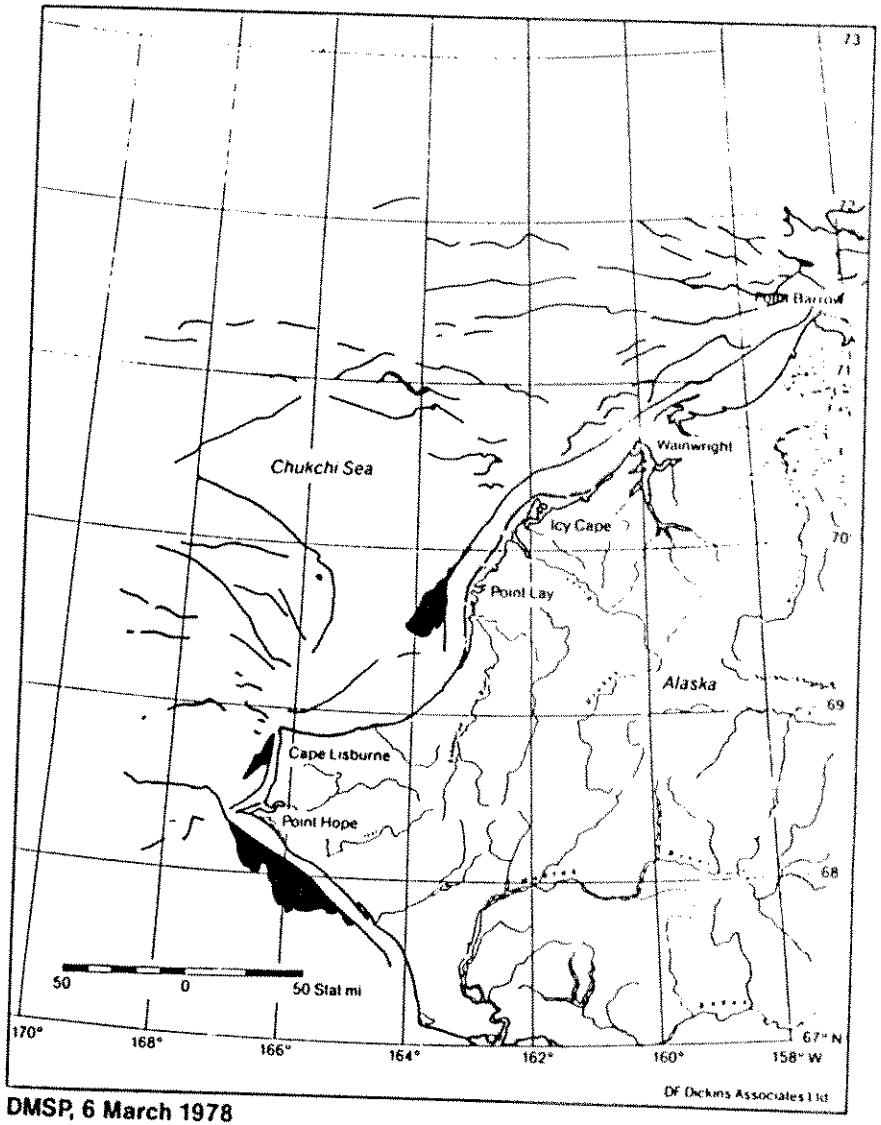

DMSP, 6 March 1978

Figure 30 Examples of Winter Lead Systems Offshore, 1975 and 1978

Table 6 Proportion of Tanker Route Easily Transited as Estimated from DMSP Images

Date	Percentage of Route	
	Zone 5	Zone 7
Nov 02 - 73	100	40
Jan 08 - 74	95	40
Jan 17 - 74	95	95
Jan 03 - 75	100	50
Jan 12 - 75	50	80
Feb 13 - 75	70	95
Nov 01 - 75	90	90
Nov 18 - 75	100	80
Nov 22 - 75	100	70
Dec 06 - 75	90	90
Dec 15 - 75	95	70
Jan 07 - 76	hazy	hazy
Jan 26 - 76	90	hazy
Mar 01 - 76	100	80
Dec 09 - 76	90	75
Dec 15 - 76	50	50
Nov 10 - 77	50	80
Dec 18 - 77	80	10
Jan 16 - 78	95	75
Jan 26 - 78	95	80
Feb 09 - 78	50	hazy
Mar 06 - 78	10	80
*Mar 23 - 78	95	75
Apr 01 - 78	hazy	80
May 17 - 78	100	hazy
Dec 07 - 78	hazy	hazy

Table 6 Proportion of Tanker Route Easily Transited as Estimated from DMSP Images (Continued)

Date	Percentage of Route	
	Zone 5	Zone 7
Jan 31 - 79	70	70
Jun 03 - 79	100	
Dec 23 - 79	50	50
Jan 15 - 80	50	90
Jan 16 - 80	30	50
Feb 17 - 80	50	60
Mar 17 - 80	hazy	hazy
*Apr 09 - 80	50	50
May 29 - 80	100	40
Jan 25 - 83	hazy	hazy
Jan 31 - 83	20?	20?
*Feb 26 - 83	80	70
*Mar 11 - 83	50	50
Mar 30 - 83	80	20
*May 09 - 83	95	30
Jan 01 - 84	10	70
Jan 15 - 84	50	30
Feb 07 - 84	90	90
*Mar 24 - 84	90	80
*May 20 - 84	50?	50?
Jun 06 - 84	90	hazy
Dec 23 - 84	hazy	90

*Landsat image available for comparison.

Figures 31 to 34 are two DMSP and Landsat image pairs for March 1978 and March 1983. The areas covered by the Landsat images are outlined on the DMSP images. Note that the DMSP images are enlarged from their original scale of 1:7,000,000 while the Landsat images are at their original scale of 1:1,000,000. The advantages and disadvantages of NOAA, DMSP, and Landsat images are compared in Appendix D.

Tanker routes to the central production site are plotted on overlays for Figures 31 and 33, the DMSP images for March 23, 1978 and March 11, 1983, respectively. (Note: the tanker routes were plotted by Valmet Corporation.) By comparing ice conditions along the tanker routes on the DMSP and the Landsat images, it is apparent that the severity of the ice conditions is overestimated from DMSP images.

Figure 31 is a high quality DMSP image which shows the lead system on March 23, 1978. The tanker route follows leads for what appears to be about 75% of its length from Cape Lisburne to the central production site (from Table 6). The corresponding Landsat image for March 27, 1978 (Figure 32) shows an even greater percentage of leads available for tanker transit. Note that all leads visible on Landsat are suitable for tanker transit (image resolution is 80 m).

Figure 33 is a poorer quality DMSP image for March 11, 1983; the lower half of the image is hazy and the leads are not clearly visible. Plotting the tanker route is more difficult. The ice cover offshore of Point Lay, in the vicinity of Zone 9, is assumed to be less than 10/10 as leads are just visible. From the Landsat image (Figure 34) for the same area, the ice cover is estimated at 7/10 seaward of the major shore lead and 8-9/10 further seaward. Aerial photography might show that the ice cover in these areas is actually only 5/10 and 7/10, respectively. The DMSP imagery indicated that only 50% or less of the route was assumed to be easily transited (Table 6). The Landsat image shows that this estimate is too conservative; the pack ice is highly fractured, with numerous leads facilitating tanker transit.

Interpretation of ice conditions from satellite imagery is largely a function of the resolution and scale of the image.

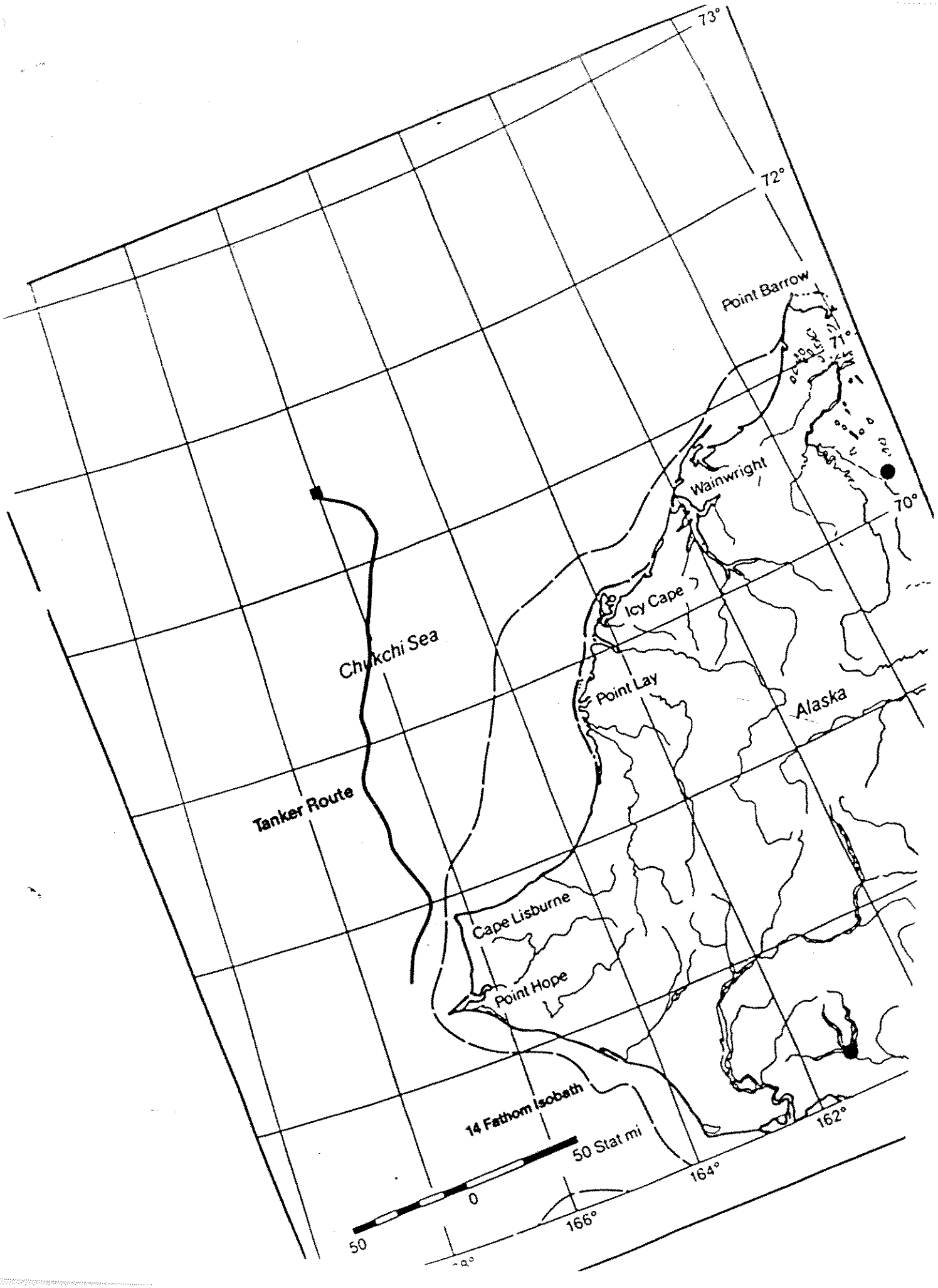
73°
72°
71°
70°
Point Barrow
Wainwright
Icy Cape
Point Lay
Chukchi Sea
Alaska
Tanker Route
Cape Lisburne
Point Hope
14 Fathom Isobath
50 Stat mi
50
0
164°
166°
162°

A survey of weekly polar pack edges between 1975 and 1989 confirms that there is no clear seasonal cycle of pack ice advance and retreat.

The extreme variability in polar pack locations, both from year to year, and within a given ice season, makes the definition of an average multi-year ice edge somewhat academic. Multi-year ice can occur within the lease sale area throughout the year, although concentrations of greater than 5/10 multi-year ice are not encountered south of 71°N more than 5 years in 14.

The occurrence of high multi-year ice concentrations is critical to tanker loading operations. The ice edge locations shown on the ice charts are based on large scale satellite imagery (NOAA imagery, original scale 1:7,000,000) . Identification of multi-year ice concentrations from satellite imagery is highly subjective (Intera, pers. comm.). The only time of year that the polar pack edge can be mapped with any certainty from satellite imagery is during the late summer or early fall.

Experience has shown that regional ice conditions interpreted from satellite imagery are often more severe than the actual ice condition at a specific location. Operating experience from the Canadian Beaufort Sea and from icebreaker voyages has confirmed this trend. Unfortunately, there is limited, publicly available field data to calibrate multi-year ice concentrations interpreted from satellite imagery (satellite imagery is used to prepare the ice charts). Lack of field data on multi-year ice concentrations is a continuing deficiency which affects long-term planning for Chukchi Sea development.

4.2 Multi-Year Floe Sizes

Public data on multi-year floe sizes is unavailable for most of the study area. One study by Weeks et al. (1977) used SLAR imagery to record multi-year floe sizes along a line northwest of Point Barrow (data replotted as Figure 20). The floe sizes in Figure 20 were assumed to have a circular shape. Mean diameters were grouped into 650 ft (200 m) bins.

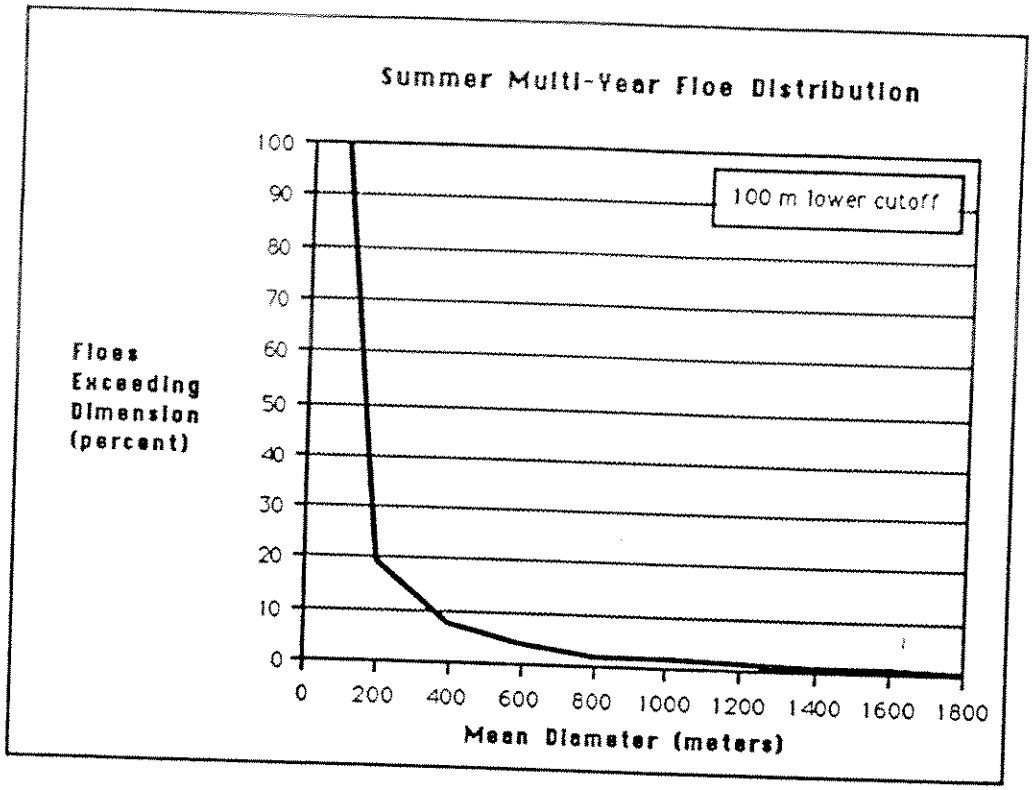

Figure 20 **Summer Multi-Year Floe Distribution for the North Chukchi Sea (Weeks et al., 1977)**

A second study measured the major and minor axes of 922 multi-year floes near the polar pack edge using aerial photo-stereo analysis (Gulf Canada, 1980), which has a higher degree of accuracy than other types of imagery such as Synthetic Aperture Radar (SAR). The photo-stereo information allowed the floes to be grouped into high, medium, and low freeboard categories. The percent exceedance versus the major axis dimension (floe length) is shown in Figure 21.

Despite the fact that the data was collected in the Canadian Beaufort Sea, it is considered reasonable to extrapolate this data to the Chukchi Sea. Multi-year ice in the northern region of the Chukchi Sea originates at the southern limits of the polar pack. Data from multi-year ice studies near the polar pack edge in the Beaufort Sea will be representative of the multi-year floe sizes likely to be encountered in the northern Chukchi Sea during the winter and early summer (mid to late summer floes will likely be reduced in size due to

dynamic interactions). Comparison of Figure 20 with the medium to high freeboard floes documented by Gulf (Figure 21) shows good agreement.

A third study analyzed multi-year floe dimensions for the Chukchi Sea based on SAR data acquired in February 1981 (Intera, 1982). Floes were counted in bins of 160 m with a lower cutoff of 91 m in the 0-160 m bin. Although less certain than aerial photography in identifying old ice, SAR offers the advantage of a wide swath which includes much larger floes than can be viewed in a single air photo strip. Figure 22 shows the floe distributions from the Intera data.

The data in the first two bins (91-320 m) was not included in Figure 22 because the number of floes reported below 320 m (17%) is unusually low. Researchers usually describe the distribution of floe sizes as either a power law or exponential function, both of which predict higher frequencies as floe sizes decrease. The apparent discrepancy in the Intera data (1982) may be caused by the resolution of the SAR imagery. SAR can have difficulty adequately differentiating small pieces of multi-year ice when the pieces are either surrounded by first-year rubble or so heavily deformed in their own right that they appear like first-year ice in the radar return.

To avoid presenting data which may be misleading, only data for floe sizes greater than 320 m were included in Figure 22.

Figures 21 and 22 present two snapshots of floe size distributions in the winter. The general trend of each data set is the same. In comparison to Figure 20, the winter ice regime has a higher percentage of floes >500 m. As multi-year ice moves away from the confines of the polar pack it will be subject to increased summer ablation and more dynamic interactions with surrounding features. Floe size distributions would then tend towards smaller mean diameters with higher freeboards (assuming that the last floes to fragment tend to be rougher and thicker). This hypothesis seems to be in agreement with the many small multi-year floes profiled on the *Polar Sea* cruises.

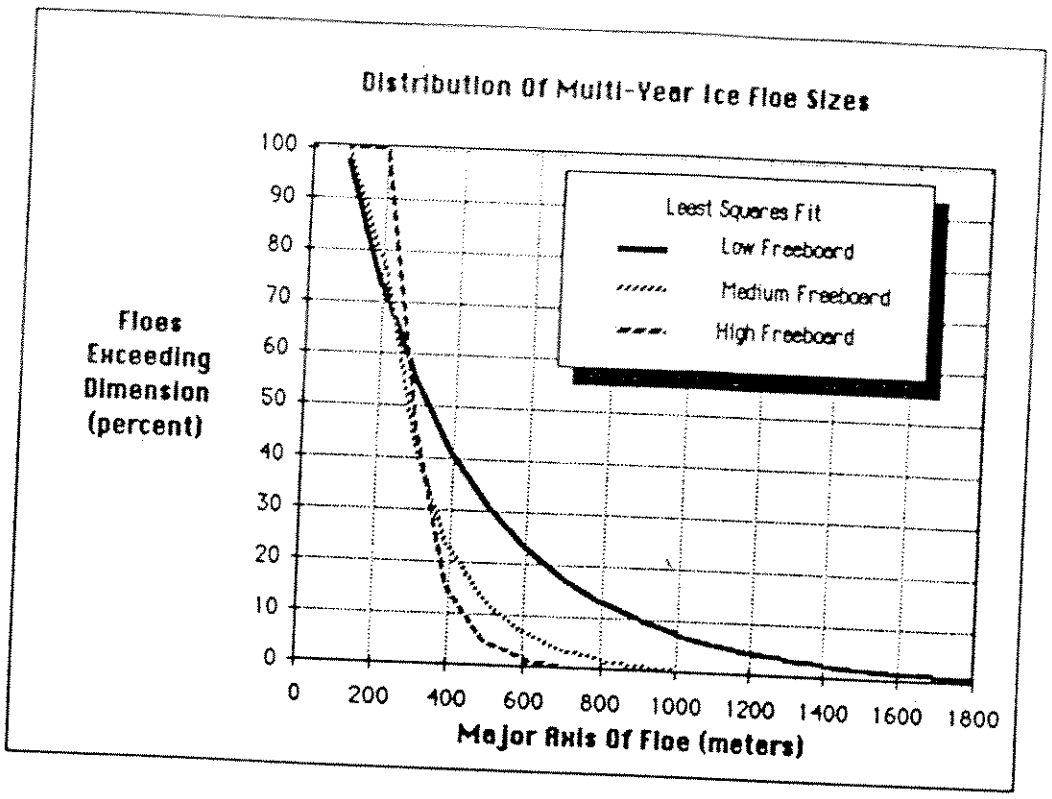

Figure 21 Winter Multi-Year Floe Distributions Measured Near the Polar Pack Edge in the Canadian Beaufort Sea (Gulf, 1980)

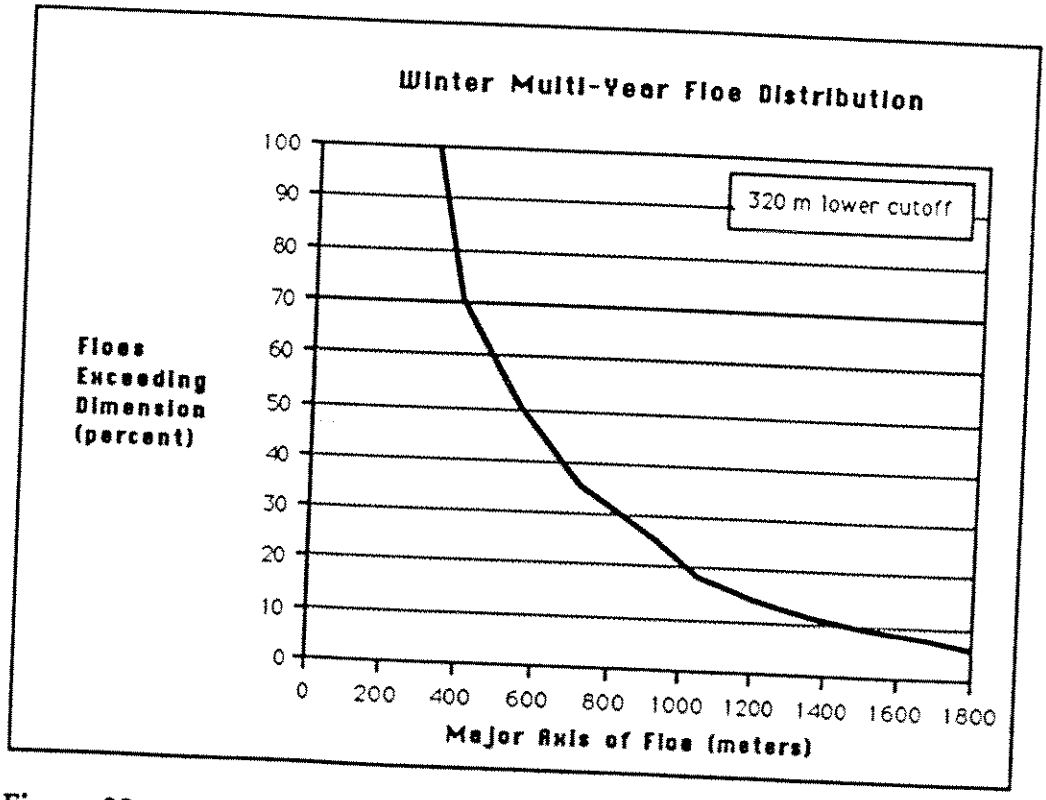

Figure 22 Winter Multi-Year Floe Distributions Measured in the Chukchi Sea, February 1981 (Intera, 1982)

4.3 Multi-Year Ice Floe Thickness

Multi-year ice thicknesses reported by published sources are tabulated in Table 3 below. These values indicate that multi-year ice floe thicknesses (ridges excluded) will likely range between 10 and 14 ft in the northern Chukchi Sea. Much higher thicknesses, in excess of 90 ft, will be associated with multi-year pressure ridges. The *Polar Sea* observed a multi-year ridge sail of 49 ft during the 1981 winter voyage in the north Chukchi Sea, indicating a total potential thickness in excess of 150 ft. (Voelker et al., 1981b).

Sixteen multi-year profiles were obtained in small floes (< 500 ft) during the April 1983 *Polar Sea* voyage in the Chukchi Sea (Voelker et al., 1983); results of deliberate drilling through the ridges showed a mean sail height of 6.8 ft and a mean keel depth of 16 ft (in reasonable comparison with the general thickness of rough floes (ridges excluded) measured in the Canadian Beaufort (Dickins, 1989).

Floes encountered at lower concentrations in the south Chukchi Sea will tend to be smaller and thicker (more likely to be multi-year fragments). The data collected by Dickins (1989) for rough multi-year floes in the Beaufort Sea represents a conservative upper bound for old ice thickness which could be encountered in the south Chukchi Sea.

Table 3 Multi-Year Ice Thicknesses

Reference	Mean (ft)	Standard Deviation (± ft)	Upper Decile Thickness (ft)	Comments
Tucker (1977)	11.8	5.0	-	31 drill holes on one floe
Wetzel (1971-75)	9.5	-	14.8	Sverdrup Basin 6300 data pts
Maykut (1977)	10.5	-	22.3	Based on theoretical thermodynamic mass balance
Wadhams and Horne (1978)	12.8	6.9	-	2600 nmi of submarine sonar profiles
C-CORE (1980)	12.1	4.9	-	50 nm of airborne radar data
Dickins (1989)	13.8	4.6	17.8	116 holes in 6 smooth floes
	17.8	5.6	25.9	56 holes plus sonar in 7 rough floes

5.0 CONTIGUOUS ICE EXTENT

Contiguous ice is defined as ice continuous to shore. This zone includes ice that may temporarily extend from shore into areas beyond the zone of most grounded ridges (7 to 12 fathoms (13 to 22 m)). The term contiguous ice has been used by Stringer to conveniently map those ice areas which, although they appear continuous to shore on satellite images, may not satisfy the stability requirements inferred by the term fast ice. According to Stringer et al. (1980), the contiguous ice edge is largely controlled by season, extending seaward as the winter progresses.

The Chukchi Sea nearshore ice environment is much more dynamic and variable than that of the Beaufort Sea (see Section 9.0). In the Beaufort Sea, the fast ice zone is relatively static throughout the winter and typically extends out beyond the 10 fathom (18 m) water depth to merge with the slowly moving pack ice offshore. Along the Chukchi coast the edge of the contiguous ice often marks the inshore boundary of an active flaw lead or young ice area (see Section 6.0) .

The stability of contiguous ice is strongly related to the nearshore bathymetry and bottom slope. In the Chukchi Sea, the distances between the 10 and 17 fathom (18 and 31 m) water depths range from about 15 to 35 nmi. By comparison, distances in the Beaufort Sea range from 5 to 20 nmi. The resulting differences in bottom slope mean that, to reach a given water depth, the contiguous ice has to extend much further from shore in the Chukchi Sea. At the same time, the lack of a distinct shelf break in the Chukchi Sea means that the grounded pressure ridges that serve as anchor points for fast ice in the Beaufort Sea are not as frequent or effective. The net result is that the contiguous ice cover in the Chukchi Sea is unreliable and subject to sudden break-away.

The average seasonal nearshore ice regimes of the Beaufort Sea and Chukchi Sea are compared in Table 4.

Table 4 Nearshore Ice Cycles in the Beaufort and Chukchi Seas[1]

Ice Phase	Central Beaufort Sea Coast	Central Chukchi Sea Coast
New Ice Forms	3 October	10 October
First Continuous Fast Ice	Mid-October	Early November
Extension/Modification of Fast Ice	Nov-Jan/Feb	Nov/Dec-Jan/Feb
Stable Ice Sheet Inside 15 m Isobath	Jan/Feb-Apr/May	Feb-Apr/May[2]
River Flooding Fast Ice	25 May	1 May
First Melt Pools	10 June	10 May
First Openings and Movement	30 June	10 June
Nearshore Area Largely Free of Fast Ice	1 August	5 July

1 These dates are based on available Landsat imagery for 1973-77. An identifiable event may occur anywhere between the dates of available clear frames which bracket the latest date of recognized non-occurrence and the earliest date of its identified occurrence; the average of these dates is used here.

2 Locally, the ice may not achieve any prolonged stability.

Source: LaBelle et al. (1983).

Figures 23, 24, and 25 map the range in contiguous ice extent in the Chukchi Sea for three periods: early winter (November and December), mid-winter (January to March), and early spring (April and May), respectively. Contiguous ice edges were mapped from 54 DMSP (Defence Meteorological Satellite Program) images for the years 1975 to 1984 and 26 NOAA (National Oceanic and Atmospheric Administration) images for the years 1975 to 1982. In mapping the ice edges from the imagery it was often difficult to determine the extent of true fast ice. Small leads inshore of the contiguous ice edge could not always be detected.

Figure 24 shows the contiguous ice edge at its maximum extent in late winter, between January and March. In some years, especially in the early winter period and in January, contiguous ice may not extend further seaward than the barrier islands between Point Lay and Wainwright (Figures 23 and 24).

Where the edge of the contiguous ice is poorly anchored, the ice tends to move seaward and leave large areas of open water behind. The recurring polynya between Point Hope and Cape Lisburne is an example of this. Another polynya formed by southward motion of the ice occurs southeast of Point Hope. In both areas the contiguous ice extent is unreliable.

Northeast of Cape Lisburne a large ridge system develops that serves to anchor the contiguous ice arch between Point Lay and Cape Lisburne (Stringer et al., 1980). However, due to the large distance involved, the contiguous ice sheet in Ledyard Bay is not stable and appears susceptible to break-away during the winter (Figures 23, 24, and 25).

In spring, the seaward limit of the contiguous ice recedes from its winter maximum, as the flaw lead expands to expose the ice edge (Figure 25). The minimum ice edge extent during April and May is greater than during the mid-winter period. This reflects the increased ice thickness and, hence, stability of the ice close to shore.

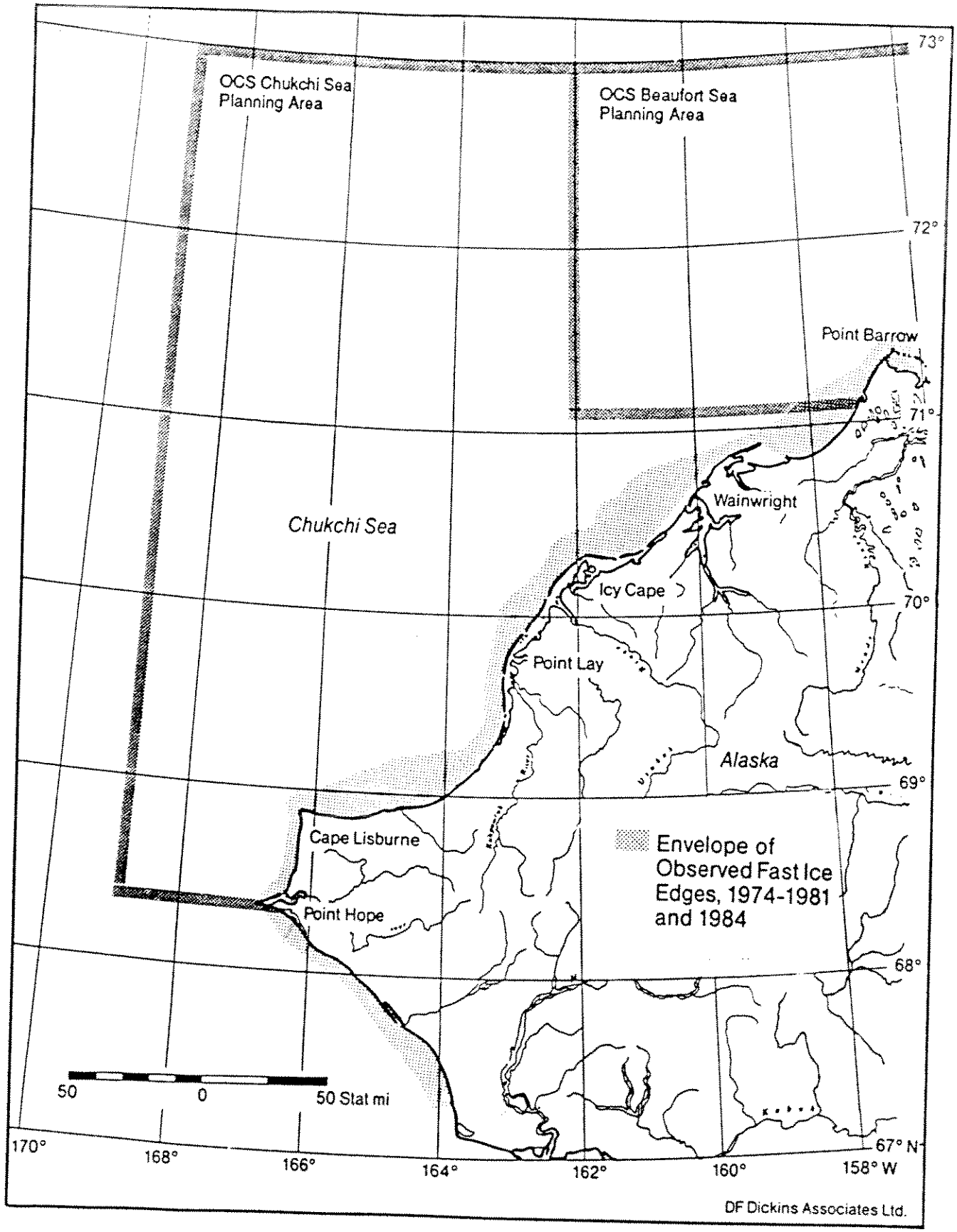

Figure 23 **Early Winter Contiguous Ice Extent (November-December)**

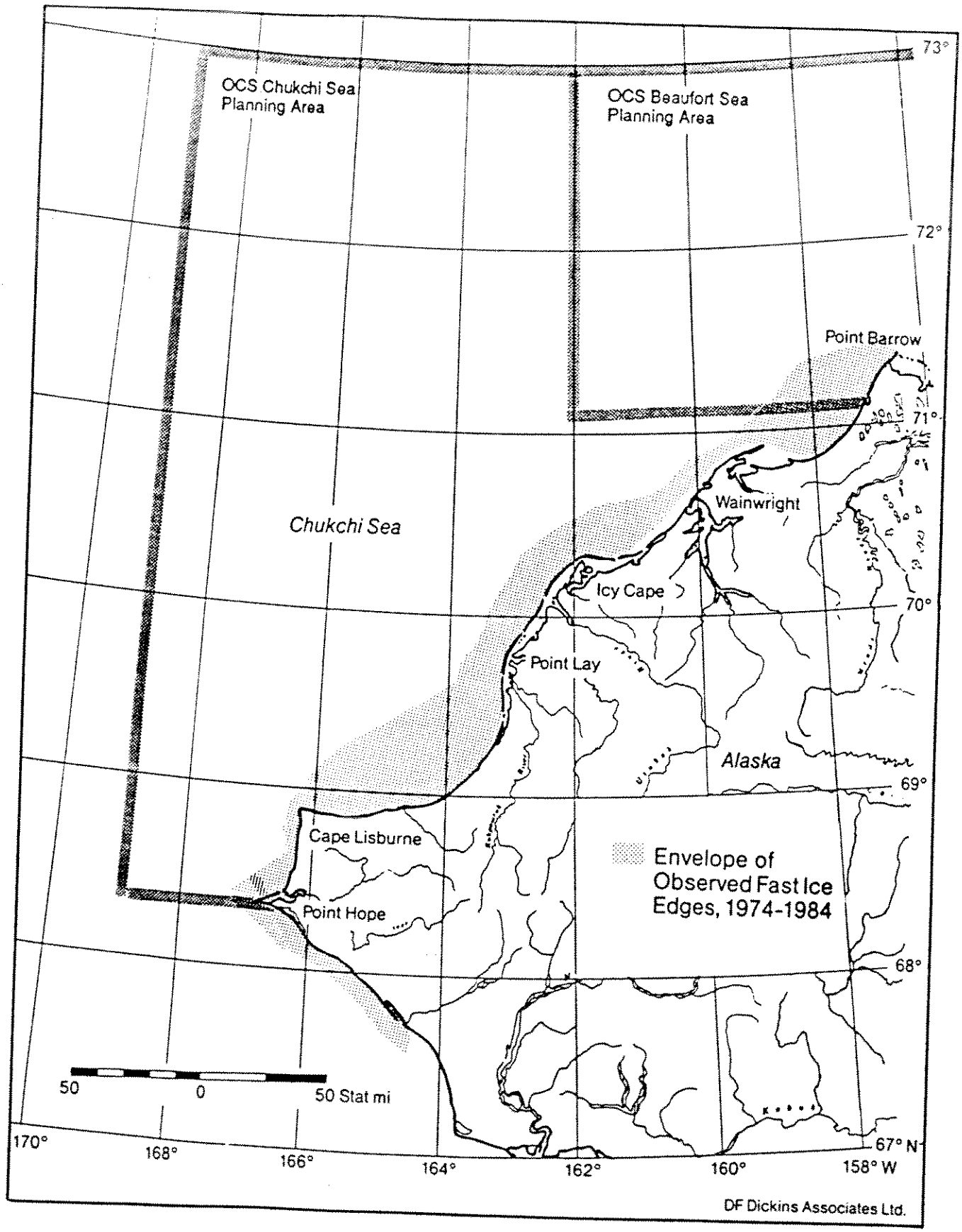

Figure 24 **Mid-Winter Contiguous Ice Extent (January-March)**

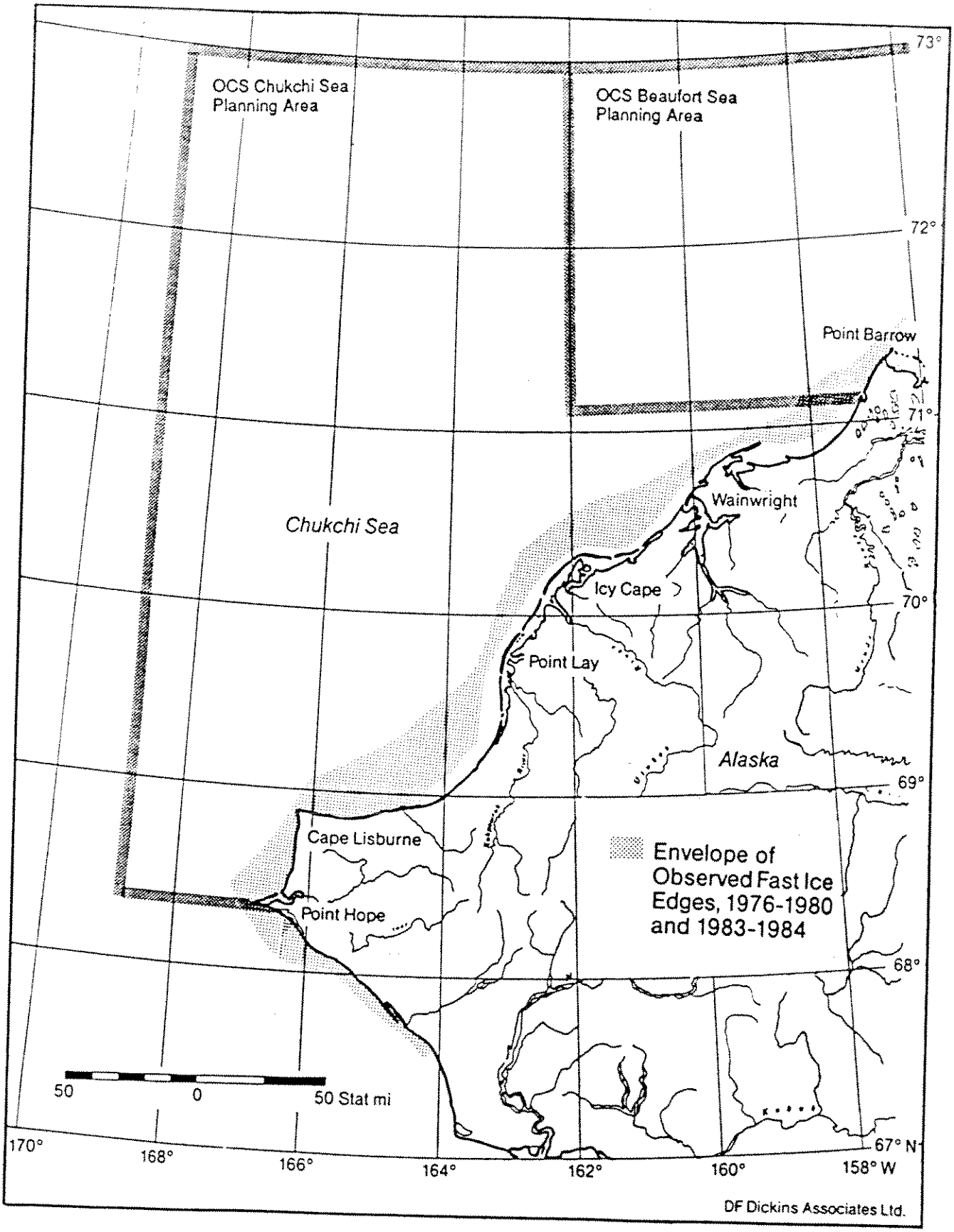

Figure 25 **Early Spring Contiguous Ice Extent (April-May)**

6.0 RECURRING FLAW POLYNYAS AND LEAD SYSTEMS

As described in Section 2.0, the nearshore ice environment in the Chukchi Sea is dominated by the presence of broad flaw polynyas, leads, and thin ice areas. These features are most persistent in the Point Hope/Cape Lisburne area but often extend as far north as Point Barrow.

Satellite images, acquired for the months November to June from 1974 to 1985, show that the flaw polynyas and leads along the Chukchi Sea coast are not limited to the spring period, but have a high probability of occurring in any month.

Figures 26 and 27 are satellite images obtained in January and February. These images show two common features of the Chukchi Sea winter ice cover, young ice stretching for 10 to 80 nmi from the coast, and major east/west oriented leads offshore covering the lease sale area. The area between Cape Lisburne and Point Lay is most often associated with a large expanse of young ice. North of Point Lay the flaw lead can narrow to less than a mile or become non-existent.

There is a problem with defining polynyas and leads in mid-winter; the formation of new ice is so rapid that true open water becomes a transient phenomenon. Leads and polynyas quickly develop a cover of new and young ice which can be as good as open water to an ice class vessel. (By definition new ice is less than 4 in. thick and young ice is from 4 to 12 in. thick.)

The persistence of the Chukchi polynya was evaluated in detail by Stringer et al. (1982) for the period February to October. During February and March, considered as winter months in this study, Stringer found that 20 to 30% of satellite observations showed a flaw lead adjacent to the fast ice edge. Stringer reported the average lead width as less than 0.3 nmi (including zero width situations). Qualitative observations of images for the November to January period show that when a flaw lead exists, it is likely to be at least several miles in extent, if only open water or new ice areas are measured. If young ice areas are included, the frequency and width of the lead increases well beyond those values indicated in previous studies.

Figure 26 NOAA Satellite Image Showing Increasing Ice Thickness Away from the Coast and Characteristic East/West Leads, 15 February 1975

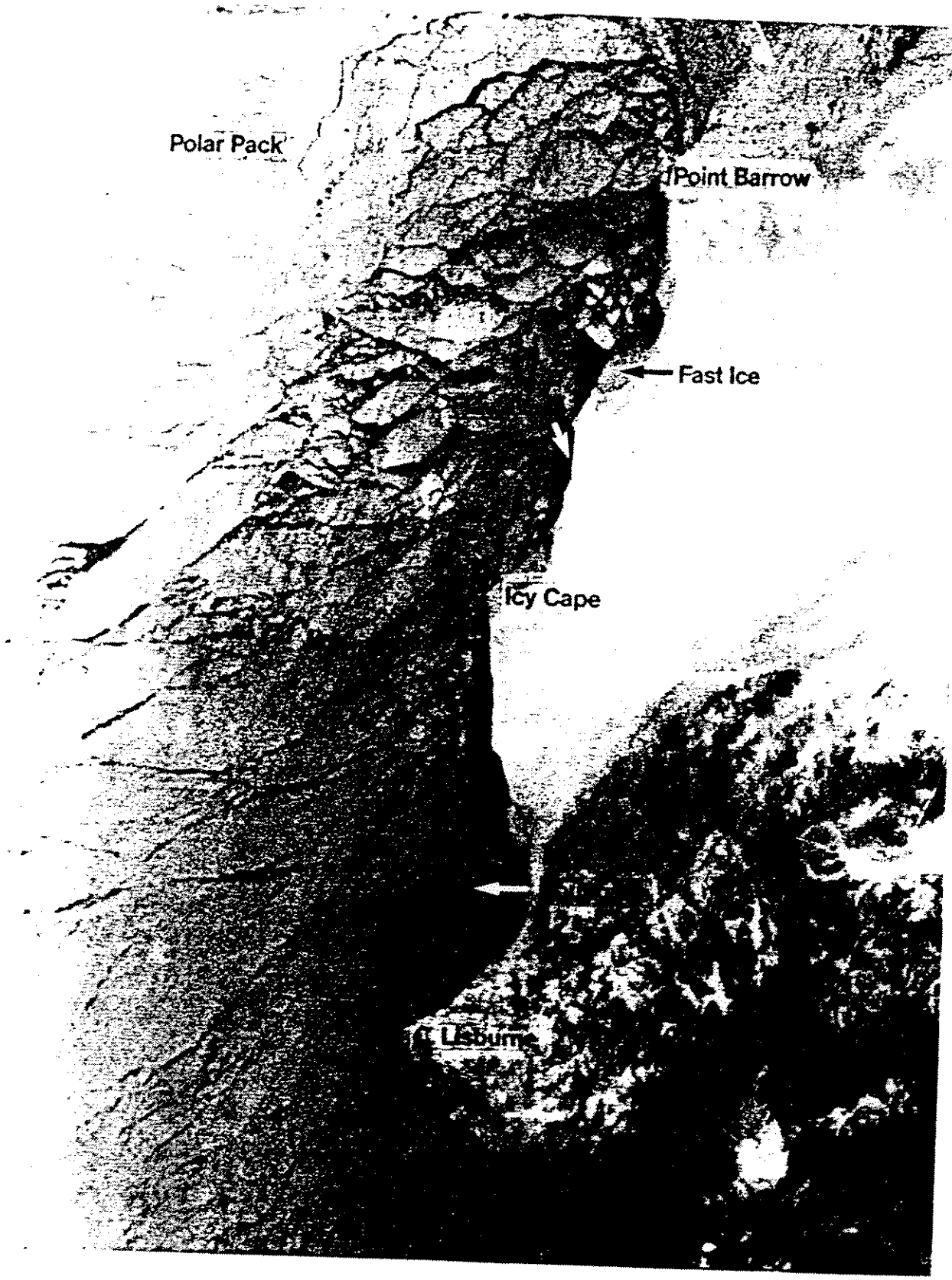

Figure 27 NOAA Satellite Image Showing North/South Gradation in Ice Thickness and New Ice Along the Fast Ice Edge, 14 January 1982

6.1 Ice Pressure

The environmental driving forces which inhibit or promote the development of leads and polynyas are currents, winds, and the Beaufort Gyre (influencing the northern sections of the lease area).

Winter current data is almost non-existent in the Chukchi Sea. Speeds under the ice are expected to be significantly lower than surface currents during periods of open water.

Winds are likely to be the most dominant driving force controlling the extent of transient open water and young ice along the Chukchi shore. Stringer et al. (1982) noted a qualitative correlation between the average ice motion away from the coast and the mean vector wind.

Four ice motion situations are related to the wind strength and direction as follows:

1. **Winds - Calm or Light (<7 kt)**
   Ice movement is current driven at speeds typically less than 0.2 kt. Leads will tend to be randomly oriented except off Point Barrow where current shear may cause an arching effect as the ice adopts the eddy motion of the near surface water. Pack ice may move up the coast slowly with a northerly set until all openings are closed and pressure builds up to resist further northerly ice movement.

2. **Winds - West to North (>6 kt)**
   Pack ice will be pushed towards shore without well defined lead systems. An exception may be direct northerly winds which could produce east/west leads along the polar pack/first-year pack ice boundary.

3. **Winds - Southwest (>6 kt)**
   Pack ice will be driven north, assisted by the nearshore currents. Pressure will build to the north as the first-year pack is driven into the polar pack. The Point Hope polynya will close. Open areas and break-away of the fast ice can occur in Ledyard Bay, northeast of Cape Lisburne. Northerly ice drift will be short lived, lasting only until openings and thin ice areas are closed or deformed.

4. Winds - Southeast to the Northeast (>6 kt)
Flaw leads and polynyas will develop as the pack ice is moved away from the fast ice edge. Winds from the prevailing northeast winter direction will develop the characteristic situation of wide thin ice zones parallel to shore, starting off Point Barrow and expanding towards Cape Lisburne. As the pack ice is driven southwest, a series of tightly spaced east/west lead systems will tend to arch away from the coast. There will be an increasing gradation in ice thickness from southeast to northwest away from the thick fast ice edge.

Of these four postulated wind-driven situations, number 4 is considered most likely. This conclusion is confirmed by satellite imagery and wind statistics. Table 5 summarizes the average percent occurrence of the different wind speed/direction groupings associated with situations 1 to 4 described above. The table combines data from Point Barrow, Wainwright, Point Lay, and Cape Lisburne (Brower et al., 1977).

Table 5 Average Wind Statistics for North Chukchi Coastal Sites - Cape Lisburne to Point Barrow

Wind Class	Percent Occurrence						
	Nov	Dec	Jan	Feb	Mar	Apr	May
1. Calm or Light <7 kt	26	37	33	38	36	35	35
2. West to North >6 kt	14	14	13	12	12	11	10
3. South to Southwest >6 kt	14	12	13	12	12	12	10
4. Southeast to Northeast >6 kt	49	43	45	46	47	48	48

Source: derived from Brower et al. (1977)

Note: Trace occurrences of winds were included in percentages. Totals may exceed 100% by up to 7%.

This table indicates that the wind class most favouring ice movement away from shore occurs between 40 and 50% of the time during the winter period. The next most common condition is calm or light winds which will lead to limited ice pressure or motion.

Wind class 3, favouring closure of the Point Hope polynya, occurs about 12% of the time. This agrees with Shapiro and Burns (1975). They associated polynya closure with short periods of southerly winds producing a northerly ice drift.

The percentage values in Table 5 should be interpreted as a relative guide to the likely proportions of different onshore/offshore ice movement patterns. The absolute values will not necessarily correspond with the actual percent occurrence of polynya formation. The rate and magnitude of ice movement associated with a particular wind will depend heavily on the duration and strength of the wind, as well as the previous history of ice development for that winter. Situations where a loose pack exists offshore may lead to an initially rapid retreat of ice away from shore with the onset of a period of relatively light north to northeasterly winds. As the pack closes and ice pressure develops, the wind strength necessary to maintain ice motion will steadily increase. If the offshore pack is already well consolidated with limited room for contraction, there may be almost little or no motion of the ice away from shore, even with a strong northeasterly wind.

The Chukchi wind climate implies a low probability of severe ice pressure situations along the shipping route. The presence of leads and thin ice areas, as the most often observed ice condition, indicates that ice pressure in the area is likely to be infrequent and short lived. Unfortunately, the state of knowledge concerning the causes and effects of ice pressure precludes any rigorous statistical treatment of the frequency of pressure situations or the actual shipping delays likely to be experienced.

Wind is the dominant driving force causing ice pressure, but there is no agreement as to what wind duration, sustained speed, or direction is necessary to generate a severe ice pressure situation. Bradford (1972) recounts the following general relationships observed between wind and ice pressure from personal observations onboard the *Manhattan, John A. MacDonald,* and *Louis St. Laurent*:

- up to a 25 knot wind speed the percentage occurrence of pressure increased by roughly an order of magnitude for every 9 knot increase in speed

- pressure was noted on 76% of all occasions of onshore winds (considered as winds between 30° and 150° angles to shore) and 51% of offshore winds

- on average, pressure situations observed during onshore winds outlasted those during offshore winds by a factor of 10.

The frequency of ice pressure situations has been interpreted from several studies of Landsat imagery. Hall (1977) measured a state of ice convergence (implying pressure) on 23% of 161 images over a three year period at a point near 77°N, 135°W. Dickins (1979) inferred a maximum winter frequency of ice pressure situations in the Chukchi Sea of 25% (January to July).

In summary, the limited database on actual ice pressure situations, combined with known wind statistics (shown in Table 5), indicates that ice pressure will not cause significant interruptions to the operation of high ice class vessels in the Chukchi Sea.

6.2 Leads Available for Tanker Transit

Recurring leads and young ice areas are an important part of the ice environment affecting icebreaking vessel operations and offshore structures in the lease sale area. Figures 28 to 30 are maps drawn from a typical cross section of DMSP and NOAA satellite images used in this study. In almost every month of every year polynyas and leads were visible on the images.

Table 6 lists the dates of all available DMSP images and the percentage of the tanker route that appears to be easily transited for a given date. The route was assumed to follow outside the 14 fathom (26 m) isobath, around Cape Lisburne, north to Icy Cape (Zone 5) and then head west to the central production site (Zone 7). Leads, open water, and thin or young first-year ice visible on the images define what was considered easily transited. The percentages are conservative visual estimates made from the DMSP images by an experienced icebreaker designer from the Valmet Corporation (A. Keinonen).

Table 6 indicates that between November and May, open water, leads, and thin ice areas occur frequently along the tanker route.

In an attempt to calibrate the ice conditions visible on the large scale DMSP and NOAA images, nine Landsat images of the lease sale area were found for dates that correspond closely to the dates of the DMSP and NOAA images. The availability of suitable Landsat images is limited by time of year (no images are available for the November to February period), by location (Landsat covers the nearshore Chukchi Sea area but not the offshore area in the vicinity of Zones 7 and 8), and by cloud cover (no images with over 50% cloud cover were ordered).

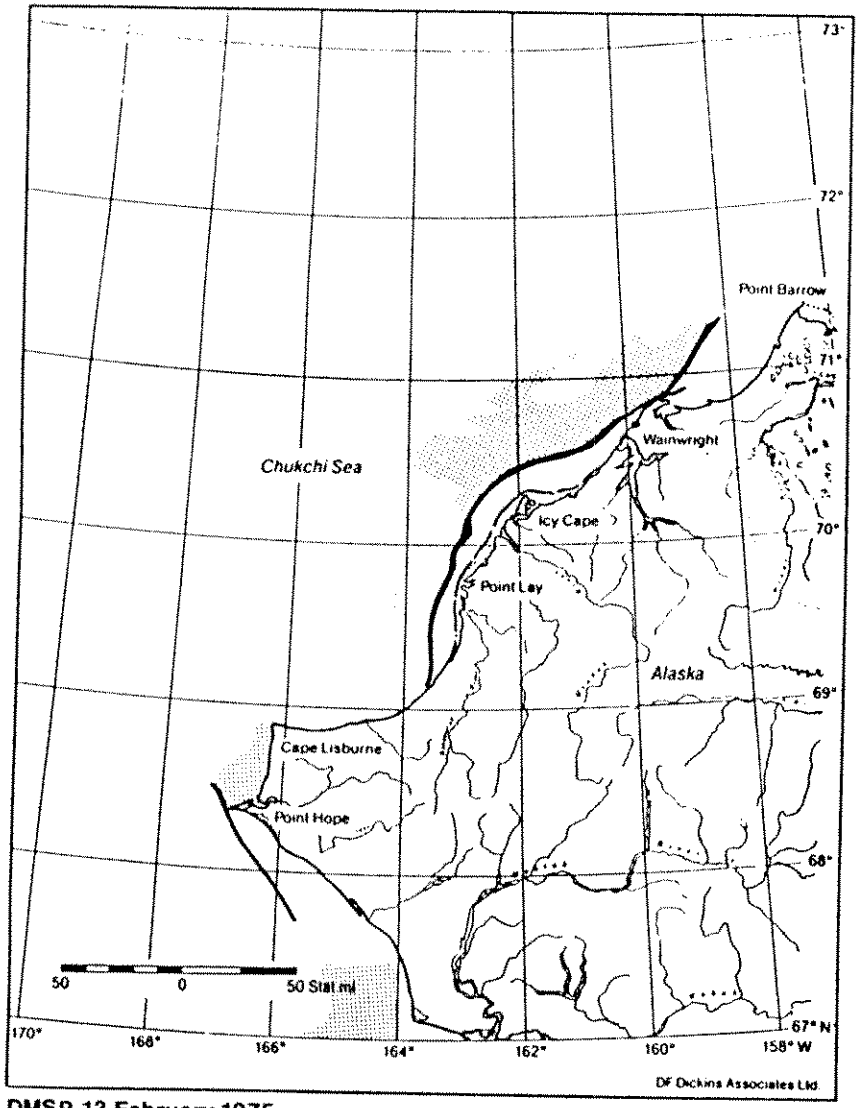

DMSP, 13 February 1975

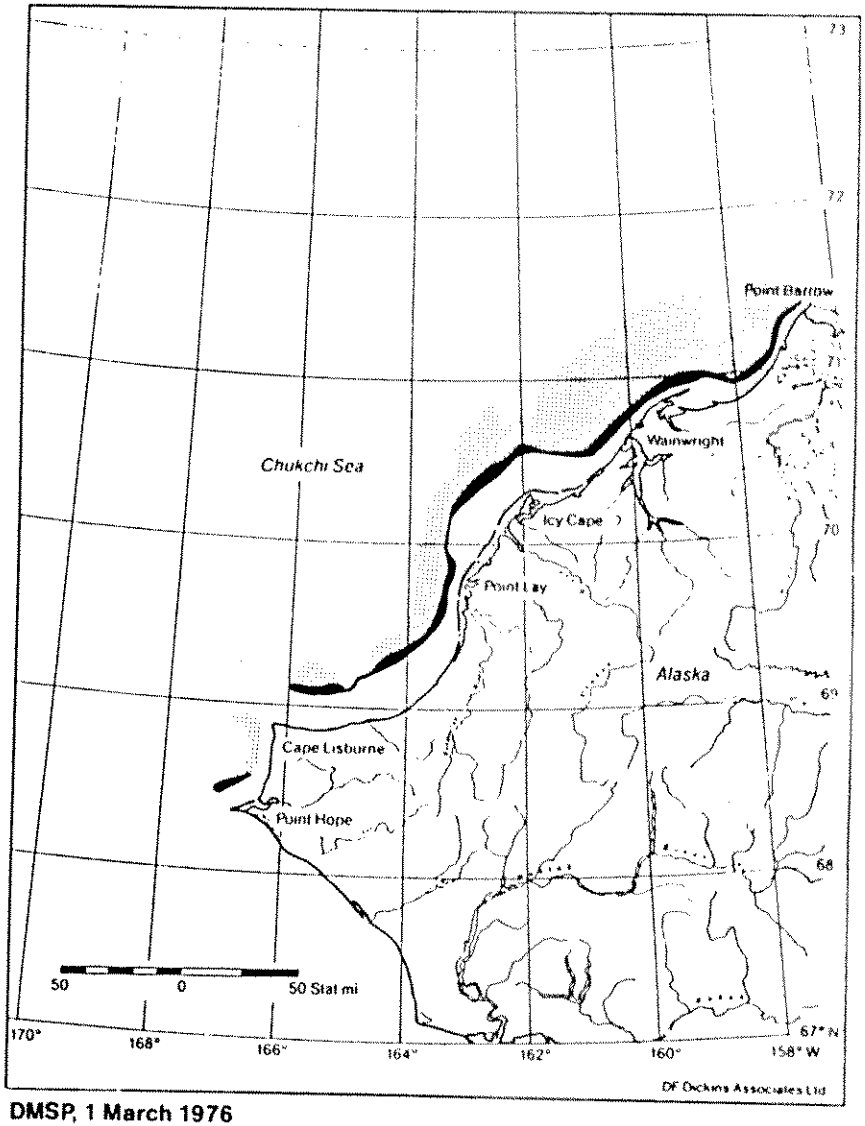

DMSP, 1 March 1976

Figure 28 **Examples of the Winter Flaw Lead and Young Ice Areas, 1975 and 1976**

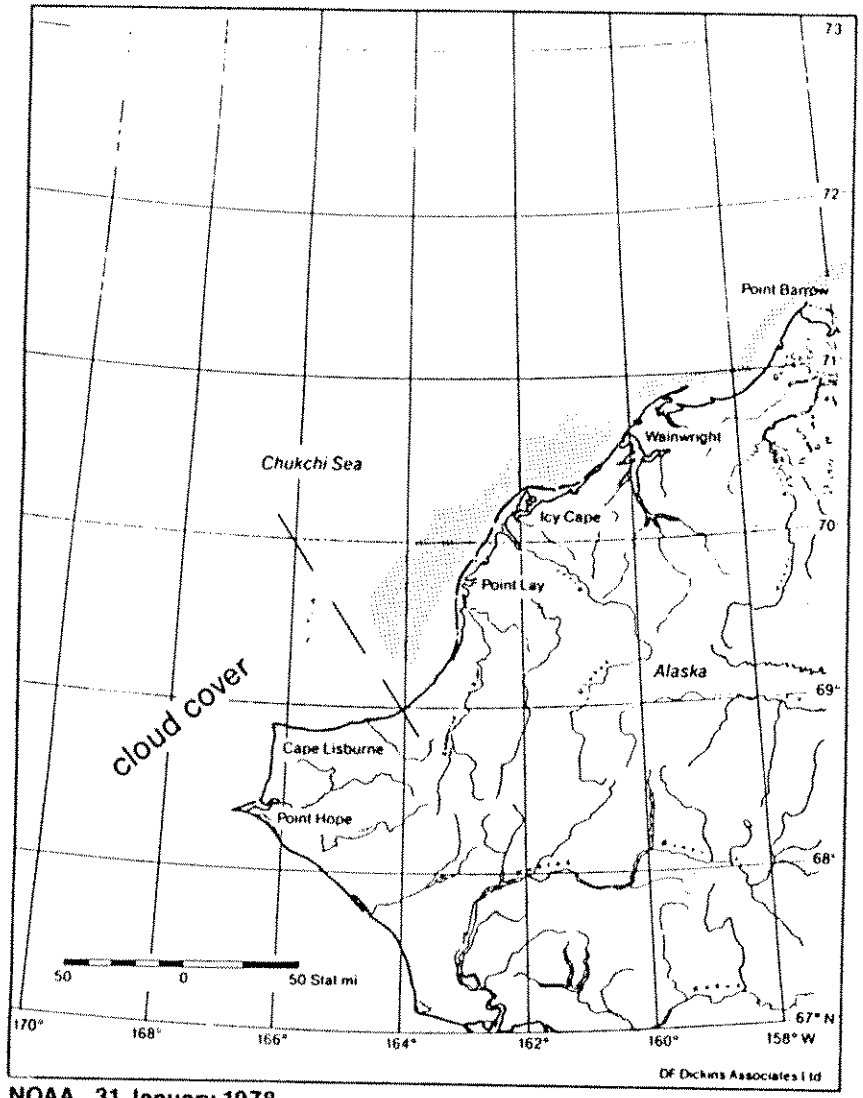

NOAA, 31 January 1978

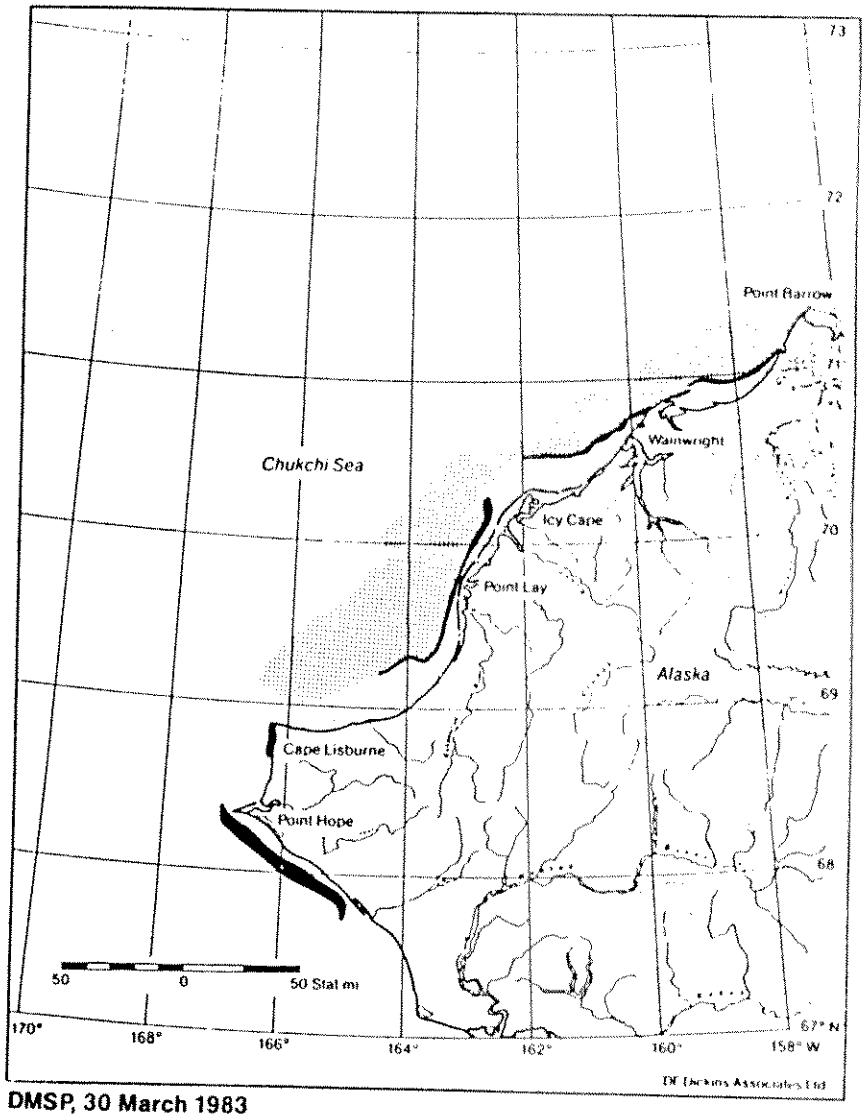

DMSP, 30 March 1983

Figure 29 **Examples of the Winter Flaw Lead and Young Ice Areas, 1978 and 1983**

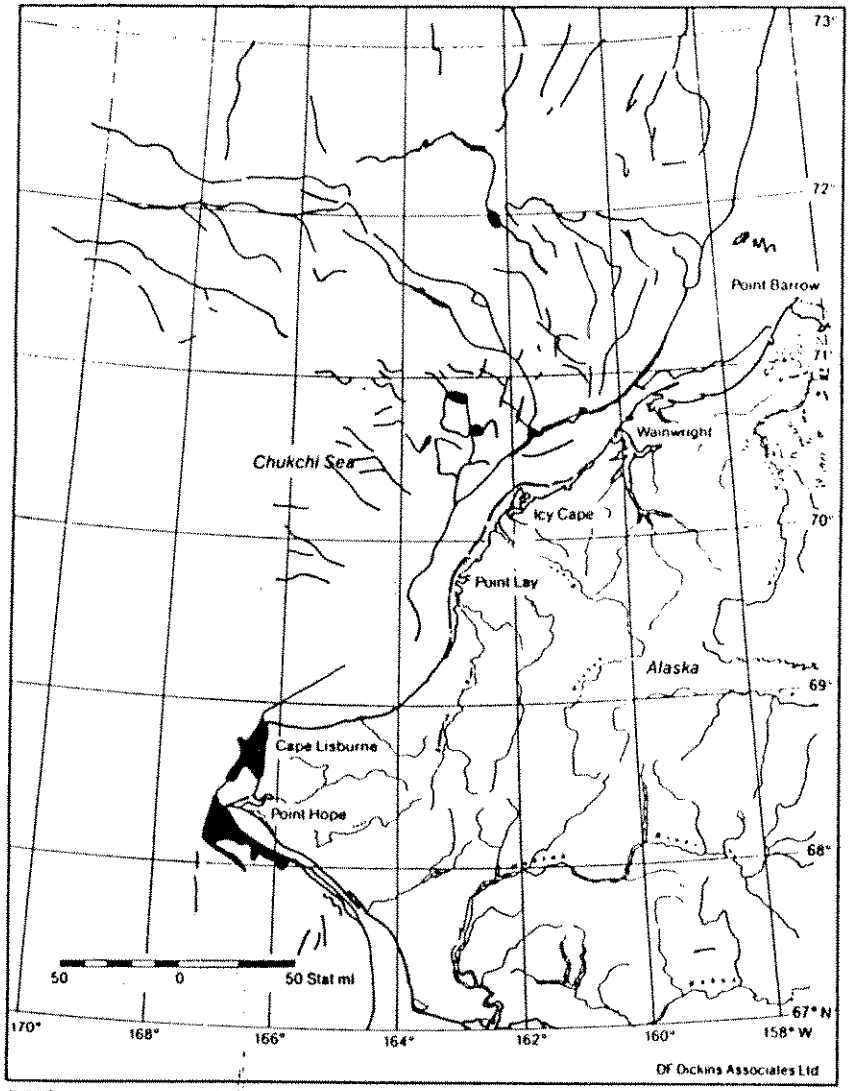

DMSP, 12 January 1975

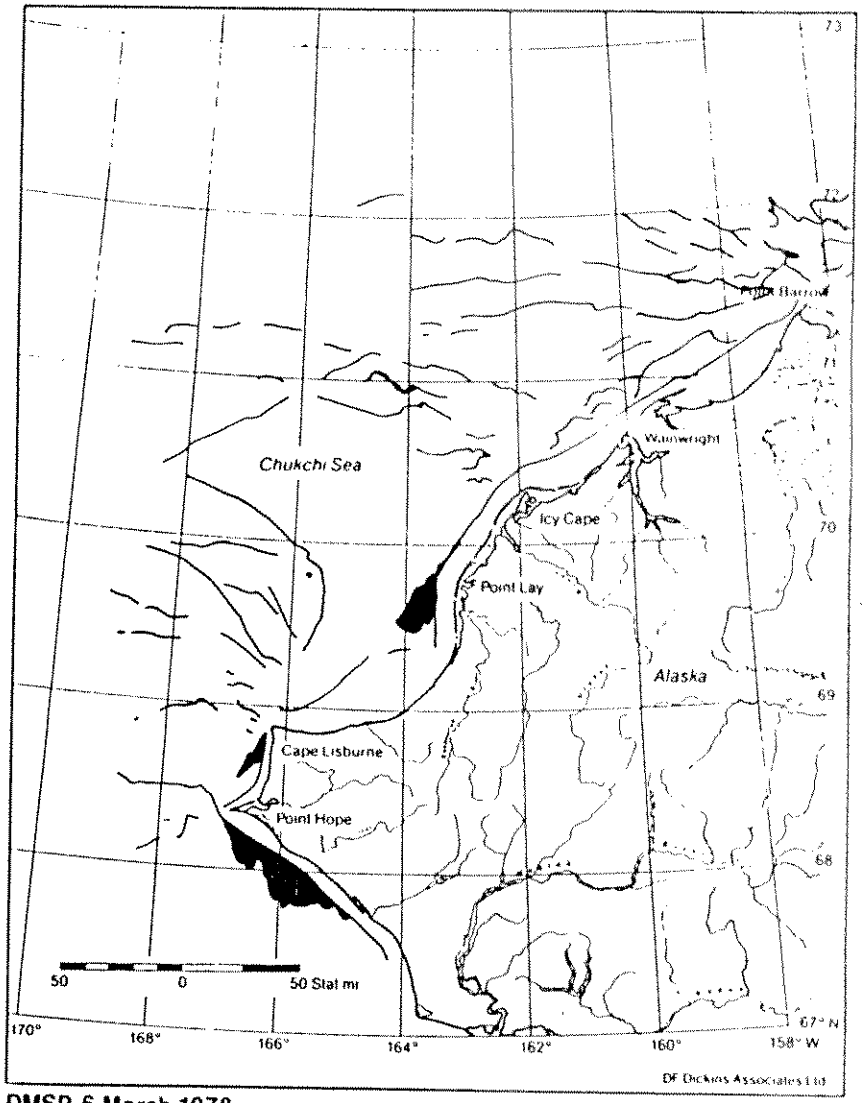

DMSP, 6 March 1978

Figure 30 Examples of Winter Lead Systems Offshore, 1975 and 1978

Table 6 Proportion of Tanker Route Easily Transited as Estimated from DMSP Images

Date	Percentage of Route	
	Zone 5	Zone 7
Nov 02 - 73	100	40
Jan 08 - 74	95	40
Jan 17 - 74	95	95
Jan 03 - 75	100	50
Jan 12 - 75	50	80
Feb 13 - 75	70	95
Nov 01 - 75	90	90
Nov 18 - 75	100	80
Nov 22 - 75	100	70
Dec 06 - 75	90	90
Dec 15 - 75	95	70
Jan 07 - 76	hazy	hazy
Jan 26 - 76	90	hazy
Mar 01 - 76	100	80
Dec 09 - 76	90	75
Dec 15 - 76	50	50
Nov 10 - 77	50	80
Dec 18 - 77	80	10
Jan 16 - 78	95	75
Jan 26 - 78	95	80
Feb 09 - 78	50	hazy
Mar 06 - 78	10	80
*Mar 23 - 78	95	75
Apr 01 - 78	hazy	80
May 17 - 78	100	hazy
Dec 07 - 78	hazy	hazy

Table 6 Proportion of Tanker Route Easily Transited as Estimated from DMSP Images (Continued)

Date	Percentage of Route	
	Zone 5	Zone 7
Jan 31 - 79	70	70
Jun 03 - 79	100	
Dec 23 - 79	50	50
Jan 15 - 80	50	90
Jan 16 - 80	30	50
Feb 17 - 80	50	60
Mar 17 - 80	hazy	hazy
*Apr 09 - 80	50	50
May 29 - 80	100	40
Jan 25 - 83	hazy	hazy
Jan 31 - 83	20?	20?
*Feb 26 - 83	80	70
*Mar 11 - 83	50	50
Mar 30 - 83	80	20
*May 09 - 83	95	30
Jan 01 - 84	10	70
Jan 15 - 84	50	30
Feb 07 - 84	90	90
*Mar 24 - 84	90	80
*May 20 - 84	50?	50?
Jun 06 - 84	90	hazy
Dec 23 - 84	hazy	90

*Landsat image available for comparison.

Figures 31 to 34 are two DMSP and Landsat image pairs for March 1978 and March 1983. The areas covered by the Landsat images are outlined on the DMSP images. Note that the DMSP images are enlarged from their original scale of 1:7,000,000 while the Landsat images are at their original scale of 1:1,000,000. The advantages and disadvantages of NOAA, DMSP, and Landsat images are compared in Appendix D.

Scale – 1:3,000,000

Figure 31 DMSP Satellite Image Showing Tanker Route (Overlay) and Corresponding Landsat Coverage (Figure 32), 23 March 1978

Figure 32 Landsat Image Showing Numerous Leads and Open Water Areas Offshore of Cape Lisburne, 27 March 1978

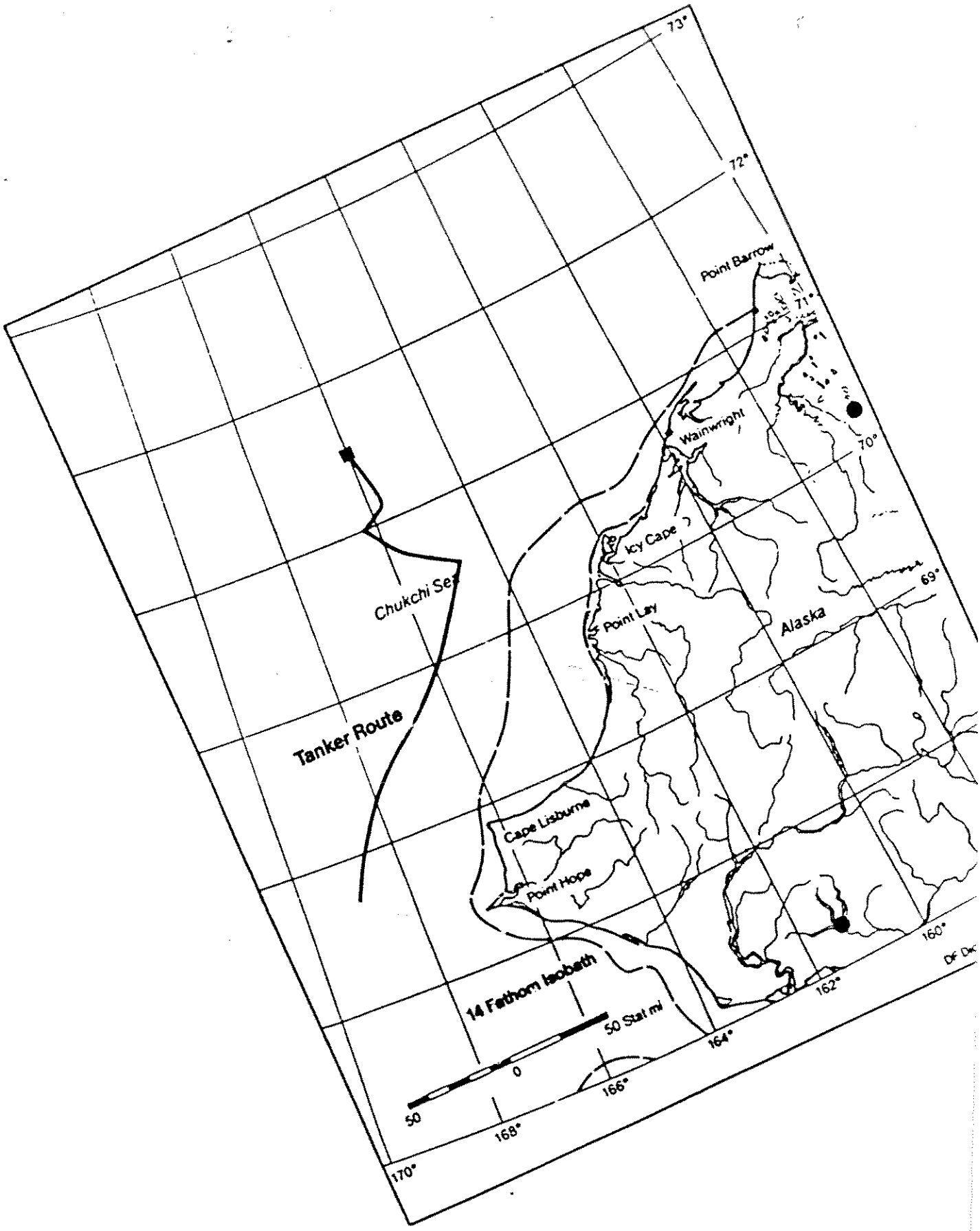
73°
72°
Point Barrow
71°
Wainwright
70°
Icy Cape
69°
Chukchi Sea
Point Lay
Alaska
Tanker Route
Cape Lisburne
Point Hope
14 Fathom Isobath
50 Stat mi
0
50
168°
166°
164°
162°
160°
170°

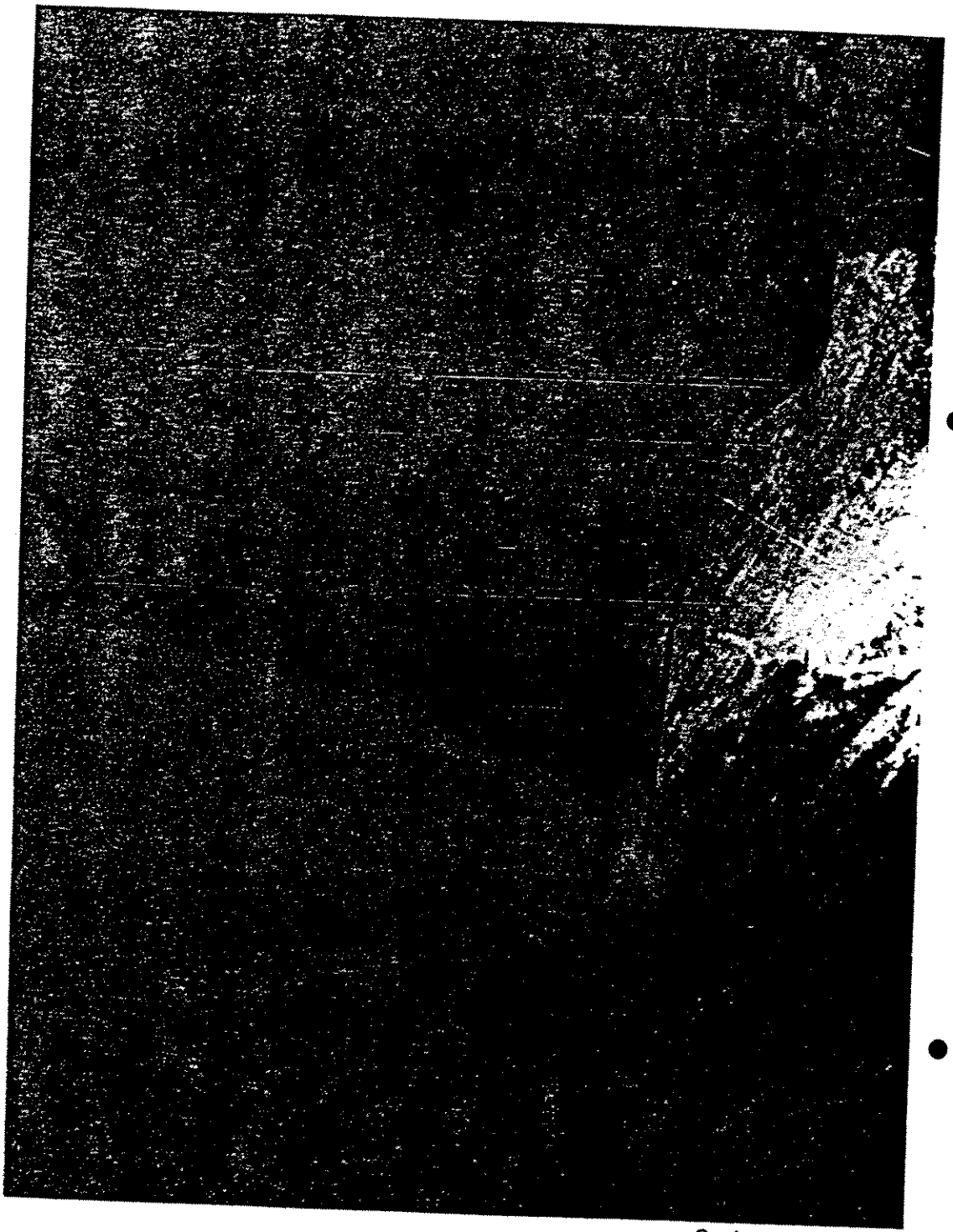

Scale – 1:4,000,000

Figure 33 DMSP Satellite Image Showing Tanker Route (Overlay) and Corresponding Landsat Coverage (Figure 34), 11 March 1983

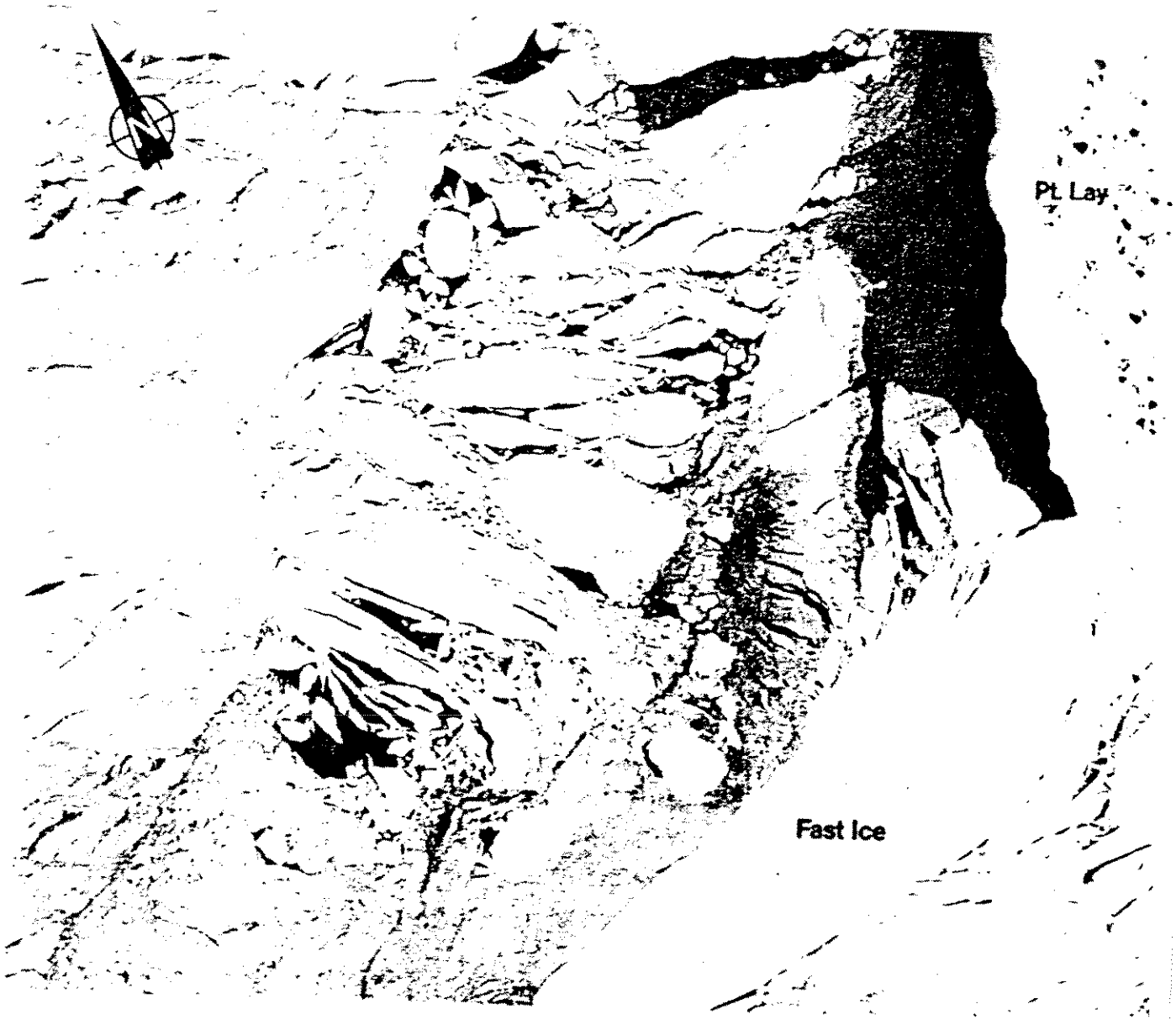

Figure 34 Landsat Image Showing Open Water and Thin Ice Areas Grading to Fractured Pack Ice Seaward of the Fast Ice Edge, 13 March 1983

7.0 FIRST-YEAR LEVEL ICE THICKNESS

Maximum level first-year ice thickness is often calculated according to the accumulation of freezing degree days (FDD), using the so-called Zubov rule (Zubov, 1945).

$$I^2 + 50\,I - 8R = 0$$

where I = ice thickness (cm)
R = cumulative freezing degree days in degrees centigrade (below -1.8°C).

This method provides reasonable results as long as the snow cover on the ice is not excessive.

Level ice thickness nearshore in the fast ice zone is most accurately calculated by using Zubov's rule with corrected FDD values. There is a significant increase in cumulative annual FDD values (based on O°C) moving from south to north through the Chukchi Sea lease sale area; from 3500 FDD at Cape Lisburne (68°50'N) to 4800 FDD at Point Barrow (71°30'N) (LaBelle et al., 1983). FDD values reported in LaBelle et al. (1983) were modified in this study by discounting freezing degree days cumulated before actual freeze-up at a particular location, and by using the freezing point of seawater (-1.8°C) as the baseline for FDD cumulation.

The maximum predicted offshore ice thickness at the end of April, calculated with these modified FDD values, ranges from 4.3 ft off Cape Lisburne to 5.2 ft off Point Barrow. These results indicate that there is 1.0 to 1.2 ft less ice than calculated for shore stations in the Alaska Marine Ice Atlas (LaBelle et al., 1983). Note: In preparing this report, it was found that the entire section entitled "Calculated Ice Thickness" in the Alaska Marine Ice Atlas is in error (confirmed by personal communication with the author J. Wise, 26/02/86).

Calculations carried out in this study compare favorably with the only long term historical ice thickness records for the study area: Point Hope in the Chukchi Sea and Mekoryuk Bay (Nunivak I.) in the Bering Sea (Bilello and Bates, 1962-1972, in LaBelle et al., 1983).

Level first-year pack ice thickness offshore is known to be significantly lower than the adjacent landfast ice thickness. For example, continuous ice draft profiles at a deep water site in the Canadian Beaufort Sea showed average level ice thickness between 20 and 35% less than landfast ice thickness measured at the same time (Hudson et al., 1980; Dickins and Buist, 1980).

Level ice thickness measurements from the *Polar Sea* in February 1981 averaged between 2 and 4 feet from Cape Lisburne to Point Barrow respectively (Voelker et al., 1981b); interestingly a level ice thickness of 4.6 ft was reported by Brigham (1986) for the same voyage in the more southerly region between the Bering Strait and Cape Lisburne - this condition probably reflects the presence of leads and thin ice areas along the ship route north of the Cape . The *Polar Sea* data was collected in association with pressure ridge profiling and represents the upper bound of level first-year ice thickness which was present in the area at the time of the voyage. Photographs and documentation of the February 1981 cruise point to large areas of new and thin ice offshore which would have thickness values of less than one foot.

In contrast, the *Polar Sea* 1983 cruise encountered thicker level ice of 6 feet offshore Wainwright on April 8, 1983. Between the Bering Strait and Cape Lisburne, first-year ice thicknesses on that voyage ranged from 3.4 to 4.8 ft (Voelker et al., 1984).

Leads and openings in the Chukchi Sea offshore ice cover are common throughout the winter (refer to satellite images in Sections 2.0 and 6.0). The overall effect of the young ice forms present offshore is to significantly reduce the average first-year ice thickness encountered in a region. This effect is demonstrated in Figure 35 which compares the calculated maximum first-year ice thickness at the end of April, with the average thickness derived from actual concentrations of different ice types (1981-1984 ice charts). The difference is quite dramatic, particularly in the southern areas of the lease sale. As the proportions of thin and young ice decrease moving north, the average thickness values begin to approach the maximum calculated values based on FDD days.

Figure 35 shows three curves for maximum first-year ice thickness that were calculated as follows:

1. from erronecus data contained within the Alaska Marine Climate Atlas;

2. from Potocsky (1975) using the correct ice growth formula for shore stations; and

3. using the correct ice growth formula with reduced FDD to account for later freeze-up offshore.

In addition, a stepped line is shown to indicate values of maximum ice thickness used in previous Alaskan shipping studies (Dickins, 1979; Halebsky, 1978; and Han-Padron Associates, 1984). Actual measurements made during the 1981 and 1983 *Polar Sea* cruises tend to fall between the curve of maximum level ice thickness and the curve of "blended" thickness which accounts for the presence of thin ice areas (solid curved line in Figure 35).

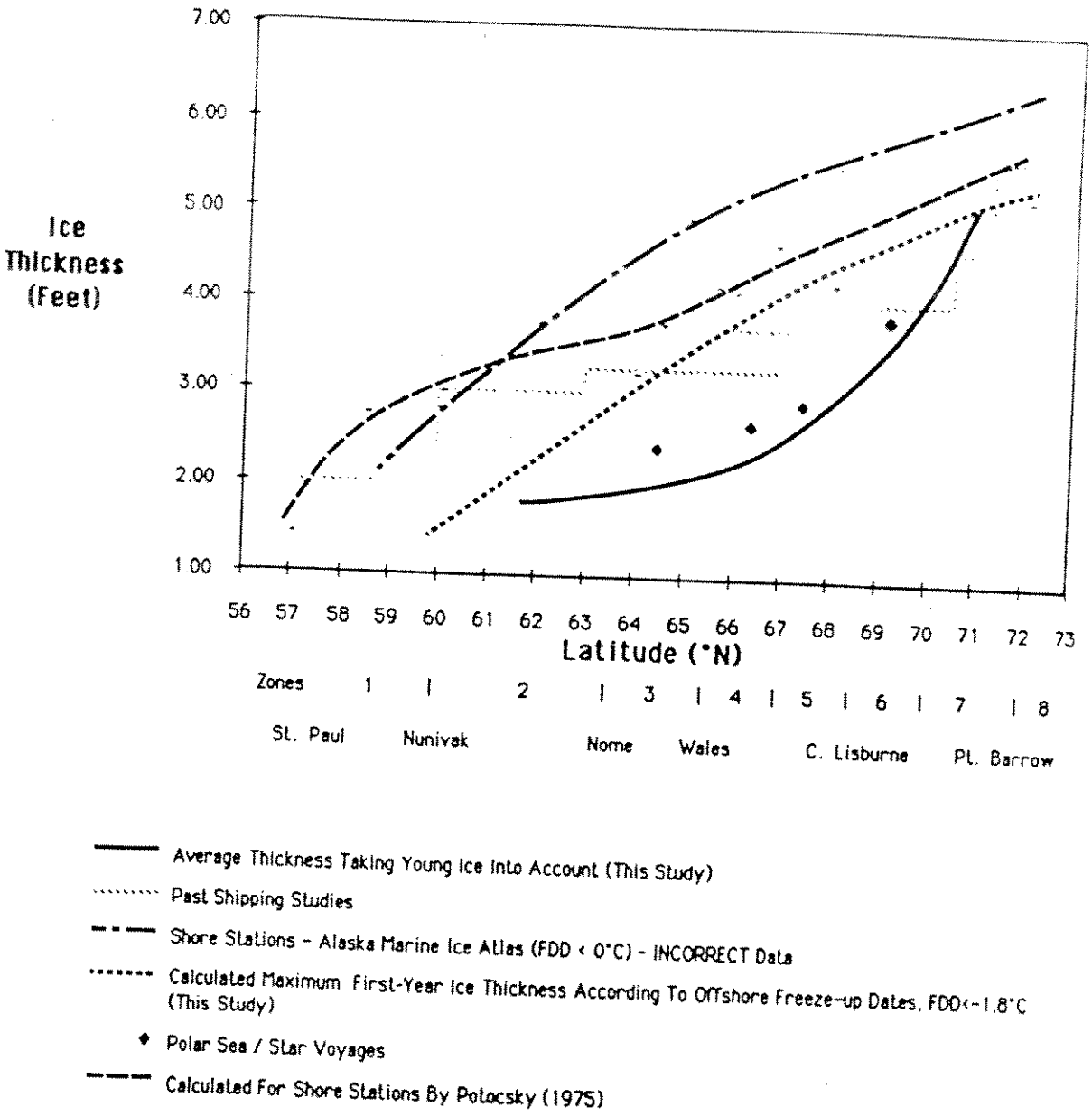

Figure 35 Comparison of Level First-Year Ice Thicknesses at the End of April

8.0 ICE ROUGHNESS

Vessel operations along the proposed route will encounter varying degrees of rough ice, in the form of discrete ridges, rubble fields, or rafted floes. Deformed ice thickness can be many times the level ice thickness values discussed in Section 7.0.

There is an extremely limited public database which provides a quantitative measure of ice roughness in the Bering and Chukchi Seas. Available information can be derived from four basic sources:

1. Airborne Laser Profiles
2. Aerial Photography
3. Subjective Airborne and Shipboard Observations
4. Individual Ridge and Rubble Field Profiles (Polar Class icebreaker voyages)
5. Synthetic Aperture Radar (SAR)

These different data sources each provide a particular representation of deformed ice. No one data source provides a complete three dimensional picture of the ice cover through which the vessel will be operating.

Laser profiles provide fine scale elevation statistics along a line. Depending on the minimum elevation measured, a laser record may or may not "see" rubble fields important to vessel performance.

SAR can map the areal extent of deformed ice but provides no quantitative information on feature height.

Shipboard observations of ridge sails are biased by the vessel's tendency to seek leads of opportunity and are limited by the subjectivity of the measurements. Actual profiles of ridge keel geometry provide the only cross sectional view of the ice cover, but necessarily involve a very small sample population.

Aerial photography provides a best compromise data source in that it allows clear discrimination between rubble and discrete ridges (something which is not possible with a laser elevation profile).

This study presents representative examples from publicly available data for the Chukchi and Bering Seas and includes first-year ridge height statistics from the much more extensive research conducted in the Beaufort Sea.

Actual spot values for ridge frequencies and maximum ridge heights (where known) are included in the individual zone summary sheets in Appendix A.

The following sections discuss examples of ridging information which apply to the Bering and Chukchi Seas.

8.1 Bering Sea Ice Roughness

Direct measurements of Bering Sea ice ridges are confined to the joint industry/Maritime Administration Polar Class icebreaker research voyages (Voelker et al., 1981a; 1981b; 1982, 183, and 1984). Figures 36 and 37 show typical representations of pressure ridges encountered in April 1980 in the south Bering Sea (Voelker et al., 1981a).

These ridges showed the following characteristics in the vicinity of 60°31'N, 177°12'W:

Average Sail to Keel Ratio	1:3.3
Average Sail Height	3.4 ft
Range in Sail Heights	1.2 to 7 .0 ft
Maximum Keel Depth	33 ft

Ridge Frequency	
Small (<3 ft)	4
Medium (≥3 ft but <6 ft)	4
Large (6 ft)	1
Total	9 ridges/mile

The 1980 cruise attempted to profile "average" rather than extreme ice features.

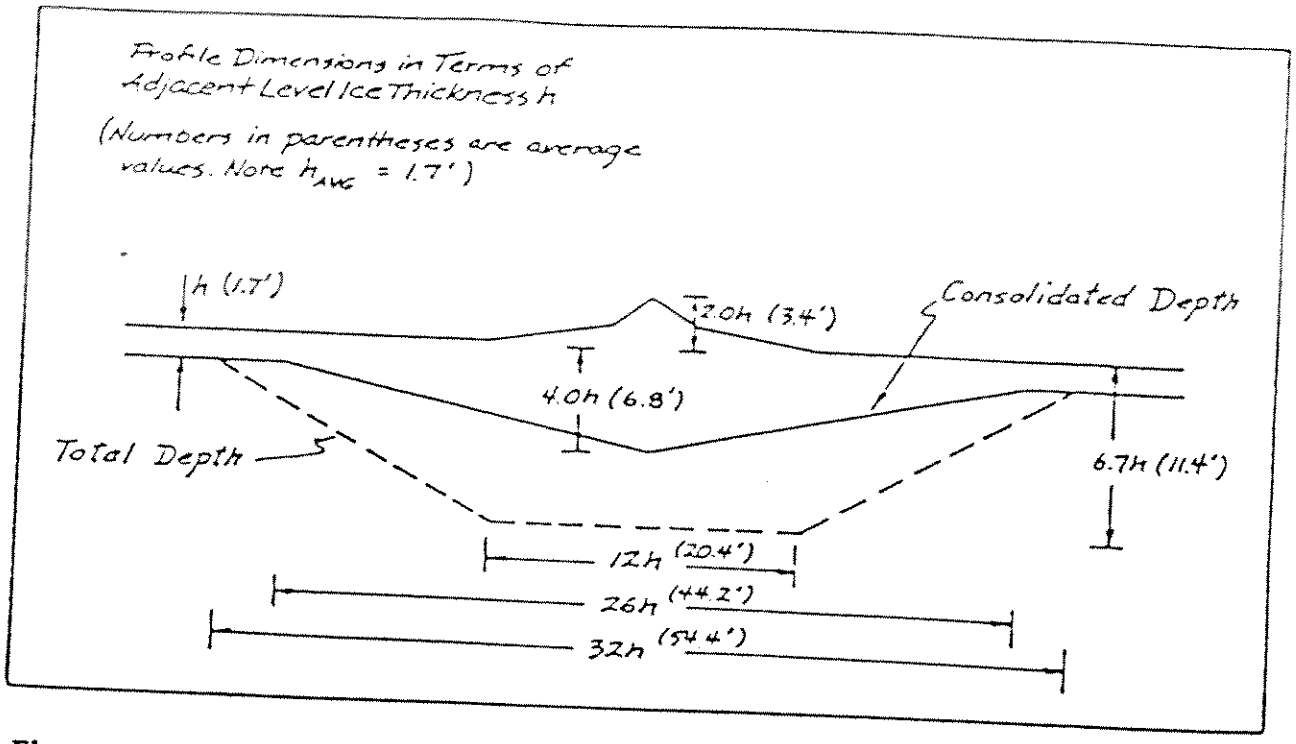

Figure 36 Average Representation of Pressure Ridges Encountered in the South Bering Sea (Voelker et al., 1981a)

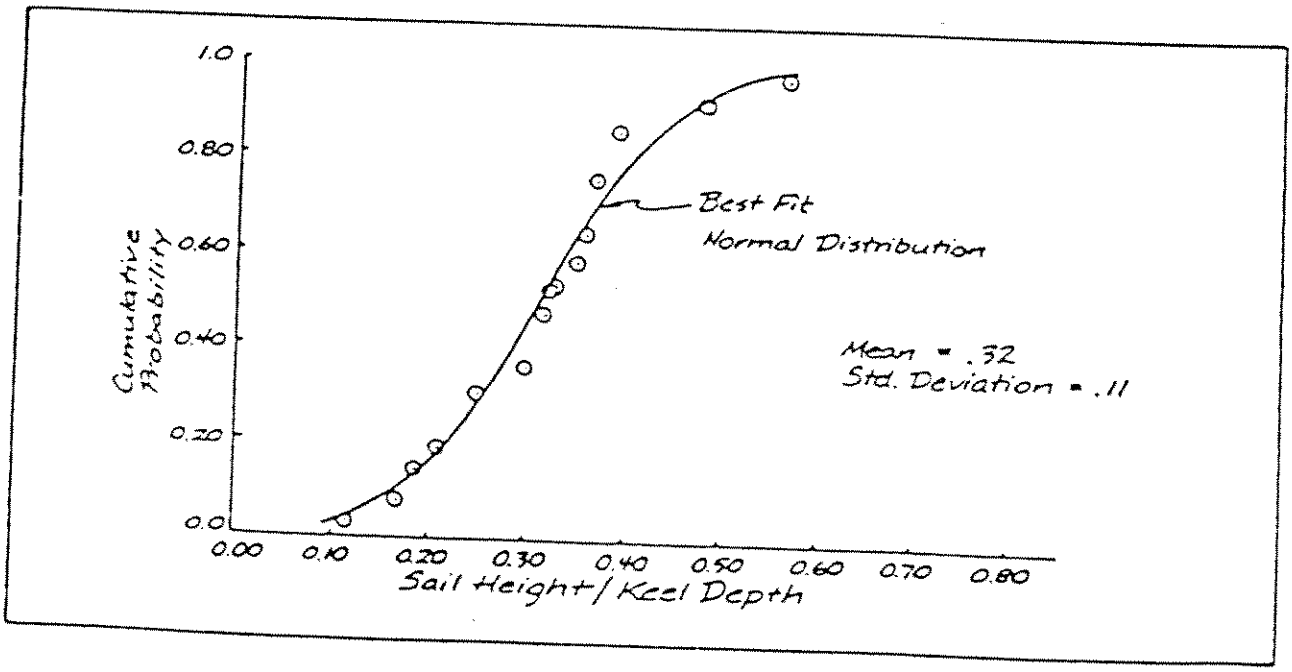

Figure 37 Cumulative Probabilities of Sail/Keel Ratios for Pressure Ridges Encountered in the South Bering Sea (Voelker et al., 1981a)

North Bering Sea

Ridge height distributions have been published for the north Bering Sea using stereo photogrammetry (Wheeler, 1981). Figure 38 shows the cumulative probability distribution of ridge sail heights in the vicinity of 63°10'N, 172°10'W during April 1977. The ridge frequency along 8.5 miles of profile line was 8.6 ridges/mile. Maximum sail height was 9.6 ft.

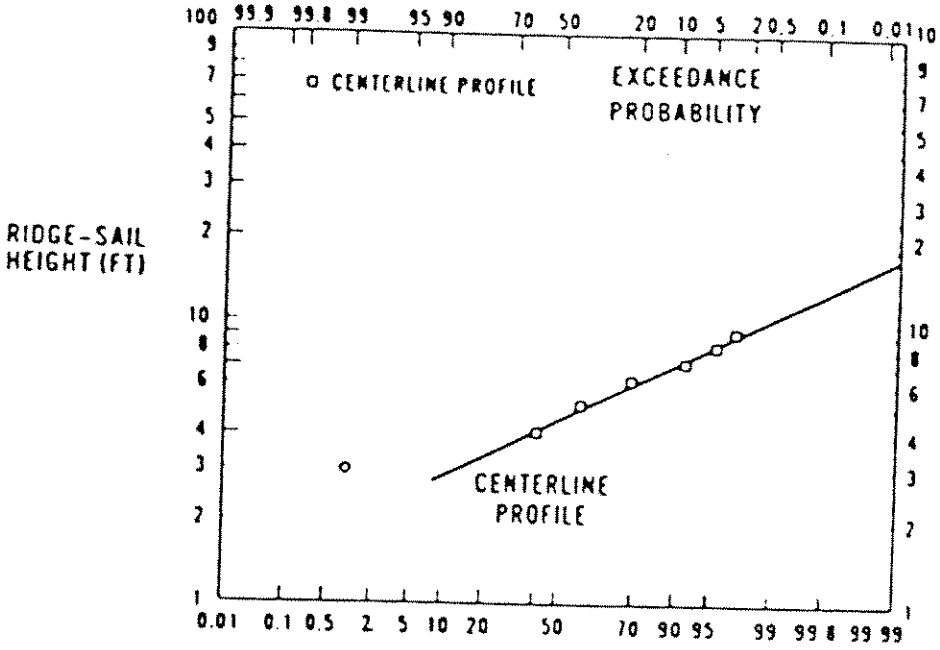

Figure 38 **Ridge Height Distribution, North Bering Sea, April 1977 (Wheeler, 1977)**

The February 1981 *Polar Sea* voyage reported the following ridge frequency in the north Bering Sea, from St. Lawrence Island to King Island (Voelker et al., 1981b):

Ridge Frequency	
Small (<3 ft)	8
Medium (>3 ft but <6 ft)	9
Large (> ft)	1
Total	18 ridges/mile

In April 1982, 19 first-year ridges were profiled in the north Bering Sea, in the area 62° to 64°N and 173° to 168°W. This project set out to profile the largest features present in the study area. Results showed the following range in ridge characteristics (Voelker et al., 1982):

Average Sail to Keel Ratio	1:3.55
Range in Sail to Keel Ratio	1:1.3 to 1:6.5
Average Sail Height	6.2 ft
Range in Sail Heights	1.0 to 11.5 ft
Range in Keel Depths	3.7 to 40.4 ft

Figure 39 shows two cross sections of ridges profiled during the 1982 cruise.

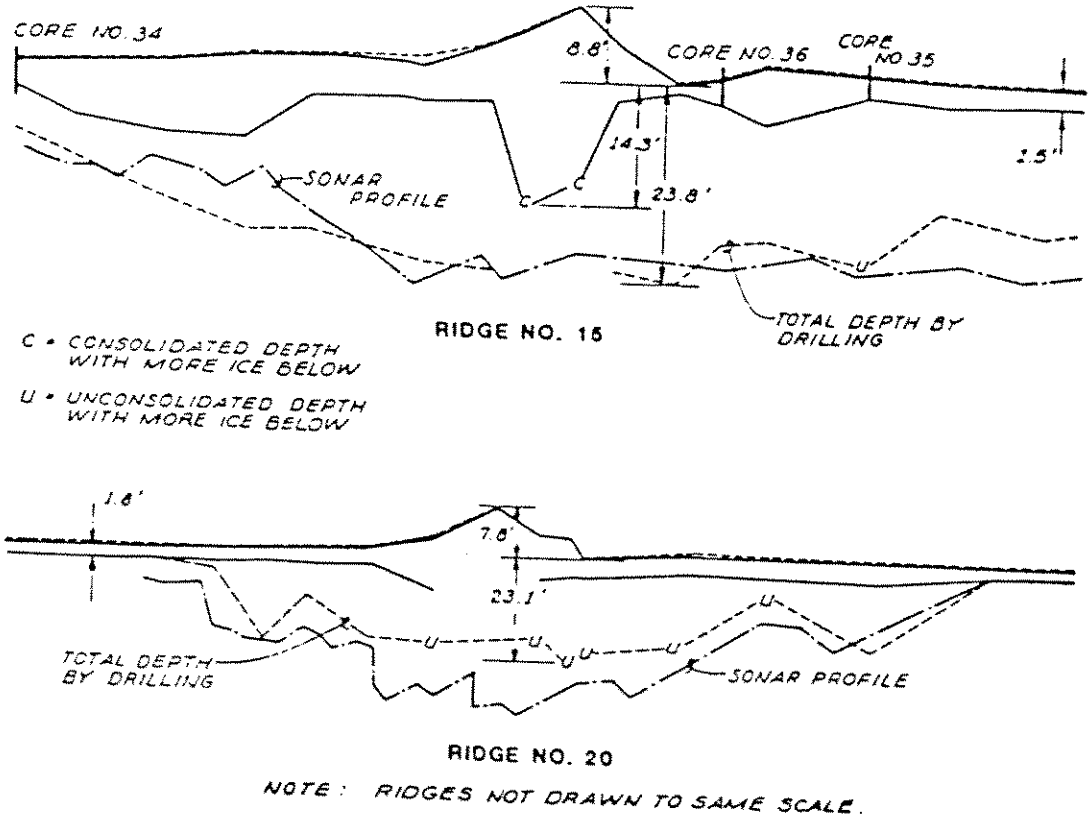

Figure 39 First-Year Pressure Ridge Profiles, North Bering Sea (Voelker et al., 1982)

8.2 Chukchi Sea Ice Roughness

Ridge severity in terms of the degree of consolidation (depth of solid ice) and height of features increases moving north from the Bering Strait. In practice, the combination of pressured ice and extensive unavoidable rubble fields often leads to more severe navigation conditions in Zone 4 from the Bering Strait to Cape Lisburne, than along the more northerly sections of the proposed shipping routes (Brigham, 1986). The experiences gained with the *Polar Sea* and *Polar Star* do not necessarily indicate that offshore ice conditions in the north Chukchi Sea are less severe than the south Chukchi, but that ships are often able to make use of recurring lead systems to avoid large areas of deformed ice north of Cape Lisburne.

Historical estimates of the areal percentage of deformed ice have shown typical mid-winter values of about 25% (U.S. Navy, 1954-66). The actual percent deformation is highly variable from year to year and over short distances at any given point in time. Aerial photography collected during the 1979/1980 winter (OSI, 1981) showed the following deformation estimates for the environmental zones used in this study (refer to Figure 1):

Table 7 Estimates of Percent Deformed Ice (OSI, 1981)

Environmental Zone	March 1980	May 1980
Zone 8	10-40	10-20
Zone 7	10-40	10-40
Zone 6	10-40	no data
Zone 5	10-60	10-80
Zone 9	10-20	10-20
Zone 4	40-80 (West)	40-80 (West)
	20-60 (East)	20-60 (East)

Note: the winter of 1980 was considered by OSI as a relatively warm winter with the ice slightly less compacted than normal

In comparison, Synthetic Aperture Radar (SAR) imagery collected in 1982 showed ice deformation north of 70° (Zone 7) to be in the range 30 to 60% vs. an equivalent value of 10 to 30% south of 70°.

The majority of the deformed ice area will be comprised of rubble fields with typical elevations of less than 1.5 ft and maximum solid ice thicknesses in the range from 4 to 6 ft. Total ice thickness, including soft unconsolidated ice, will typically be double the solid ice thickness (i.e., 8 to 12 ft).

Extreme first-year ridge heights in the Chukchi Sea can reach 18 to 20 ft. The maximum first-year keel depth profiled in the Chukchi Sea was 78 ft in 1983. The ratio of keel to sail height derived from a limited number of Chukchi ridge profiles is 3.6:1, compared with 3.1:1 derived from a larger Bering Sea database. In the north Chukchi Sea, a ratio of about 4.5:1 is considered more representative. (based on profiles by CRREL researchers in the Beaufort Sea).

Laser profiles flown perpendicular to the Chukchi coast line from Point Barrow, Wainwright, and Point Lay in 1976 showed that ridge frequencies more than doubled from December to April (Tucker et al., 1979). Typical offshore ridge frequencies ranged from 4 to 12 ridges/mile (counting all features over 2 ft in elevation). Compared with more recent data collected by industry AOGA studies, and shipboard observations, it appears that ridge frequencies in 1976 were lower than average. For example, OSI in May 1980 documented ridge frequencies of 8 to 17 ridges/mile (counting all features over 4 ft) along lines oriented similarly to the earlier 1976 flights.

Care is needed in interpreting ridge frequency data. The choice of cut-off height is extremely important in determining the absolute frequency. For example, Hanson (1985) reported ridge frequencies up to 36 features per mile counting any sail over one foot in height; this value is 2 to 3 times the frequency values tabulated from laser records using a 2 to 3 foot cutoff height.

A number of areas have been identified as having consistently higher ridging intensities. Tucker et al. (1979) singled out two areas, north of Icy Cape and Cape Lisburne, as having the most extensive ridging (13-14 ridges/mile).

Two other areas of recurring ice deformation have been detected by satellite and visual observations. One, Herald Shoal, lies just outside the lease area boundary between 70° and 71°N. The second site corresponds to an area of grounded islands of sea ice referred to as "Katie's Floeberg." These islands recur at roughly 72°N, 162°W, in the vicinity of charted shoals. Although a localized phenomenon, the ice grounded on these shoals affects the distribution of leads in the Chukchi Sea pack ice for tens of miles. A large polynya (open water area) often forms in the lee of the pack ice motion past the grounded ice islands (Kovacs, 1976).

The most extensive data base on first-year ridge height distributions relevant to the north Chukchi Sea is Gulf Canada Resources Ltd. (now Gulf Canada Corporation) observations of 12,436 first-year ridges in the Canadian Beaufort Sea over an eight year period.

A comparison was made between the Gulf Canada data set and the available profile line of 1329 ridges off Point Lay in the Chukchi Sea (Tucker et al., 1979). Mean height values for the Beaufort and Chukchi Sea data sets were almost identical, at 5.2 and 4.95 ft, respectively. Figure 40 shows the ridge height distributions from the publicly available Gulf Canada data set (Wright and Schwab, 1973-1981).

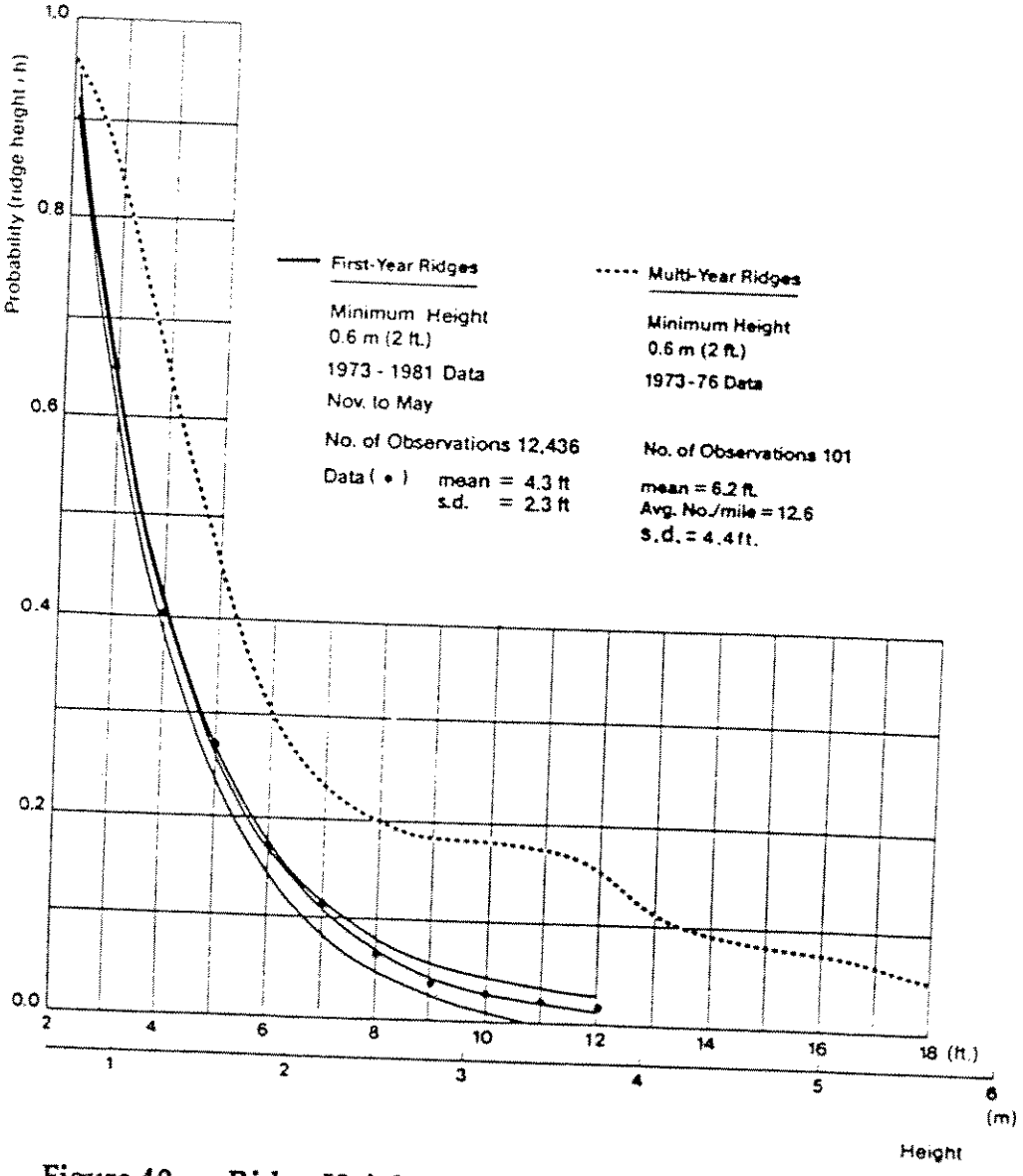

Figure 40 Ridge Height Distributions in the Canadian Beaufort Sea (Wright and Schwab, 1973-1981)

9.0 Ice Motion

9.1 Chukchi Sea Ice Motion

Winter ice speeds in the Chukchi Sea are shown in Figure 41. Daily ice speeds derived from drifting buoys are presented for two regions: 67°-70°N and 70°-73°N. Figure 41 shows that 10% of the time the speeds exceed 0.6 knots in the southern region and 0.5 knots in the northern region. Table 8 shows the average and maximum speeds in the Chukchi Sea for the two regions.

Table 8 Chukchi Sea Winter Ice Motions

Region	Average	Maximum	Observations
67°-70°	0.27 knots	1.0 knots	96
70°-73°	0.21 knots	1.24 knots	438

Ice speeds are slightly higher south of 70°, as one would expect in more open ice conditions.

The ice motion data was obtained from a drifting buoy database maintained by the Polar Science Center at the University of Washington (Colony, pers comm). The database includes the work of the Arctic Buoy Program at the Polar Science Center and other buoy deployments for groups such as OCSEAP. Buoys become frozen into the ice during the winter and can predict ice motions with a high degree of confidence.

The buoy database was filtered to select buoy trajectories within an area bounded by 67° and 73° N, and 156° and 170° W. Altogether, 10 buoy trajectories were available for the study area. Daily buoy velocities were calculated from the buoy positions. The possible error in the positions is ±300 m.

The buoys typically drifted west-northwest in the Central Chukchi Sea, while between Cape Lisburne and Cape Barrow, buoys in the nearshore ice moved back and forth along the shoreline (Pritchard and Hanzlick, 1988). Pritchard

and Hanzlick (1988) found that both winds and currents played a role in controlling the buoy drift, but that current was the dominant factor.

Sea ice is much more dynamic in the Chukchi Sea than in the Beaufort Sea. The average winter ice speeds are two to three times greater in the Chukchi Sea (0.21 and 0.27 versus 0.1 in the Beaufort Sea). Ice speeds tend to be greatest nearshore within the flaw polynyas. Lower ice speeds can be expected in the more consolidated pack ice to the northwest.

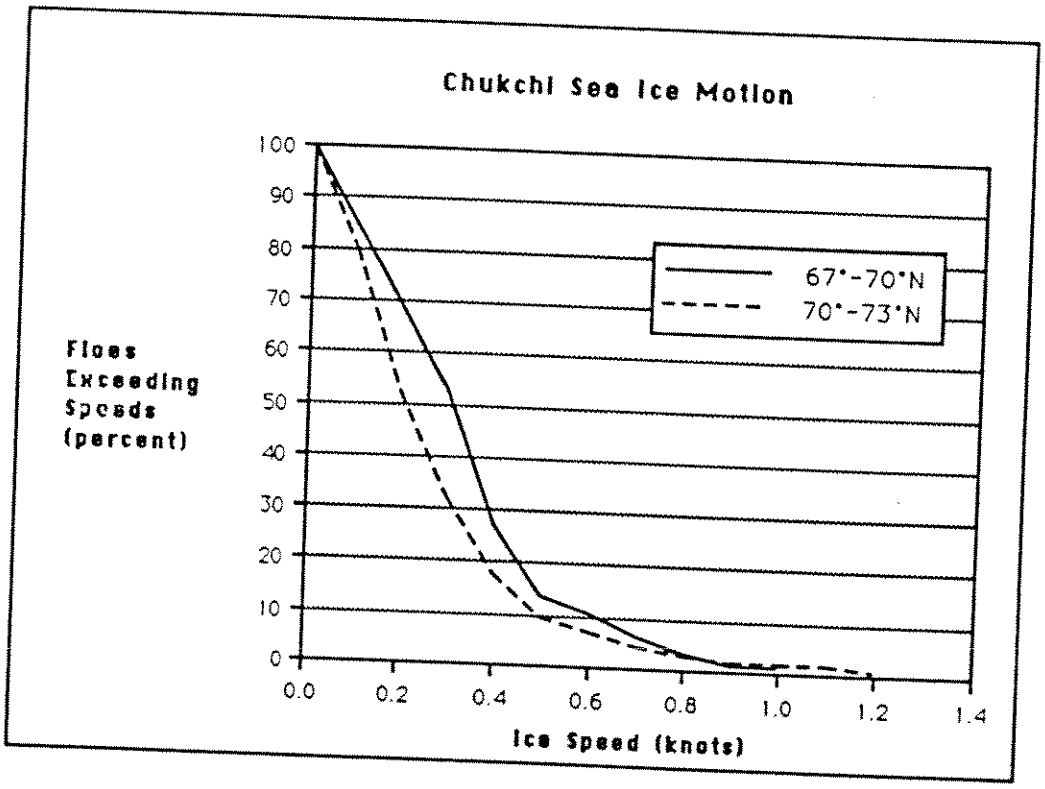

Figure 41 Distribution of Chukchi Sea Winter Ice Motion

9.2 North Bering Sea Ice Motion

Large scale ice motions are driven primarily by regional winds, except in local areas where opposing currents are strong enough to move ice against the wind (Muench and Ahlnas, 1976). The predominant current direction in the Bering Sea is north. Southward movements of ice from the Chukchi Sea into the Bering Sea occur several times a year and are associated with wind induced current reversals in the Bering Strait.

In heavy ice winters the dominant arctic high pressure system produces northerly winds and moves the ice southward. In light ice winters and in spring the Aleutian low pressure system produces more frequent storms and southerly winds, causing the ice to retreat northward.

Ice velocities are greatest where polynyas develop rapidly, such as south of Nome-Point Hope, or where ice divergence occurs, such as east of St. Lawrence Island. Ice speeds are slowest in sheltered areas, as in Norton Sound (McNutt, 1981).

Table 9 lists ice velocities for comparison with the data in Figure 42. Data for Figure 42 were based on drift speeds reported in the 1982 USCGC *Polar Star* trafficability study (Voelker et al., 1982) . The speed distribution in Figure 42 indicates a median speed of roughly 0.4 knots. This speed is of the same order of magnitude as the values reported by McNutt (1981) for the eastern Bering Sea.

Table 9 Bering Sea Ice Velocities

Source	Data		Comments
Myers (1985)	• maximum velocity for 5, 25 and 100 year return periods were 2.2, 2.6 and 3.0 kt respectively		• estimates were based on a statistical analysis of wind speeds • wind speeds were multiplied by 0.024 for ice speeds
McNutt (1981)	February: (1976, 1979)	0.9 kt max. speed 0.3 kt avg. speed	• based on Landsat and NOAA image analysis of eastern Bering Sea
	March: (1976, 1977)	1.2 kt max. speed 0.35 kt avg. speed	
	April: (1977)	0.5 kt max. speed 0.2 kt avg. speed	
Muench & Ahlnas (1976)	March: April: May:	0.7 kt max. speed 0.7 kt max. speed 0.6 kt max. speed	• 1974 NOAA image analysis

The peak velocity recorded during the *Polar Star* drift study was 1.9 kt. This value is only 0.3 kt less than the 5 year return period ice speed.

The average ice speed in the north Bering Sea is 0.2-0.4 kt during the months of February to April. Extreme ice speeds will occur after a wind reversal in areas of rapid polynya development. Maximum velocities of up to 2.0 kt are likely to occur in any year. More extreme ice speeds of up to 3.0 kt are theoretically reasonable for the northern Bering Sea region.

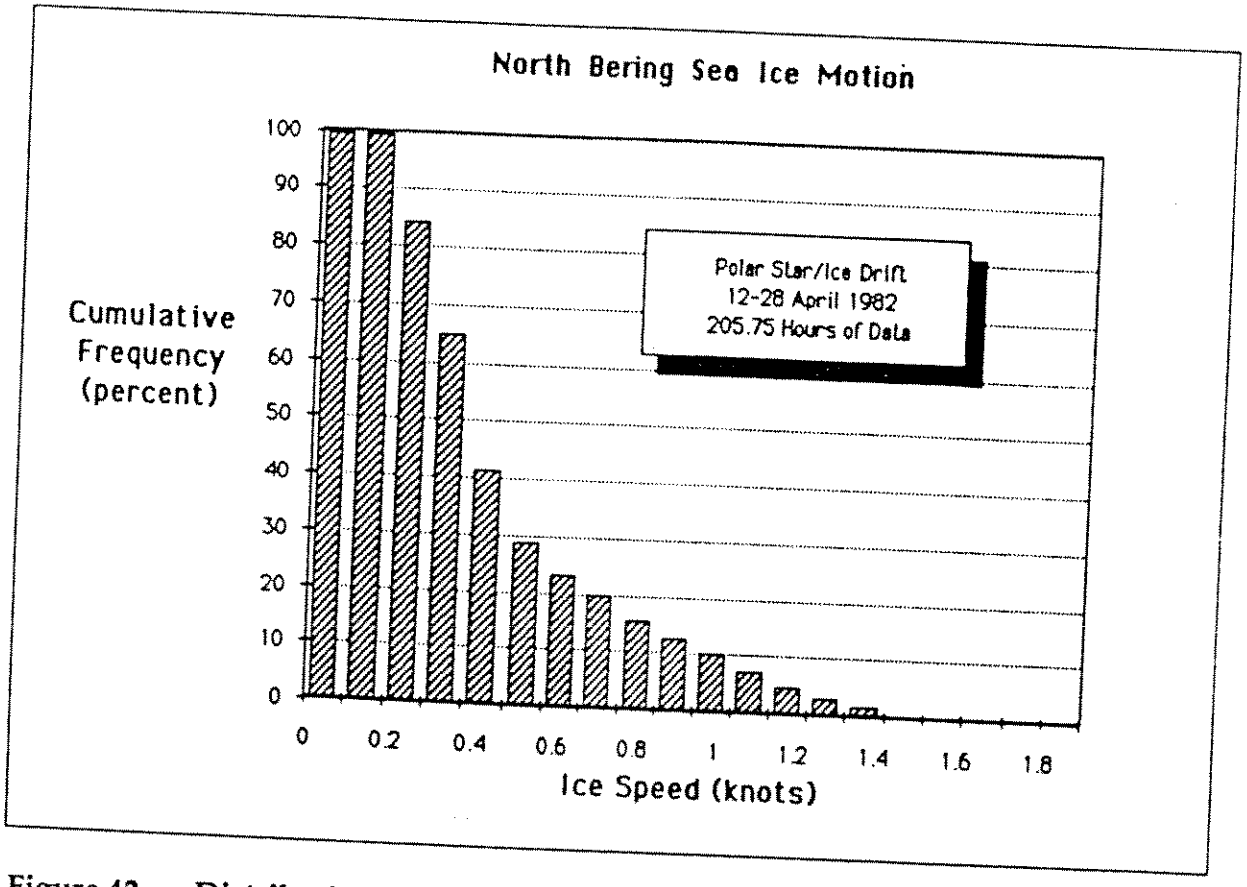

Figure 42 Distribution of North Bering Sea Ice Motion During April 1982

Frankenstein, G. and R. Garner. 1966. Linear Relationship of Brine Volume and Temperature from -0.5 C for Sea Ice of 1% Salinity. U.S. Army, CRREL Report December 1966.

Hanson, A.M. 1985. Observations of Ice and Snow in the Eastern Part of the Chukchi Sea: A Serindipitous Cruise on the *Polar Sea*. VI: MIZEX-WEST Bulletin, CRREL Special Report 85-6

Halebsky, et al. 1978. A Preliminary Feasibility Study of a Tanker Transportation System Serving the Northwest Coast of Alaska for Maritime Administration, Washington, D.C.

Hall, R.T. 1977. AIDJEX Modelling Group Studies Involving the Use of Remote Sensing Data. AIDJEX Symposium, Seattle.

Han-Padron Associates. 1984. Evaluation of Bering Sea Crude Oil Transportation Systems for Minerals Management Service, Alaska Outer Continental Shelf Region. Technical Report No. 110.

Hoare, R.E. et al. 1980. Seasonal Pack Ice Characteristics in the Shear Zone of the Beaufort Sea. Canadian Marine Drilling Ltd., APOA Report No. 147.

Intera Environmental Consultants Inc. 1982. Synthetic Aperture Radar (SAR) Study of the Beaufort and Chukchi Sea Ice, 1981. APOA Project No. 144.

Kovacs, A. 1976. Grounded Ice in the Fast Ice Zone Along the Beaufort Sea Coast of Alaska. CRREL Report 76-32.

LaBelle, J.C., J.L. Wise, R.P. Voelker, R.H. Schulze, and G.M. Wohl. 1983. Alaska Marine Ice Atlas. Arctic Environmental Information and Data Center, University of Alaska.

Lainey, L. and R. Tinawi. 1984. The Mechanical Properties of Sea Ice - A Compilation of Available Data. Can. J. Civ. Eng., Vol. 11, pp. 884-923.

Lane, J.S. 1979. Strength of Sea Ice and Correlation Between the Various Strength Tests. NRC, Low Temperature Laboratory, LTR-LT-104.

Marcellus, R.W. and T.B. Morrison. 1982. Ice Design Statistics for the Canadian Beaufort Sea. Canadian Marine Drilling Ltd., Report No. 1015.

Martin, S., R.D. Muench, C. Pease, and J.E. Overland. 1982. The Nature of the Winter Bering Sea Marginal Ice Zone. Oceans '82. Conference sponsored by Marine Technology Society and IEEE Council on Oceanic Engineering, Washington, D.C., September 20-22, 1982.

Maykut, G.A. 1977. Estimates of the Regional Heat Mass Balance of the Ice Cover in the Central Arctic. AIDJEX Symposium, Seattle.

McNutt, L. 1981. Ice Conditions in the Eastern Bering Sea from NOAA and LANDSAT Imagery: Winter Conditions 1974, 1976, 1977, 1979. NOAA Technical Memorandum ERL PMEL-24.

Muench, R.D. and K. Ahlnas. 1976. Ice Movement and Distribution in the Bering Sea from March to June 1974. J. Geophysical Research, Vol. 81, No. 24, pp. 4467-4476.

Murphy, D.L., P.A. Tebeau, and I.M. Lissauer. 1981. Long-Term Movement of Satellite-Tracked Buoys in the Beaufort Sea - An Interim Report. Washington, D.C., United States Coast Guard, Report No. CG-D-48-82.

Oceanographic Services Inc. 1981. Aerial Mapping of Sea Ice in the Chukchi Sea - 1980. AOGA Project Report 111 (confidentiality expired).

Overland, J.E. and C.H. Pease. 1982. Cyclone Climatology of the Bering Sea and its Relation to Sea Ice Extent. Monthly Weather Review, Vol. 11, pp. 5-13.

Paquette, R.G. and R.H. Bourke. 1981. Ocean Circulation and Fronts as Related to Ice Melt-Back in the Chukchi Sea. J. Geophysical Research, Vol. 86, No. C5, pp. 4215-4230.

Pease, C.H. 1980. Eastern Bering Sea Ice Processes. Monthly Weather Review, Vol. 10, No. 2, pp. 2015-2023.

Potocsky, G.J. 1975. Alaskan Area 15- and 30-Day Ice Forecasting Guide. Washington, D.C., Naval Oceanographic Office, Report No. NOO SP-263.

Pritchard, T.S. and D.J. Hanzlick. 1988. Chukchi Sea Ice Motion 1981-82. Proceedings, Port and Ocean Engineering Under Arctic Conditions, Volume III, Fairbanks, Alaska.

Shapiro, H. and J. Burns. 1975. Major Late-Winter Features of Ice in Northern Bering and Chukchi Seas as Determined from Satellite Imagery. Sea Grant Report 75-8, University of Alaska, Fairbanks.

Siebold, F. 1985. A Review of Research to Aid the Development of Commercial Arctic Marine Transportation: 1982 Trafficability Tests on the USCGC *Polar Star*. Marine Technology, Vol. 22, No. 1, pp. 28-35.

Stringer, W.J., S. Barrett, and L. Schreurs. 1980. Nearshore Ice Conditions and Hazards in the Beaufort, Chukchi, and Bering Seas. Geophysical Institute, University of Alaska.

Stringer, W.J., J. Zender-Romick, and J.E. Groves. 1982. Width and Persistence of the Chukchi Polynya. Geophysical Institute. University of Alaska.

Stringer, W.J., D.G. Barrett, and R.H. Godin. 1984. Handbook for Sea Ice Analysis and Forecasting. Geophysical Institute, University of Alaska.

Thorndike, A.S. and J.Y. Cheung. 1977. AIDJEX Measurements of Sea Ice Motion, 11 April 1975 to 14 May 1976. AIDJEX Bulletin No. 35.

Tucker, W.B., W.F. Weeks, and M.D. Frank. 1979. Sea Ice Ridging Over the Alaskan Continental Shelf. CRREL Report 79-8.

U.S. Navy. 1954-66. Birdseye Flight Series. (No longer available - data extracted from NOAA/BLM Beaufort/Chukchi Environmental Assessment, 1978.)

Vaudrey, K.D. 1977. Determination of Mechanical Sea Ice Properties by Large Scale Field Beam Experiments. POAC 1977, pp. 529-543.

Voelker, R.P., F.W. DeBord, J.J. Nelka, J.W. Jacobi, and J.L. Coburn. 1981a. Assessment of Ice Conditions in the South Bering Sea Based on April 1980 USCG Polar Class Trafficability Test Data, Volumes 1 and 2. Washington, D.C., Maritime Administration, Report No. 500C-2.

Voelker, R.P., F.W. DeBord, F.A. Geisel, J.L. Coburn, and K.E. Dane. 1981b. Winter 1981 Trafficability Tests of the USCGC *Polar Sea*, Volume 2: Environmental Data. Washington, D.C., Maritime Administration, Report No. 583C-3.

Voelker, R.P., F.A. Geisel, G.M. Wohl, and K.E. Dane. 1982. Arctic Deployment of USCGC *Polar Star*, Winter 1982. Volume 2. Environmental Data. Washington, D.C., Maritime Administration, Report No. 730B.

Voelker, R.P., F.A. Geisel, and K.E. Dane. 1983. Arctic Deployment of USCGC *Polar Sea*, Winter 1983. Executive Summary. Washington, D.C., Maritime Administration, AOGA Project 208 Vol. 1.

Voelker, R.P., F.A. Geisel, and G.M. Wohl. 1984. Bering Sea Data Collection Aboard USCGC *Polar Star*, February to March 1984. Volume 1 - Environmental Data, Washington, D.C., Maritime Administration, AOGA Project 208 Vol. 1.

Wadhams, P. and R.J. Horne. 1978. An Analysis of Ice Profiles Obtained by Submarine Sonar in the AIDJEX Area of the Beaufort Sea. Scott Polar Research Inst. Tech. Rept. No. 78-1, Cambridge.

Webster, B.D. 1982. Empirical Probabilities of the Ice Limit and Fifty Percent Ice Concentration Boundary in the Chukchi and Beaufort Seas. National Weather Service, NOAA.

Webster, B.D. 1981. A Climatology of the Ice Extent in the Bering Sea. NOAA Technical Memo NWSAR-33.

Weeks, W.F. and A. Assur. 1967. Mechanical Properties of Sea Ice. U.S. Army, CRREL Monograph IIC3.

Wetzel, V.F. 1971-1975. Statistical Study of Late Winter Ice Thickness Distribution in the Arctic Islands. APOA Projects 96-1 to 96-11, Sun Oil Company.

Wheeler, J.D. 1981. Ridge Statistics from Aerial Stereophotography. In Proceedings POAC 81, Helsinki, pp. 1209-1226.

Wilson, J.C., W.W. Wade, M.L. Feldman, and D.R. Younger. 1982. Alaska OCS Socioeconomic Studies Program Barrow Arch Planning Area (Chukchi Sea). Petroleum Technology Assessment. OCS Lease Sale No. 85 for Minerals Management Service.

Wright, B.D. and D.L. Schwab. 1973-1981. Beaufort Sea Ice, Stereo- Photo Analysis. 4 Volumes. Gulf Canada Resources Inc., Calgary.

Zubov, N.N. 1945. Arctic Ice. Northern Sea Route Administration, Moscow, USSR. Translated by U.S. Naval Oceanographic Office.

APPENDIX A
REGIONAL ICE SUMMARY TABLES

REGIONAL ICE SUMMARY

Environmental Zone: Zone 1

Geographic Name: South Bering Sea

Location: 56°N to 60°N
Pribilof Islands to Nunivak Island

Length: 240 n.mi.

	Earliest	Mean	Latest
Break-Up (<6/10)	-	-	1 Apr-18 May
Freeze-Up (>6/10)	25 Dec-12 Mar	-	-

Month	Ice Concentration (tenths)								Level First Year Ice Thickness (ft)
	Total			MY			Mean		
	Mean	Max	Min	Mean	Max	Min	Thick FY	Thin FY	Thick FY
Oct	0	0	0				0	0	0
Nov	0	0	0				0	0	0
Dec	0	1	0				0	0	0
Jan	0.5	4.8	0	NOT PRESENT			0	0.5	0.47
Feb	2.4	9.8	0				0	2.4	0.97
Mar	2.8	9.4	0				0	2.8	1.33
Apr	1.9	6	0				0.7	1.2	1.49 (1.52)
May	1.3	1.6	0				1.0	0.3	0
June	0	0	0				0	0	0
July	0	0	0				0	0	0
Aug	0	0	0				0	0	0
Sept	0	0	0				0	0	0

Other Data

Month	Snow Depth (in)	Ridge Frequency (#/mi)	Max Ridge Height (ft)
April 1980	-	8.0 (cut off ht = 2.0 ft)	7.0

Comments:

- Ice concentration and thickness values represent mid-month conditions.
- Ice thickness is based on mean freeze-up date.
- ( ) maximum ice thickness is based on earliest freeze-up date.
- February 1981 ridge data is low as the USCG Polar Sea route avoided severe features.
- Thin first year ice is defined as ice less than 12 inches thick.

REGIONAL ICE SUMMARY

Environmental Zone: Zone 2

Geographic Name: South Bering Sea

Location: 60°N to 63°N
Nunivak Island to St. Lawrence Island

Length: 205 n.mi.

	Earliest	Mean	Latest
Break-Up (<6/10)	13 Feb	6 May	13-18 June
Freeze-Up (>6/10)	13-18 Nov	13 Dec	25-30 Jan

Month	Ice Concentration (tenths)							Level First Year Ice Thickness (ft)
	Total			MY			Mean	
	Mean	Max	Min	Mean	Max	Min	Thick FY / Thin FY	Thick FY
Oct	0	0	0				0 / 0	0
Nov	5.4	8.7	0				3.9 / 1.5	0
Dec	8.3	10	0				1.7 / 6.6	1.0
Jan	9.2	10	2.5				5.1 / 4.1	1.0
Feb	9.4	10	6.3	Isolated floes			4.8 / 4.6	1.44
Mar	9.1	10	2.5	Observed			5.8 / 3.3	1.97 [2.7]
Apr	7	10	0	March 1984 from			5.2 / 1.8	2.24
May	5.3	9.4	0	"Polar Star"			4.5 / 0.8	2.32 (2.52)
June	0.9	4.4	0				0.9 / 0	0
July	0	0	0				0 / 0	0
Aug	0	0	0				0 / 0	0
Sept	0	0	0				0 / 0	0

Other Data

Month	Snow Depth (in)	Ridge Frequency (#/mi)	Max Ridge Height (ft)
April 1981	-	8.6 (cut off ht = 3.0 ft)	9.6
Feb 1981	4	9 (cut off ht = 3.0 ft)	8.0
Mar 1984		2-4 (over 3.0 ft)	12
Mar 1983	1.8		

Comments:

- Ice concentration and thickness values represent mid-month conditions.
- Ice thickness is based on mean freeze-up date.
- ( ) maximum ice thickness is based on earliest freeze-up date.
- February 1981 ridge data is low as the USCG Polar Sea route avoided severe features.
- Thin first year ice is defined as ice less than 12 inches thick.
= [ ] floe thickness reported by the Polar Sea 30 nmi north of

REGIONAL ICE SUMMARY

Environmental Zone: Zone 3

Geographic Name: North Bering Sea

Location: 63°N to 66°N
St. Lawrence Island to Bering Strait

Length: 160 n.mi.

	Earliest	Mean	Latest
Break-Up (<6/10)	19-24 Apr	25 May	19-24 June
Freeze-Up (>6/10)	6 Nov	1-6 Dec	19-24 Dec

Month	Ice Concentration (tenths)								Level First Year Ice Thickness (ft)
	Total			MY			Mean		
	Mean	Max	Min	Mean	Max	Min	Thick FY	Thin FY	Thick FY
Oct	0	0	0				0	0	0
Nov	4.4	9.7	0				1.5	2.9	0
Dec	9	10	5.4	NOT			2.9	6.1	0.76
Jan	9.6	10	5.9	PRESENT			5.7	3.9	1.60
Feb	9.5	10	6.3	EXCEPT			7.2	2.3	2.20
Mar	9.3	10	6.6	TRACE			7.0	2.3	2.68
Apr	8.4	10	1.6	AMOUNTS			7.1	1.3	2.98
May	5.9	10	0				5.6	0.3	3.04 (3.22)
June	1.1	6.9	0				1.1	0	0
July	0	0	0				0	0	0
Aug	0	0	0				0	0	0
Sept	0	0	0				0	0	0

Other Data

Month	Snow Depth (in)	Ridge Frequency (#/mi)	Max Ridge Height (ft)
Feb 1981	5	10(cut off ht = 3.0 ft) 18-23 worst case frequency reported NE of St. Lawrence Island	8.0

Comments:

- Ice concentration and thickness values represent mid-month conditions.
- Ice thickness is based on mean freeze-up date.
- ( ) maximum ice thickness is based on earliest freeze-up date.
- February 1981 ridge data is low as the USCG Polar Sea route avoided severe features.
- Thin first year ice is defined as ice less than 12 inches thick.

REGIONAL ICE SUMMARY

Environmental Zone: Zone 4

Geographic Name: South Chukchi Sea

Location: 63°N to 69°N
Bering Strait to Point Lay

Length: 230 n.mi.

	Earliest	Mean	Latest
Break-Up (<6/10)	25-30 Mar	25-30 May	19-24 June
Freeze-Up (>6/10)	6 Nov	25-30 Nov	13-18 Dec

Month	Ice Concentration (tenths)							Level First Year Ice Thickness (ft)
	Total			MY		Mean		
	Mean	Max	Min	Mean	Max Min	Thick FY	Thin FY	Thick FY
Oct	0	0	0			0	0	0
Nov	5.8	10	0			2.2	3.6	1.00
Dec	9.6	10	8.9	TRACE		4.8	4.8	1.17
Jan	9.8	10	8.3	CONCENTRATIONS		6.2	3.6	2.19
Feb	9.9	10	9.6	ONLY		7.9	2.0	2.88 [4.1Avg]
Mar	9.9	10	9.6			8.1	1.8	3.43
Apr	9.6	10	7.1			8.3	1.3	3.65
May	7.3	10	2.9			6.7	0.6	3.91 (4.10)
June	0.7	5	0			0.6	0.1	2.60
July	0.2	1.7	0			0.2	0	0
Aug	0	0	0			0	0	0
Sept	0	0	0			0	0	0

Other Data

Month	Snow Depth (in)	Ridge Frequency (#/mi)	Max Ridge Height (ft)
Feb 1981	6-7 12 (Max)	4 (cut off ht = 3.0 ft)	12.0
May 1980		8 (< 4 ft)	25
Mar 1983	1.0		

Comments:

- Ice concentration and thickness values represent mid-month conditions.
- Ice thickness is based on mean freeze-up date.
- ( ) maximum ice thickness is based on earliest freeze-up date.
- February 1981 ridge data is low as the USCG Polar Sea route avoided severe features.
- Thin first year ice is defined as ice less than 12 inches thick.
- [ ] range in first-year ice reported by the Polar Sea between Bering Strait and Cape Lisburne (1981 & 1983)

REGIONAL ICE SUMMARY

Environmental Zone: Zone 5

Geographic Name: Chukchi Sea - Nearshore

Location: 68°N 165°30'W to 70°30' 162°W
Cape Lisburne to Icy Cape

Length: 180 n.mi.

	Earliest	Mean	Latest
Break-Up (<6/10)	25-30 Mar	25 May	25 July
Freeze-Up (>6/10)	7-12 Oct	6 Nov	19-24 Nov

Month	Ice Concentration (tenths)								Level First Year Ice Thickness (ft)
	Total			MY			Mean		
	Mean	Max	Min	Mean	Max	Min	Thick FY	Thin FY	Thick FY
Oct	2.1	7.3	0				0.4	1.7	0
Nov	9.4	10	7				1.5	7.9	1.00
Dec	9.9	10	9.3				2.3	7.6	1.47
Jan	9.9	10	9.8				3.2	6.7	2.29
Feb	9.9	10	9.3	TRACE			4.3	5.6	2.98
Mar	9.6	10	7.3	CONCENTRATIONS			3.8	5.8	3.61
Apr	9.8	10	8.8	ONLY			4.9	4.9	4.10
May	6.3	10	0				3.8	2.5	4.22 (4.33)
June	2.9	9.5	0				2.5	0.4	3.20
July	0.7	3.8	0				0.7	0	0
Aug	0.4	1.8	0				0.4	0	0
Sept	0.05	0.25	0				0.05	0	0

Other Data

Month	Snow Depth (in)	Ridge Frequency (#/mi)	Max Ridge Height (ft)
Feb 1976	-	11.5-12.1 (cut off ht = 3.0 ft)	-
Apr 1976	-	7.7-8.7 (cut off ht = 3.0 ft)	-
Feb 1981	4	17 (cut off ht = 2 ft)	12

Comments:

- Ice concentration and thickness values represent mid-month conditions.
- Ice thickness is based on mean freeze-up date.
- ( ) maximum ice thickness is based on earliest freeze-up date.
- February 1981 ridge data is low as the USCG Polar Sea route avoided severe features.
- Thin first year ice is defined as ice less than 12 inches thick.

REGIONAL ICE SUMMARY

Environmental Zone: Zone 6

Geographic Name: Chukchi Sea - Nearshore

Location: 70°30'N to 71°30'N
Icy Cape to Barrow

Length: 60 n.mi.

	Earliest	Mean	Latest
Break-Up (<6/10)	25 April	07 July	12 Sept
Freeze-Up (>8/10)	01 Oct	25 Oct	06 Nov

Month	Ice Concentration (tenths)								Level First Year Ice Thickness (ft)
	Total			MY			Mean		
	Mean	Max	Min	Mean	Max	Min	Thick FY	Thin FY	Thick FY
Oct	4.9	10	0	0	0	0	1.1	3.8	0
Nov	9.8	10	8.2	0	0	0	2.2	7.6	1.00
Dec	9.8	10	6.9	0	0	0	5.6	4.2	2.10
Jan	10	10	10	0	0.6	0	7.5	2.5	3.02
Feb	10	10	9.4	0	0.6	0	7.9	2.1	3.76
Mar	9.8	10	6.9	0.1	1.3	0	6.1	3.6	4.41
Apr	9.8	10	7.6	0	0	0	6.4	3.4	4.90[6.0]
May	7.7	10	0	0	0	0	5.7	2.0	5.15
June	5.0	10	0	0	0	0	4.6	0.4	5.19 (5.19)
July	4.4	10	0	0.3	3.1	0	4.1	0	4.00
Aug	0.9	10	0	0	0	0	0.8	0.1	0
Sept	0.8	4.4	0	0.2	1.3	0	0.4	0.2	0

Other Data

Month	Snow Depth (in)	Ridge Frequency (#/mi)	Max Ridge Height (ft)
Feb 1976	-	6.7-7.0 (cut off ht = 3.0 ft)	
Apr 1976	-	7.2-8.3 (cut off ht = 3.0 ft)	
Apr 1983	2.5		

Comments:

- Ice concentration and thickness values represent mid-month conditions.
- Ice thickness is based on mean freeze-up date.
- ( ) maximum ice thickness is based on earliest freeze-up date.
- Thin first year ice is defined as ice less than 12 inches thick.
- [ ] maximum thickness reported by the Polar Sea offshore Wainwright Apr. 2, 1983

REGIONAL ICE SUMMARY

Environmental Zone: Zone 7

Geographic Name: Chukchi Sea - Offshore

Location: 70°N to 72°N
Point Lay to Barrow - Offshore

Length: 130 n.mi.

	Earliest	Mean	Latest
Break-Up (<6/10)	13-18 May	25 June	25 July
Freeze-Up (>6/10)	25 Sept	30 Oct	19-24 Nov

Month	Ice Concentration (tenths)								Level First Year Ice Thickness (ft)
	Total			MY			Mean		
	Mean	Max	Min	Mean	Max	Min	Thick FY	Thin FY	Thick FY
Oct	3.1	10	0	0	0	0	0.4	2.7	0
Nov	10	10	10	0.3	2.5	0	4.1	5.6	1.00
Dec	10	10	10	0.3	2.5	0	8.3	1.4	1.81
Jan	10	10	10	0.6	2.5	0	8.6	0.8	2.68
Feb	10	10	10	0.6	3.8	0	8.9	0.5	3.40
Mar	9.9	10	9.4	0.6	5.0	0	8.7	0.6	4.04
Apr	9.8	10	8.8	0.1	1.3	0	9.2	0.5	4.50
May	8.3	10	4.4	0.1	1.3	0	7.6	0.6	4.74 (4.86)
June	5.5	10	0	0	0	0	5.2	0.3	4.74
July	2.3	9.4	0	0	0	0	2.3	0	3.70
Aug	0.6	8.8	0	0.3	2.5	0	0.3	0	0
Sept	0.4	3.8	0	0	0	0	0	0.4	0

Other Data

Month	Snow Depth (in)	Ridge Frequency (#/mi)	Max Ridge Height (ft)
Feb 1976	-	5.8 (cut off ht = 3.0 ft)	12.0
Apr 1976	-	7.6 (cut off ht = 3.0 ft)	-
Feb 1981	5	9 (cut off ht = 2.0 ft)	10
May 1980	-	11 (< 4ft) from laser	38

Comments:

- Ice concentration and thickness values represent mid-month conditions.
- Ice thickness is based on mean freeze-up date.
- ( ) maximum ice thickness is based on earliest freeze-up date.
- February 1981 ridge data is low as the USCG Polar Sea route avoided severe features.
- Thin first year ice is defined as ice less than 12 inches thick.

REGIONAL ICE SUMMARY

Environmental Zone: Zone 8

Geographic Name: Chukchi Sea

Location: 72°N to 73°N
Northern Limit of OCS Lease Sale Area 109

Length: 30 n.mi.

	Earliest	Mean	Latest
Break-Up (<6/10)	13-18 June	25-30 July	-
Freeze-Up (>6/10)	-	25-30 Oct	19-24 Nov

Month	Ice Concentration (tenths)								Level First Year Ice Thickness (ft)
	Total			MY			Mean		
	Mean	Max	Min	Mean	Max	Min	Thick FY	Thin FY	Thick FY*
Oct	4.8	10	0	0.6	3.8	0	1.7	2.5	1.00
Nov	10	10	10	0.9	3.1	0	4.8	4.3	1.00
Dec	10	10	10	1.3	5.6	0	7.9	0.8	2.10
Jan	10	10	10	2.1	5.6	0	7.6	0.3	3.02
Feb	10	10	10	2.3	5.6	0	7.5	0.2	3.76
Mar	10	10	10	2.8	7.5	0.6	6.9	0.3	4.41
Apr	10	10	10	2.8	7.5	0	6.9	0.3	4.90
May	10	10	10	1.9	6.3	0	7.6	0.5	5.15
June	8.8	10	0	2.1	6.3	0	6.4	0.3	5.19 (5.19)
July	6.9	10	0	1.6	5.0	0	5.3	0	4.00
Aug	3.1	10	0	1.6	4.4	0	1.5	0	3.00
Sept	6.9	10	0	0.6	3.1	0	5.9	0.4	1.00

Other Data

Month	Snow Depth (in)	Ridge Frequency (#/mi)	Max Ridge Height (ft)
Feb 1976	-	5.5 (cut off ht = 3.0 ft)	17.0 (laser)
Apr 1976	-	5.3 (cut off ht = 3.0 ft)	- (laser)
Feb 1981	5		20 (ship obs.)
May 1980		17 (< 4ft) from laser	27 (from laser)

Comments:

- Ice concentration and thickness values represent mid-month conditions.
- Ice thickness is based on mean freeze-up date.
- ( ) maximum ice thickness is based on earliest freeze-up date.
- February 1981 ridge data is low as the USCG Polar Sea route avoided severe features.
- Thin first year ice is defined as ice less than 12 inches thick.
- *Ice thickness values for Zone 8 are low as based on Pt. Barrow shore station freezing degree days.

REGIONAL ICE SUMMARY

Environmental Zone: Zone 9

Geographic Name: Chukchi Sea - Offshore

Location: 69°N to 70°N
Point Lay to Icy Cape - Offshore

Length: 60 n.mi.

	Earliest	Mean	Latest
Break-Up (<6/10)	1-6 June	18 June	19-24 July
Freeze-Up (>8/10)	19 Oct	12 Nov	13-18 Nov

Month	Ice Concentration (tenths)								Level First Year Ice Thickness (ft)
	Total			MY			Mean		
	Mean	Max	Min	Mean	Max	Min	Thick FY	Thin FY	Thick FY
Oct	0.7	5	0				0	0.7	0
Nov	9.8	10	8.8				2.8	7.0	1.00
Dec	10	10	10	TRACE			6.2	3.8	1.53
Jan	10	10	10	CONCENTRATIONS			8.6	1.4	2.48
Feb	10	10	10	ONLY			9.3	0.7	3.22
Mar	10	10	10				9.2	0.8	3.89
Apr	10	10	10				9.3	0.7	4.37
May	9.8	10	8.8				9.3	0.5	4.58
June	6	10	0				5.8	0.2	4.59 (4.79)
July	1.5	10	0				1.5	0	3.50
Aug	0.2	1.3	0				0.2	0	0
Sept	0	0	0				0	0	0

Other Data

Month	Snow Depth (in)	Ridge Frequency (#/mi)	Max Ridge Height (ft)
Apr 1981	2 in (smooth ice) 19 in (rough ice)	16-36 (cut off ht = 1.0 ft)	16.4
May 1980		16 (< 4ft) from laser	28

Comments:

- Ice concentration and thickness values represent mid-month conditions.
- Ice thickness is based on mean freeze-up date.
- ( ) maximum ice thickness is based on earliest freeze-up date.
- February 1981 ridge data is low as the USCG Polar Sea route avoided severe features.
- Thin first year ice is defined as ice less than 12 inches thick.

APPENDIX B

POLAR PACK EDGES

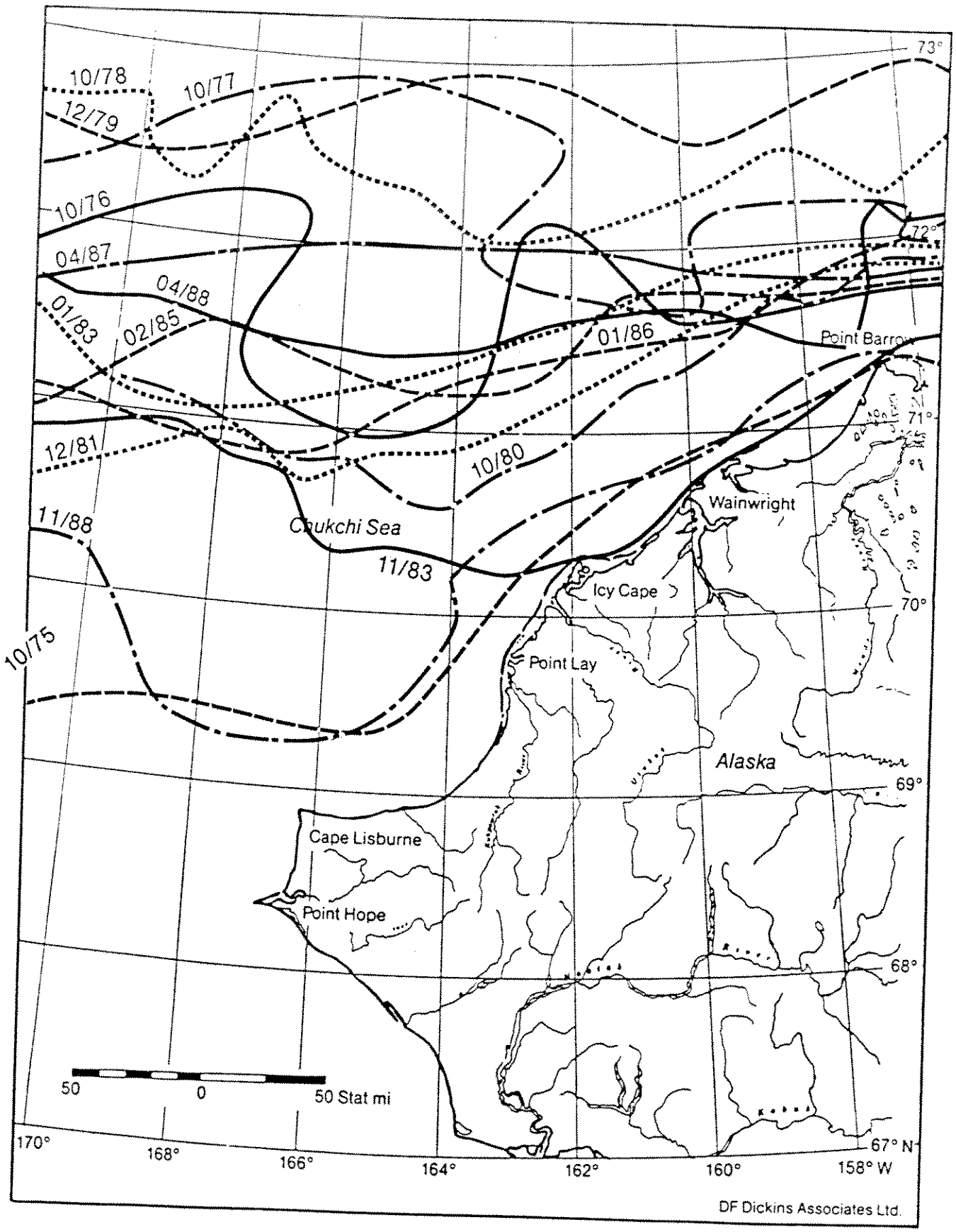

Locations of the Most Southerly Annual Winter Polar Pack Edges (October to May, 1975-89)

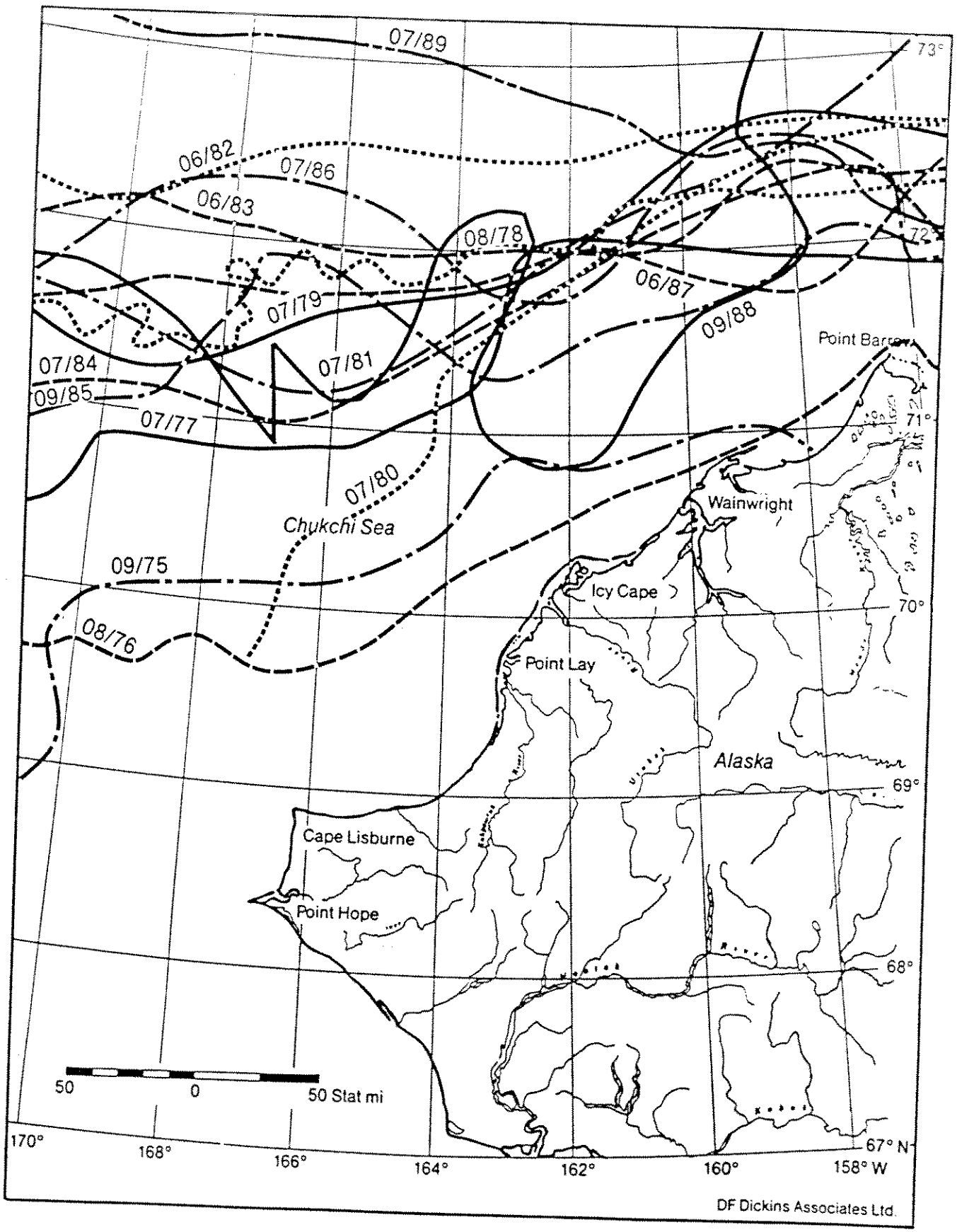

Locations of the Most Southerly Annual Summer Polar Pack Edges (June to September, 1975-89)

APPENDIX C
FLEXURAL ICE STRENGTH

FLEXURAL ICE STRENGTH

Flexural ice strength in the Chukchi Sea has not been measured directly. During the USCGC Polar Sea (February 1981) and USCGC Polar Star (April 1982) cruises, measurements of temperature and salinity were used to calculate flexural ice strength. Flexural ice strength estimates were given for the top 75% of each ice core. Strength estimates were based on three formulae, namely: Vaudrey (1977), Lane (1979), and Weeks and Assur (1967) equations.

Flexural strength of ice is a function of temperature, brine volume (salinity), and stress rate. Figure 1 (from Lainey and Tinawi (1984)) shows the relationship between flexural strength and stress rate. At stress rates greater than 100 kPa/s there is very little variation in flexural strength. Also, at stress rates between 100 kPa/s and 10,000 kPa/s the stress rate has almost no effect on flexure strength.

Figure 2 presents four curves relating salinity to flexural strength. Instead of plotting a family of curves to account for salinity changes caused by temperature, the variable brine volume is used. The brine volume is related to salinity and temperature by three equations reported by Frankenstein and Garner (1967).

$$V_b = S\left(-\frac{52.56}{T} - 2.28\right) \qquad -0.5 < T < -2.06°C$$

$$= S\left(-\frac{45.917}{T} + 0.930\right) \qquad -2.06 < T < -8.2°C$$

$$= S\left(-\frac{43.795}{T} + 1.189\right) \qquad -8.2 < T < -22.9°C$$

Where V_b = brine volume, S = salinity (%), T = temperature (°C)

Three equations are required to calculate brine volume because Na_2S0_4 precipitates at -8.2°C and NaCl precipitates at -22.9°C. The precipitation of NaCl causes an increase of ice strength because the precipitate bonds to the ice. Bonding of NaCl almost eliminates the brine channels in sea ice.

Measurements from the two USCGC trafficability studies indicate a range of brine volume values from 0.4 ppt to almost 200 ppt. This is equivalent to the square root of brine volume varying between 0 and 0.4 in Figure 2. A large variation in brine volume is expected to occur because of the range of ice temperatures from -2 to -20°C.

The relationship between temperature and flexural strength is not well defined. Figure 3 shows the range of values found by 8 different authors. The average of the ranges is also indicated and corresponds closely with Vaudrey's (1977) equation for a salinity of 5%. The data range is caused by differences of stress rates and salinity. Random variations between identical samples also contribute to the data range. The slope of the curves increases after -22.9°C, reflecting the strength increases caused by precipitation of NaCl.

Estimates for Chukchi Sea flexural ice strength (Polar Sea, 1981 and Polar Star, 1982 cruises) were from 360 to 930 kPa. These values were calculated for ice at temperatures from -2 to -20°C and average salinities from 2 to 6 ppt. The flexural strength values quoted were based on Vaudrey's (1977) equation. Flexural ice strengths were roughly 100 kPa lower when based on the Lane (1979) or Weeks and Assur (1967) equations.

The ice strength estimates from the Polar Sea and Polar Star cruises should be representative of Chukchi Sea ice. The values estimated fall well within the range of experimental values shown in Figure 3.

Chukchi Sea ice will be weakest during the fall and spring when ice temperatures are warmest (as warm as -2°C). Ice in the fall will have more brine channels and hence a higher salinity than ice later in the winter. The ice will be strongest after sustained low air temperatures have cooled the ice below -22.9°C to a depth of a few feet. This is most likely to occur from January through March.

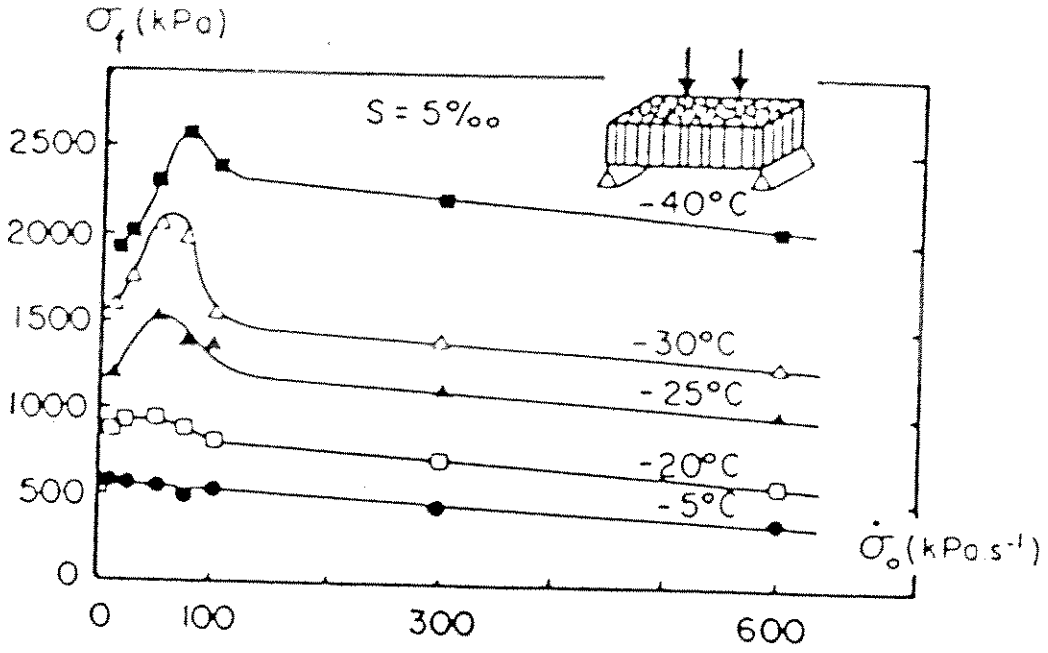

Figure 1 Flexural Ice Strength vs Stress Rate (Lainey and Tinawi), 1984

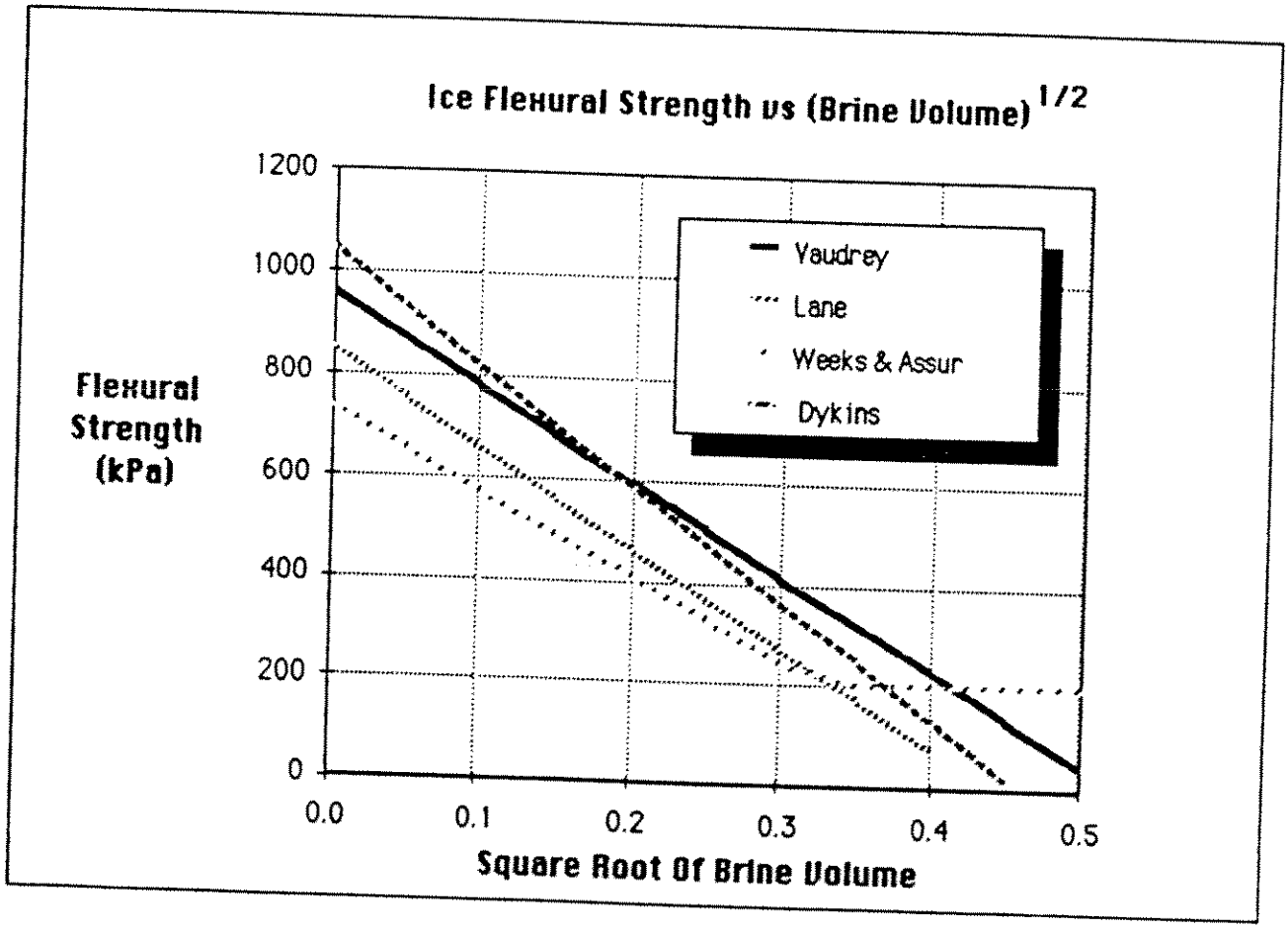

Figure 2 Variation of Flexural Strength with Changes of Brine Volume

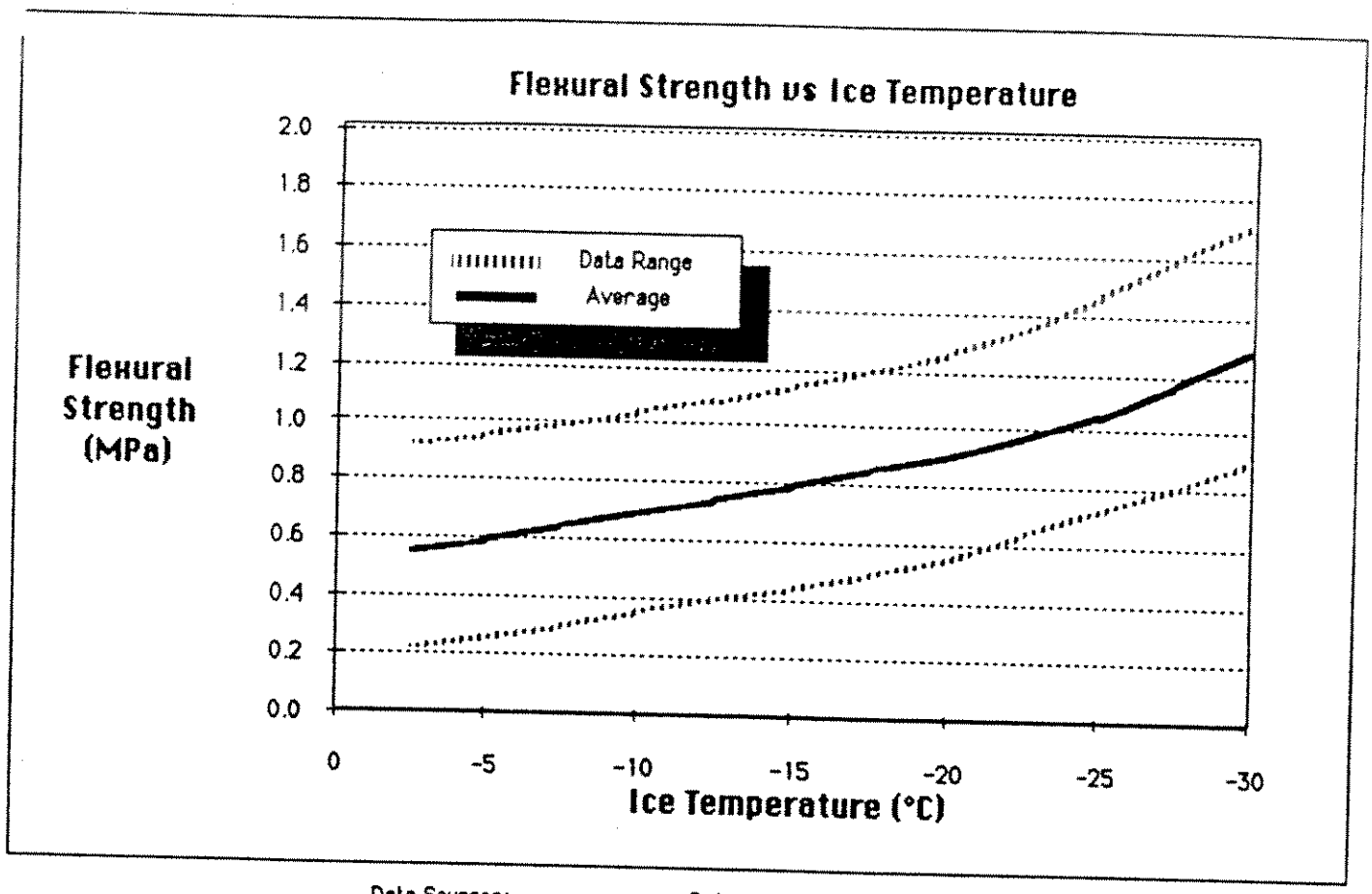

Data Sources:	Dates	Stress Rates (kPa/s)
Timco & Frederking	1983	?
Lainey & Tinawi	1981	10-600
Saeki et al.	1981	100-300
Saeki et al.	1978	20-2000
Murat	1978	50-120
Dykins	1971	160-260
Tabata	1966	6-200
Butkovich	1956	50-700

Figure 3 Experimentally Measured Variation of Flexural Strength With Ice Temperature

APPENDIX D

COMPARISON OF NOAA, DMSP, AND LANDSAT IMAGES

COMPARISON OF NOAA, DMSP, AND LANDSAT IMAGES

NOAA Images

Agency	- National Oceanographic and Atmospheric Administration
Nominal Scale	- 1:7,000,000
Resolution	- 0.6 to 1.0 nmi (1 to 1.8 km) but deteriorates towards images' edges
Advantages	- daily coverage year round
	- some cloud penetration
Disadvantages	- significant optical distortion of images
	- if many small floes occur, the ice concentration can be overestimated
	- difficult to distinguish multi-year from thick first-year ice

DMSP Images

Agency	- Defense Meteorological Satellite Program
Standard Scale	- 1:7,000,000
Resolution	- high resolution mode gives 0.3 nmi (0.6 km) resolution
Advantages	- less optical distortion than NOAA images, it is possible to register image using coastline
	- can identify major lead features greater than 0.5 nmi
Disadvantages	- images are blocked by cloud cover
	- difficult to estimate multi-year ice cover
	- errors in estimating ice cover when floe size approaches pixel resolution or less (0.3 nmi)

Landsat Images

Agency	- University of Alaska Geophysical Institute
Scale	- 1:1,000,000
Resolution	- 80 m (0.043 nmi) resolution and virtually no distortion
Advantages	- excellent for calibrating other remote sensors - good definition of general ice conditions
Disadvantages	- cannot obtain images without daylight (no images available for November to February period)
	- cannot obtain images through clouds (results in an 80% or more data loss)
	- 16-18 days between repeat images of same area (8-9 days if two satellites are operating)